FRIEDRICH-SCHILLER-
UNIVERSITÄT
JENA

Anion receptors based on hydrogen and halogen bonding

Dissertation

(kumulativ)

zur Erlangung des akademischen Grades

doctor rerum naturalium (Dr. rer. nat.)

vorgelegt dem Rat der Chemisch-Geowissenschaftlichen Fakultät

der Friedrich-Schiller-Universität Jena

von Dipl.-Chem. Ronny Tepper

geboren am 06.11.1987 in Hohenmölsen

Gutachter:

1. Prof. Dr. Ulrich S. Schubert (Friedrich-Schiller-Universität Jena)
2. Prof. Dr. Benjamin Dietzek (Friedrich-Schiller-Universität Jena)
3. Prof. Dr. Carsten Schmuck (Universität Duisburg-Essen)

Tag der öffentlichen Verteidigung: 19.09.2018

Table of content

Documentation of authorship

This section contains a list of individual authors' contributions to the publications reprinted in this thesis.

P1) "Halogen bonding in solution: Anion recognition, templated self-assembly, and organo-catalysis" R. Tepper,[1] U. S. Schubert,[2] *Angew. Chem. Int. Ed.* DOI: 10.1002/anie.201707986; *Angew. Chem.* DOI: 10.1002/ange.201707986.		
Author	**1**	**2**
Conceptual contribution	x	
Preparation of the manuscript	x	
Correction of the manuscript	x	x
Supervision of R. Tepper		x
Proposal for crediting publication equivalents	0.5	

P2) "Preorganization in a cleft-type anion receptor featuring iodo-1,2,3-triazoles as halogen bond donors" R. Tepper,[1] B. Schulze,[2] H. Görls,[3] P. Bellstedt,[4] M. Jäger,[5] U. S. Schubert,[6] *Org. Lett.* **2015**, *17*, 5740-5743.						
Author	**1**	**2**	**3**	**4**	**5**	**6**
Conceptual contribution	x	x				
Synthesis / characterization of compounds	x					
ITC binding studies	x					
computational calculations					x	
single-crystal X-ray diffraction analysis			x			
assistance with special NMR measurements				x		
Preparation of the manuscript	x					
Correction of the manuscript	x	x			x	x
Supervision of R. Tepper		x				x
Proposal for crediting publication equivalents	1.0					

P3) "Halogen-bond-based cooperative ion-pair recognition by a crown-ether-embedded 5-iodo-1,2,3-triazole"

R. Tepper,[1] B. Schulze,[2] P. Bellstedt,[3] J. Heidler,[4] H. Görls,[5] M. Jäger,[6] U. S. Schubert,[7] *Chem. Commun.* **2017**, *53*, 2260-2263.

Author	**1**	**2**	**3**	**4**	**5**	**6**	**7**
Conceptual contribution	x	x					
Synthesis / characterization of compounds	x			x			
NMR binding studies	x						
computational calculations						x	
single-crystal X-ray diffraction analysis					x		
assistance with special NMR measurements			x				
Preparation of the manuscript	x						
Correction of the manuscript	x	x				x	x
Supervision of R. Tepper		x					x
Proposal for crediting publication equivalents	1.0						

P4) "Polymeric halogen-bond-based donor systems showing self-healing behavior in thin films"

R. Tepper,[1] S. Bode,[2] R. Geitner,[3] M. Jäger,[4] H. Görls,[5] J. Vitz,[6] B. Dietzek,[7] M. Schmitt,[8] J. Popp,[9] M. D. Hager,[10] U. S. Schubert,[11] *Angew. Chem. Int. Ed.* **2017**, *56*, 4047-4051; *Angew. Chem.* **2017**, *129*, 4105-4110.

Author	**1**	**2**	**3**	**4**	**5**	**6**	**7**	**8**	**9**	**10**	**11**
Conceptual contribution	x	x								x	
Synthesis / characterization of compounds	x	x									
ITC binding studies	x										
self-healing tests		x									
Raman studies			x								
computational calculations				x							
single-crystal X-ray diffraction analysis					x						

nanoindentation studies						x					
Preparation of the manuscript	x	x	x								
Correction of the manuscript	x	x	x				x	x	x	x	x
Supervision of R. Tepper											x
Supervision of R. Geitner							x	x	x		
Proposal for crediting publication equivalents	1.0		0.5								

P5) "A healing ionomer crosslinked by a bis-bidentate halogen bond linker: a route to hard and healable coatings"

J. Dahlke,[1] R. Tepper,[2] R. Geitner,[3] S. Zechel,[4] J. Vitz,[5] R. Kampes,[6] J. Popp,[7] M. D. Hager,[8] U. S. Schubert,[9] *Polym. Chem*. **2018**, *9*, 2193-2197.

Author	**1**	**2**	**3**	**4**	**5**	**6**	**7**	**8**	**9**
Conceptual contribution	x	x		x					
Synthesis / characterization of compounds	x	x				x			
ITC binding studies		x							
self-healing tests	x								
Raman studies			x						
nanoindentation studies					x				
Preparation of the manuscript	x	x							
Correction of the manuscript	x	x	x	x			x	x	x
Supervision of R. Tepper									x
Proposal for crediting publication equivalents	1.0	0.5							

Erklärung zu den Eigenanteilen des Promovenden/der Promovendin sowie der weiteren Doktoranden/Doktorandinnen als Co-Autoren an den Publikationen und Zweitpublikationsrechten bei einer kumulativen Dissertation

Für alle in dieser kumulativen Dissertation verwendeten Manuskripte liegen die notwendigen Genehmigungen der Verlage („Reprint permissions“) für die Zweitpublikation vor.

Die Co-Autoren der in dieser kumulativen Dissertation verwendeten Manuskripte sind sowohl über die Nutzung, als auch über die oben angegebenen Eigenanteile der weiteren Doktoranden/Doktorandinnen als Co-Autoren an den Publikationen und Zweitpublikationsrechten bei einer kumulativen Dissertation informiert und stimmen dem zu (es wird empfohlen, diese grundsätzliche Zustimmung bereits mit Einreichung der Veröffentlichung einzuholen bzw. die Gewichtung der Anteile parallel zur Einreichung zu klären).

Die Anteile des Promovenden sowie der weiteren Doktoranden/Doktorandinnen als Co-Autoren an den Publikationen und Zweitpublikationsrechten bei einer kumulativen Dissertation sind in der Anlage aufgeführt.

Name Promovend	Datum	Ort	Unterschrift
Ronny Tepper		Jena	

Ich bin mit der Abfassung der Dissertation als publikationsbasiert, d.h. kumulativ, einverstanden und bestätige die vorstehenden Angaben. Eine entsprechend begründete Befürwortung mit Angabe des wissenschaftlichen Anteils des Doktoranden/der Doktorandin an den verwendeten Publikationen werde ich parallel an den Rat der Fakultät der Chemisch-Geowissenschaftlichen Fakultät richten.

Name Erstbetreuer(in)	Datum	Ort	Unterschrift
Prof. Dr. Ulrich S. Schubert		Jena	

1 Introduction

The field of anion complexation, from its beginnings in the late 1960s and 1970s,[1-3] has developed very dynamically from a field of solely academic interest to one of the most important research areas in supramolecular chemistry. Over the last 10 years, the reversible binding of an anion to a receptor was used as dynamic and switchable process in a wide variety of applications (**Figure 1.1**).[4-7] One of the most active areas is the selective recognition of anions indicated by a measurable response (*e.g.*, optical or electrochemical),[6, 8-9] which is particularly useful for the detection and extraction of environmentally deleterious anions (*e.g.*, phosphate, nitrate).[10] Due to a wide range of accessible geometries and sizes, anions can be seen as important information carriers at the molecular level and, thus, are predestined for applications in template-based syntheses to self-assembly molecular structures (*e.g.*, macrocycles, helicates, interlocked structures and polymers).[11-13] If multiple binding pockets with different anion affinities are incorporated within one molecule, these structures are able to perform controlled molecular motions,[14] which is a very current topic awarded with the Noble prize for Chemistry in 2016.[15] Although the selective molecular recognition is also of central importance in the field of organo-catalysis, the role of anion complexation is often overlooked in this area.[16] Nevertheless, small-molecule organo-catalysts based on, in particular, hydrogen bond (HB) interactions often convince due to their rapid synthetic access, the possibility of introducing chiral information, the increased tolerance against water and oxygen as well as an improved environmental sustainability compared to metal-catalyzed processes.[17-18] In addition, the selective recognition of relevant anions *in vivo* and their directed transport, for example across lipid bilayers, is of immense importance in the biological field as well.[19-22] Thus, the selective recognition in water remains a key challenge as proposed applications in biological and medical fields typically require aqueous conditions to be realized.[23-24]

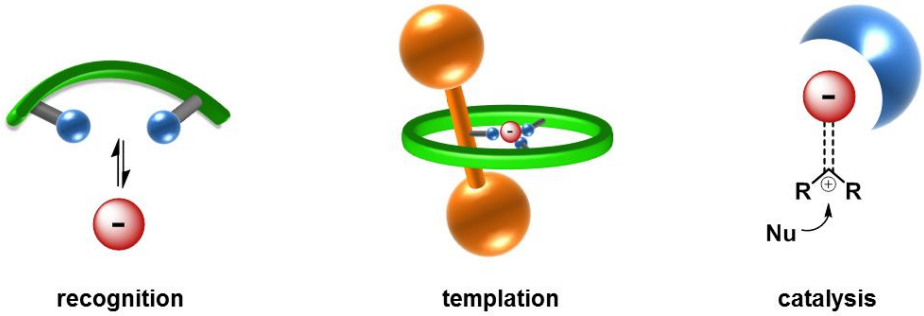

Figure 1.1: Schematic representation of different application fields of anion complexation (blue indicating active anion binding sites).

In contrast to cation receptors, the design of strong and selective anion receptors is often more challenging due to certain intrinsic challenges of negatively charged species, namely, the higher solvation energy hampering the recognition in polar / protic solvents, the diffuse charge distribution (smaller charge-to-size ratio) influencing the effectiveness of electrostatic interactions as well as the pH sensitivity and the wide range of possible geometries.[6, 24-25] While selective binding of anions could nonetheless already be achieved by the well-known HB and several other supramolecular interactions (*e.g.*, ion−ion, anion−π, and electrostatic interactions),[8] the familiar halogen bond (XB), where a covalently bound and strongly polarized halogen atom is able to act as the electrophilic species,[26] represents a fascinating but long-time overlooked interaction within this toolbox.

Thus, the goal of this thesis is to develop new XB-based anion receptors and to compare them with their related HB systems to gain a profound knowledge concerning the different binding behaviors in solution. To understand the nature as well as characteristics of the fairly uncommon XBs, a detailed description will be given in **Section 2.1**. Since this kind of interaction strongly depends on the electron-withdrawing moiety polarizing the covalently bound halogen,[27-28] a variety of different neutral and charged organic groups (*e.g.*, polyfluorinated alkenes and arenes as well as cationic halogenated imidazolium systems) evolved.[29-33] However, this work will concentrate on, up to now, less common 1,2,3-triazole derivatives as electron-withdrawing group. The heterocycle not only convince with a facile synthetic access to functionalized HB / XB donors and a wide range of possibilities of supramolecular interactions (*e.g.*, anion complexation *via* HB / XB as well as *C*- or *N*-coordination of metals) but also with a reasonable electron-withdrawing character to polarize the corresponding donor atom (see **Section 2.2**).[34-35] The modular synthetic character further enables a rapid

variation of the receptor structure as well as a straightforward incorporation into more complex and functionalized systems. In this regard, **Section 3** deals with the improvement of anion binding affinities of 1,2,3-triazole based receptors by either integration of this building block in a highly preorganized and multidentate architecture (see **Section 3.1**)[36] or a concurrent recognition of both cation and anion species in a heteroditopic ion-pair receptor system (see **Section 3.2**).[37] In both cases, the 1,2,3-triazole moiety proved very beneficial due to the Lewis-basic nitrogen atoms that enable the introduction of additional supramolecular interactions. These design concepts would not have been possible with the more common electron-withdrawing groups like polyfluorinated alkenes / arenes or imidazolium derivatives and enabled strongly boosted anion affinities. On the other hand, for the purpose of application, the combination of XBs with polymeric architectures is of increasing interest. In particular, the combination of the high directionality and potential tuneability of the interaction strength renders the XB to an interesting tool for the organization of macromolecular building blocks as well as the design of polymeric self-assembled components.[38-39] In this context, **Section 4** deals with the embedding of anion receptors into a polymer backbone and the analysis if this polymeric donor concerning binding behavior in solution as well as the evaluation of material properties in films.

2 Theoretical background

Parts of this chapter have been published in **P1)** R. Tepper, U. S. Schubert, "Halogen bonding in solution: Anion recognition, templated self-assembly, and organo-catalysis", *Angew. Chem. Int. Ed.* DOI: 10.1002/anie.201707986; *Angew. Chem.* DOI: 10.1002/ange.201707986.

2.1 The halogen bond

The development of the XB interaction starts already two centuries ago, when Colin probably prepared the first complex based on XB interactions, namely the adduct between elemental iodine and ammonia.[40] The exact stoichiometry of this complex was established 50 years later by Guthrie.[41] However, only in the mid-1950s, pioneer discoveries from Mulliken (on charge-transfer interactions)[42] and Hassel (on the crystallographic description of various halogen-bonding adducts, awarded with a Nobel prize in 1969)[43] allowed an advanced understanding of the underlying interactions. Subsequently, it was largely forgotten and only from 1998 onwards, a series of seminal papers by Resnati, Metrangolo and co-workers established the XB interaction as a reliable tool for crystal engineering,[44-45] which dominated the area for a long time. In the last decade, the utility of XBs for anion coordination and supramolecular chemistry in general became increasingly apparent and, thus, also the number of publications on XB interactions has grown rapidly (**Figure 2.1 A**). The current research still has its main focus on the theoretic[46-47] and crystallographic[48-53] characterization of XBs and their application in the design of functional supramolecular materials (**Figure 2.1 B**).[38-39, 54-55] Nevertheless, beside some topical interesting studies of XBs in biological systems,[19, 56-59] there is, in particular in the last five years, an enormous interest in the exploration of XB-based molecular recognition events in solution (**Figure 2.1 A**).[60-65] In this regard, the current research focuses on the use of XB receptors in anion recognition and sensing processes,[65] the XB-templated self-assembly of interlocked structures[61] as well as the XB-mediated organo-catalysis (**Figure 2.1 B**).[62, 66]

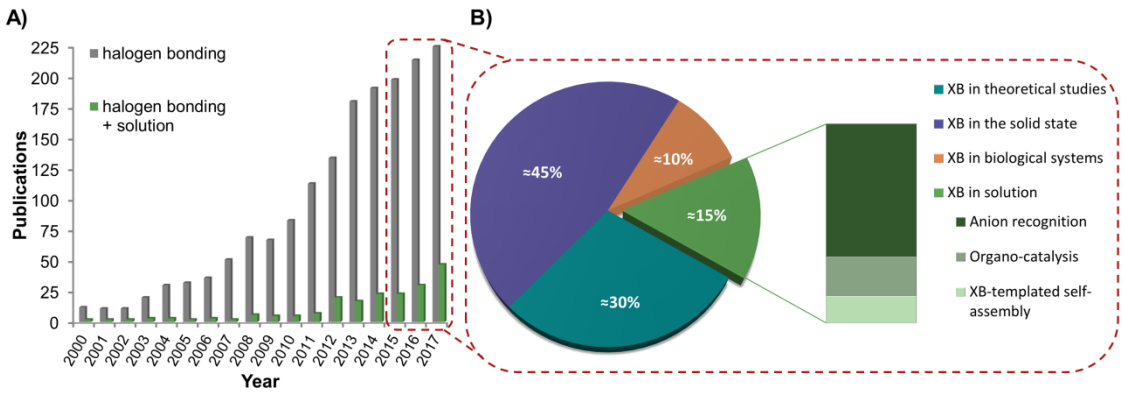

Figure 2.1: A) Number of publications per year including the keyword "halogen bonding" in the title (grey) and the additional keyword "solution" in the topic (green) (source: Thomson Reuters Web of Science, search performed in 12.03.2018). B) Distribution of publications dealing with XBs in different fields of supramolecular chemistry in the last approximately three years (numbers based on comprehensive literature research, which was in accordance (±5%) with search on Thomson Reuters Web of Science regarding publications from 2015 to 2017 including the keyword "halogen bonding" in the title and topic-specific additional keywords *e.g.* "theory", "crystal", "solution", "biological" in the topic, search performed in 01.06.2017).

The IUPAC has provisionally defined the XB interaction in 2013 by: "A halogen bond occurs when there is evidence of a net attractive interaction between an electrophilic region associated with a halogen atom in a molecular entity and a nucleophilic region in another, or the same, molecular entity."[26]

In general, the XB is a highly directional supramolecular interaction in which a covalently bound halogen in compounds of the general form R–X (X = I, Br, Cl, F) is polarized by an electron-withdrawing group R, and, thus, is able to act as the electrophilic species / XB donor in the presence of a neutral or anionic Lewis base (LB) / XB acceptor.[26, 67] The terms XB donor and XB acceptor are somewhat confusing. The Lewis acid halogen (*i.e.*, the electron acceptor) is typically referred to as the XB donor, which "donates" the bond to the XB acceptor, namely the Lewis base (*i.e.*, the electron donator). Accordingly, the polarizability of X (I > Br > Cl > F) as well as the electron-withdrawing group R, which could be either inorganic (*e.g.*, other halogens) or organic (*e.g.*, carbon, nitrogen), represent the most important key factors to tune the strength of the XB interaction.

2.1.1 Nature of halogen bonds

At first appearance, an attractive interaction between a Lewis base and an – at least to Lewis formula – likewise electron-rich halogen substituent X seems hardly plausible. Nevertheless, in fact there are even several different attractive components of the interaction energy, which are described in more detail in the following part.

Electrostatic interactions

A key feature for the interaction is the anisotropic electron density distribution around the interacting halogen atom X, which is the result of the halogen atom being covalently bound to an electron-withdrawing group R. The resulting region of positive electrostatic potential (see red regions in **Figure 2.2 B**) enables the interaction with an electron-rich binding partner and is called the σ-hole.[68]

To discuss the concept of the σ-hole in more detail, the electronic nature of the R–X bond needs to be analyzed at first. Halogen atoms larger than fluorine show only a weak sp-hybridization resulting in an approximate $s^2p_x^2p_y^2p_z^1$ configuration, where the z-axis is along the R–X bond. Due to the unshared pairs of electrons, a belt of negative electrostatic potential is formed around X perpendicular to the R–X bond (see blue regions in **Figure 2.2 B**). Upon bond formation with R, electron density of X is displaced toward R (**Figure 2.2 A**), which cannot be compensated by the electron density of the underlying s orbital and, thus, resulted in a local electron deficit (σ-hole) on the reverse side of the R–X bond. The size of the σ-hole and, consequently, the strength of the XB increases with the polarizability of X (I > Br > Cl > F) (**Figure 2.2 B**) as well as with increasing electronegativity of R. Moreover, in order to minimize electronic repulsion with the electron-rich belt surrounding the σ-hole, the XB features a strong preference for a bond angle (R–X···LB) close to 180°.[69]

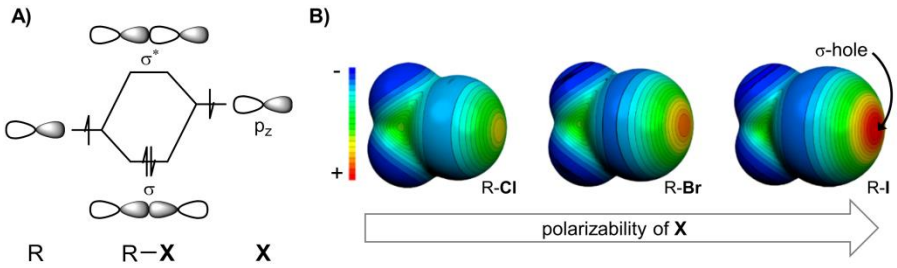

Figure 2.2: A) Simplified molecular-orbital diagram of R–X bond to illustrate the σ-hole. B) Calculated molecular electrostatic potential surfaces (from ref. [68]) for R–X ($R = CF_3$) visualizing the formation and size dependence of the σ-hole as function of halogen heaviness.

While IUPAC suggested that "the forces involved in the formation of the halogen bond are primarily electrostatic",[26] various recent computational and experimental studies have demonstrated that a purely electrostatic model cannot explain all observed trends. Thus, additional contributions from charge transfer and dispersion components have to be considered.[70-72] Nevertheless, the exact magnitude / importance of each contribution is controversially discussed and strongly depends on the studied system.[71, 73-75]

Charge transfer interactions

The XB can further be interpreted as the interaction of the antibonding orbital of the R–X covalent bond with electron donors and in terms of electron transfer between the HOMO of the Lewis base and the LUMO mainly localized on the halogen X (**Figure 2.3 A**).

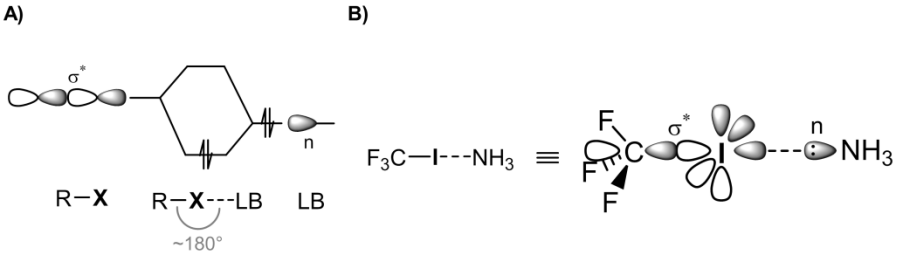

Figure 2.3: A) Simplified molecular-orbital diagram of intermolecular complex R–X···LB resulting from HOMO / LUMO mixing (HOMO of LB with LUMO of R–X). B) Example of XB-based complex and corresponding schematic representation of n(LB) → σ*(R–X) charge transfer.

Thereby, the accepting orbital is the σ*-orbital of the R–X bond, *i.e.* the halogen bond R–X···LB is a n(LB) → σ*(R–X) hyperconjugation stabilizing the lone pair (n) of the LB (**Figure 2.3 B**). The dimension of stabilization depends on the energetic difference between the interacting orbitals as well as on the orbital overlap, *i.e.* the orbital coefficients. Accordingly, also the charge transfer contribution benefits from a strong electron-withdrawing behavior of R, which causes an energetic lowering and, thus, a stronger localization of the σ*(R–X) orbital on the halogen substituent X. In order to maximize the overlap with the σ*(R–X) orbital, a linear geometry of the XB is required, which provides an alternative explanation for the strict linearity of the interaction (**Figure 2.3 A**).[71] Notably, due to the population of a σ* orbital, the R–X bond is weakened and slightly extended upon complex formation (R–X···LB).[72] In contrast, an up to 20% shortening of the interatomic distance of the participating atoms (X···LB) below the sum of their van der Waals radii ($\sum r_w$) is observable.[76]

Dispersion force

While the electrostatic as well as charge transfer contributions are very important to correctly describe XB-based systems, also polarization and dispersion contributions cannot be neglected since two atoms with high polarizability (X and the LB) are arranged closer than the $\sum r_w$. In general, the dispersion force describes the weak interaction arising from a spontaneous polarization in molecules and the resulting induced dipoles that can attract each other. Its strength strongly depends on the intermolecular distance r ($E \sim r^{-6}$) and on the polarizability of the molecules. This component of XBs is often ignored because of its supposedly small contribution compared to the electrostatic interactions. However, theoretical studies have shown that in particular for larger halogen atoms with a high polarizability this interaction cannot be neglected.[75]

Charge assistance

If R–X and the LB are charged species, the XB is accompanied by Coulombic interactions, which essentially contribute to the anion binding event. The isotropic strength of the interaction is proportional to $E \sim r^{-1}$ as well as $E \sim n_1 \cdot q_1 \cdot n_2 \cdot q_2$, which makes it important even at larger distances r between XB donor and acceptor and receives even more importance for systems carrying multiple charges.

2.1.2 Comparison between halogen and hydrogen bonds

There are some obvious parallels between HBs (R–H···LB) and XBs (R–X···LB). Both are attractive interactions between covalently-bonded electron-poor species (H or X) acting as Lewis acids, and electron-rich Lewis bases (LBs). In both systems, the bond donor (H or X) is polarized by an electron-withdrawing group R and the interaction becomes stronger, the more electron-withdrawing this group R.

However, the potential of XBs arise more from its characteristic differences, than from the similarities to HBs. In the following, the five most important differences will be discussed in detail.

Directionality. While HBs allow a high variance of the R–H···LB angle, the R–X···LB angle of XBs is always close to 180°.[77-78] This can be explained by the strong anisotropy of the electron density at the halogen X (**Figure 2.2**) that would lead to a repulsion of the LB with the unshared pairs of electrons of the halogen at smaller

angles. In contrast, the positive region of HB donors is not that narrowly confined but rather distributed over the whole surface of the hydrogen atom. This high directionality of XBs offers great opportunities for the construction of structurally defined supramolecular assemblies.

Moreover, in the case of a combined interaction of HBs and XBs with a common LB, a preferred orthogonality of both interactions is observable. As a result, the design of a multivalent receptor with orthogonal XB and HB moieties can lead to an increased specificity towards the guest molecule.[69, 79-80]

Tuneability. While the strength of HBs is mainly influenced by the electron-withdrawing ability of R,[5, 7] the XB interaction additionally strengthens with the polarizability of X (I > Br > Cl > F)[27-28, 81] (**Figure 2.2**) and, thus, can be tuned through a single-atom mutation. Due to the high electronegativity of fluorine it can only act as a XB donor when attached to particularly strong electron-withdrawing groups (*e.g.*, F_2, $(CF_3SO_2)_2NF$, $C(NO_2)_3F$).[82-84] There are only few cases of fluorine-based XB donors, which in general attracted little attention up to now.

Size of donor atom. Another difference between XB and HB is the larger steric demand of halogen atoms (van der Waals radii (r_w) $r_w(I) = 1.98$ Å and $r_w(Br) = 1.85$ Å) compared to the small hydrogen atom ($r_w(H) = 1.20$ Å).[85] The steric demand of the XB donors may on the one hand pose some limitations, *e.g.* for applications of XBs in biological systems, where the large iodine could cause difficulties fitting into the small sized binding pockets of the LB (*e.g.* artificial proteins or nucleotides) with the appropriate orientation.[86-87] On the other hand, the large size of the iodine atom can also be used beneficial to create special architectures like *anti* and *syn* conformers of cyclic structures.[88]

Next to the differences regarding the steric demand of the donor atoms, also their polarizability strongly differs. HBs are based on a small, less polarizable and, thus, very "hard" hydrogen atom, while in particular iodine (as the most common XB donor) represent a very "soft" Lewis acid. Consequently, due to the variations in orbital size and softness of the donor atoms, different classes of LBs (hard *vs.* soft) were preferred.[89]

Hydrophobicity. Numerous HB donors feature polar moieties, such as NH or OH groups, which cause HBs to be a hydrophilic interaction. In contrast, halogenated organic fragments, in particular polyfluorinated residues of XB donors, are often apolar and increase the lipophilicity / hydrophobicity of a molecule.[90] Thus, the use of less competing / low-polarity solvents (*e.g.*, cyclohexane) for subsequent applications could be enabled. Moreover, the hydrophobic character of XBs can be a pivotal aspect in particular for drug design, since many parameters (*e.g.* absorption, transport into organs and cells, interaction with target molecules) are at least partly controlled by the lipophilicity of the drug.[19]

Solvent dependency. The competition between anion and solvent always plays a crucial role if interactions are considered in solution. In this case, the polarity as well as the donor / acceptor ability (donor numbers by Gutmann)[91] of the solvent must be taken into account. Thereby, the stabilities of the XB-based complexes proofed to be remarkably more insensitive to solvents leading to the ability to outperform HB-based analogues in competitive solvents.[92-93] These results suggest that, in contrast to HBs, where electrostatics regulate thermodynamic stability, charge transfer interactions make a major contribution to the stability of XB-based complexes. In particular, the improved water resistance[94] of organic XBs compared the HB-based systems is beneficial for biological and medical applications, which typically require aqueous conditions.[23]

2.2 Influence of the electron-withdrawing group

2.2.1 General aspects

As mentioned above, next to the polarizability of X (I > Br > Cl > F), the electron-withdrawing ability of R is a key factor to tune the XB interaction strength. In general, depending on the group R, the XB donor can be either inorganic (halogens like I_2, Br_2 or inter-halogens like ICl, IBr) or organic. Although neutral inorganic XB donors are usually stronger compared to neutral organic donors,[60] the organic systems convince by the modifiability of R. Thus, they offer the possibility to apply a combination of strategies like charge-assistance, multidentate binding motifs, preorganization as well as cooperativity effects during the receptor design in order to create highly sophisticated host systems.[27-28] As a consequence, a variety of different neutral and charged organic groups R evolved (**Figure 2.4**).

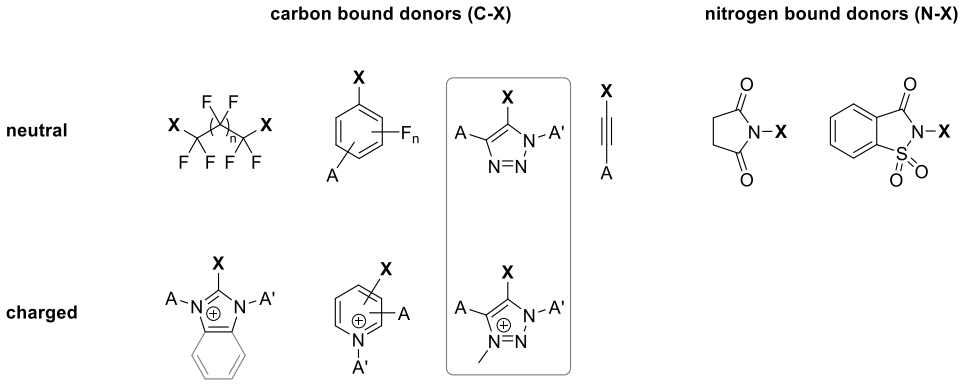

Figure 2.4: Schematic representation of an overview of most common studied electron-withdrawing groups R, generally divided into neutral and charged moieties as well as carbon and nitrogen bound donors with different substituents (A, A'). [29, 95-102]

Neutral. In comparison to charged XB donor systems, in which the binding efficiency strongly benefits from charge-assistance, the interaction strength of neutral XB donors depends much stronger on the electronic properties of the organic backbone. As most of the studies focus on XB donors where the halogen is bound to a carbon atom (C–X) (**Figure 2.4**), particularly the *sp*-hybridization at this *ipso*-carbon represents an important key factor to tune the XB strength. It was revealed that the greater the degree of s character in a *sp*-hybridized carbon (C(sp)–X > C(sp^2)–X > C(sp^3)–X), the greater its electron-withdrawing ability and, thus, the stronger the formed XB.[68]

Charged. Cationic XB donors generally consists of five- or six-membered nitrogen heterocycles as electron-withdrawing groups (R), in which one of the nitrogen atoms is quaternized to create a charge and to strongly polarize the covalently bound halogen.[27-28] While these systems usually achieve very high anion affinities due to the charge-assistance, their interaction with anionic species is less directional compared to neutral XB donors because of the isotropic nature of the additional Coulomb attraction. In addition, highly competitive solvents are usually required to dissolve the charged receptors and / or to prevent precipitation of the formed complex, which lowers their effective binding strength.[99] The charge not only boosts the binding affinity, it also modifies the entropy (TΔS)-enthalpy (ΔH) distribution of these receptors compared to analogous neutral ones. While the binding of anions by cationic receptors is more entropically driven by the release of polar-bound solvent molecules during the binding event,[98] neutral receptors benefit from negative enthalpy changes and normally suffer from an unfavorable entropic penalty (aside from some exceptions, *vide infra*).[36, 97]

2.2.2 The triazole unit as electron-withdrawing group

To date, neutral systems based on polyfluorinated alkenes and arenes as well as cationic halogenated imidazolium derivatives are the most frequently studied electron-withdrawing groups R.[29-31, 102-104] Nevertheless, not least in view of the efficient synthesis by the copper(I)-catalyzed azide–alkyne cycloaddition (CuAAC) reaction, also triazole and triazolium moieties have attracted recent growing interest as valuable electron-withdrawing groups.[14, 105-107] Moreover, the associated modular character of the synthesis offered the possibility of a simple linkage to numerous functional units (A and A'), which enabled various applications in supramolecular chemistry (*vide infra*).[34] The following paragraph is dedicated to some fundamental properties of 1,2,3-triazoles to allow a better understanding of the various advantageous offered by this building block.

Synthesis. A particular advantage of the 1,2,3-triazole moieties is their facile synthesis *via* CuAAC reaction,[34-35, 108-110] which is wide in scope, modular, regioselective, and highly efficient and, thus represents the prime example for the concept of "click chemistry".[111] The catalytically active copper(I) species of this 1,3-dipolar cycloaddition reaction can be introduced either directly as a copper(I)-salt or through *in situ* reduction of a copper(II)-salt.[112] Through the activation of the alkyne as well as the azide by σ- and π-coordinated metal centers,[113-115] two C–N bonds are regioselectively formed resulting in a copper(I) triazolide, which is protonated to obtain the 1,4-disubstituted heterocycle (**Scheme 2.1 A step I**).[112, 116] By the use of additional bridging ligands, *e.g.*, tris[(1-benzyl-1H-1,2,3-triazol-4-yl)methyl]amine (TBTA), the copper(I) species can be stabilized by protection from oxidation and disproportionation while simultaneously enhancing its catalytic activity.[117]

In order to enable the use of the triazole fragment also in the context of XB interactions, the hydrogen atom in the 5-position of the heterocycle had to be exchanged against a halogen atom X. For this purpose, the acidic 5-position ($pK_a = 27$[118]) can be deprotonated using strong organometallic bases (*e.g.*, *n*-Butyllithium (*n*-BuLi)) and subsequently subjected to an electrophile X^+ (**Scheme 2.1 A step I'**).[99] Alternatively, 5-halo-1,2,3-triazoles can be obtained by direct copper(I)-catalyzed cycloaddition between organic azides and halo-alkynes (named CuAXAC[34] or CuAHAC[119]) (**Scheme 2.1 A step II**)[116, 120] or by trapping the intermediately formed copper(I)

triazolide with a corresponding electrophile X^+, which can be added directly (*e.g.*, *N*-chlorosuccinimide[121]) or generated *in situ via* oxidation of a halide (*e.g.*, by using NaI–$Cu(ClO_4)_2$[122] or CuI–*N*-bromosuccinimide[123]) (**Scheme 2.1 A step III**).

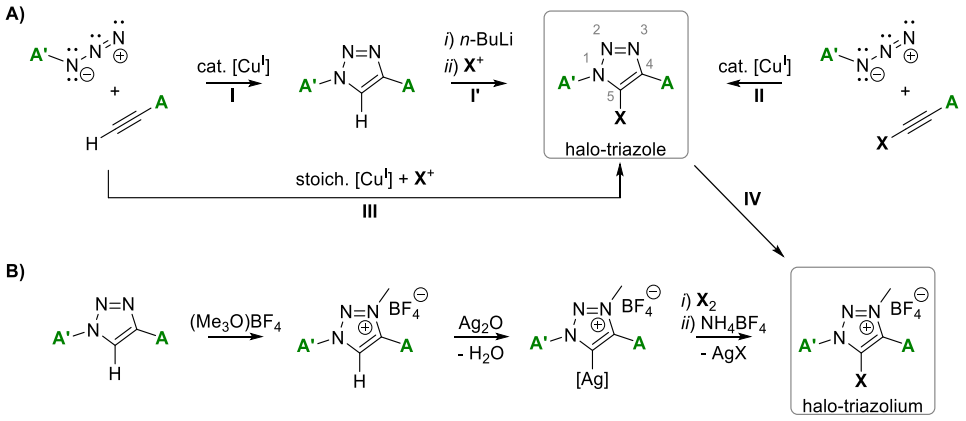

Scheme 2.1: A) Schematic representation of different synthetic pathways to obtain the 5-halo-1,2,3-triazole and B) the analogous 5-halo-1,2,3-triazolium salt (green substituents A and A' demonstrating modular synthetic character).

The analogous 5-halo-1,2,3-triazolium salts can be obtained by methylation of the corresponding halo-triazoles using alkylating reagents like trimethyloxonium tetrafluoroborate or methyl triflate (**Scheme 2.1 A step IV**).[124-125] Alternatively, a stable silver(I)-1,2,3-triazolylidene precursor is readily achieved from the triazolium salt with Ag_2O under mild reaction conditions. Afterwards, this precursor can be treated with different elemental halogens X_2 giving rise to the precipitation of the corresponding silver(I)-halide and the trapping of the nucleophilic carbene by the resulting halonium ion X^+ to yield the halo-triazolium salt (**Scheme 2.1 B**).[99]

Electron-withdrawing character. The triazole unit not only convince by a very efficient and modular synthesis but also by the truly wide range of supramolecular interactions offered by the formed heterocycle. In general, the presence of three electronegative nitrogen atoms in the five-membered ring generate a dipole moment of 4.3 D[126] aligned almost parallel to the C–H bond and further cause a highly polarized C–H / C–X bond **Figure 2.5 C, left**)[99] allowing the complexation of a LB by HB / XB interactions. On the other hand, the two basic nitrogen atoms simultaneously enable the coordination of different metal centers (M^+) as well as the possibility to act as HB / XB acceptor **Figure 2.5 A**).[34]

The facile conversion into the corresponding 1,2,3-triazolium salt **Figure 2.5 B**) enables an enhanced C–H / C–X bond polarization **Figure 2.5 C, right**) and, thus, strong HB / XB interactions accompanied by Coulomb interactions with anions. Moreover, the simple transformation from a neutral to a charged group R without substantial structural changes guarantees a good comparability between the systems.

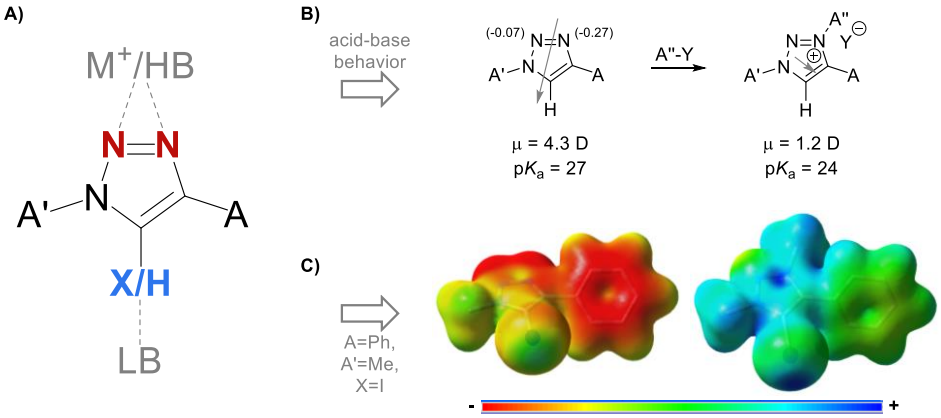

Figure 2.5: A) Schematic representation of the wide range of supramolecular interactions offered by 1,2,3-triazole employing Lewis-basic nitrogen atoms (red) or Lewis-acidic XB / HB donor atom (blue). B) Acid–base parameters of 1,2,3-triazole and corresponding 1,2,3-triazolium system (dipole moments indicated as grey arrows,[126] pK_a values taken from ref. [118, 127], nitrogen natural bond orbital (NBO) charge in brackets[128]). C) Calculated molecular electrostatic potential surfaces for iodo-1,2,3-triazole (left) and iodo-1,2,3-triazolium (right) model systems mapped on total density (isovalue 0.01).[99]

Consequently, all these aspects rendered the 1,2,3-triazole unit a frequently used functional building block in supramolecular chemistry and, in particular, also a very interesting moiety for the XB-based complexation of anions. Especially in recent years, halogenated 1,2,3-traizole derivatives have been established in different areas like templated synthesis of interlocked structures,[129-131] selective anion recognition[132-133] or redox-active sensor units.[107, 134] The field of organo-catalysis using this building block has also been developed [125] and current studies of chiral triazole-based receptors represent the first example of enantio-discrimination achieved by XB interactions.[106, 135-136]

3 Tuning the binding strength of triazole-based donors in solution

Parts of this chapter have been published in P2) R. Tepper, B. Schulze, H. Görls, P. Bellstedt, M. Jäger, U. S. Schubert, *Org. Lett.* **2015**, *17*, 5740-5743; P3) R. Tepper, B. Schulze, P. Bellstedt, J. Heidler, H. Görls, M. Jäger, U. S. Schubert, *Chem. Commun.* **2017**, *53*, 2260-2263.

The quest to improve the binding strength of neutral XB donors to combine the benefits of these systems (see **Section 2.2.2**) with sufficiently strong XB interactions has stimulated considerable research efforts.[29, 135, 137-140] In particular the increased solubility in less competitive solvents, the absence of counterions as well as the more directional binding to anionic guests of neutral XB donors might be advantageous when designing strong and selective receptors, *e.g.*, for application in organo-catalysis.[62, 141-142] One of the most promising approaches is the chelation through incorporation of multiple XB donor groups into an appropriate orientation using a preorganized scaffold. Although the synthesis of efficient multidentate and simultaneously preorganized donor systems is rather challenging due to the strict linearity of the XB interaction as well as the large size of the donor atom (mostly iodine), it also offers the opportunity to create more rigid and ordered structures with higher binding affinities and an improved guest selectivity compared to monodentate receptor systems. Some recent examples utilizing the 1,2,3-triazole motif illustrate how high-affinity anion recognition can be achieved using this concept (**Figure 3.1**).

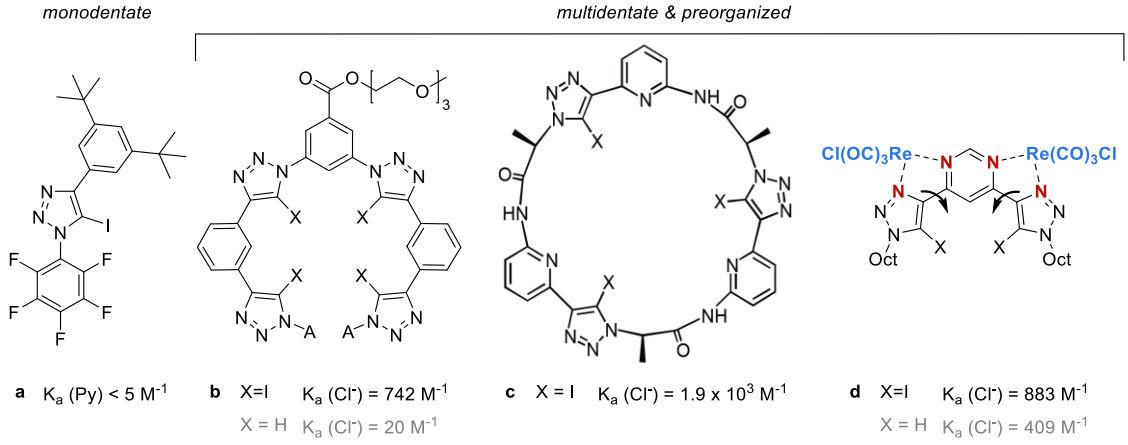

Figure 3.1: Schematic representation of exemplary receptors based on either monodentate or multidentate and preorganized XB donors. K_a values obtained by **a**: ^{1}H NMR titration in toluol-d_8 at 293 K (Py = Pyridine derivative), **b**: ^{1}H NMR titration in $CDCl_3$ at 298 K, **c**: ^{1}H NMR titration in 2.5% H_2O in DMSO-d_6 at 298 K, **d**: ^{1}H NMR titration in $CDCl_3$:CD_3OD 1:1 at 298 K.[135, 137-138, 140]

In this context, 5-halo-1,2,3-triazoles have been established as versatile, charge-neutral building blocks for XB donors due to their good accessibility *via* modular CuAAC reactions as well as their sufficient electron-withdrawing character (see **Section 2.2.2**). Moreover, the intrinsic heteroditopic character of the triazole moiety *i.e.*, the Lewis-acidic donor atom (H or X) combined with the Lewis-basic nitrogen atoms **Figure 2.5 A**), enables different ways to tune the binding strength of triazole-based XB donors. In the following parts, the concept of preorganization *via* intramolecular HBs[36] as well as the simultaneous cation-anion binding in a cooperative ion-pair receptor will be described in detail.[37]

3.1 Preorganization *via* intramolecular hydrogen bonds

The excellent XB donor ability as well as HB acceptor function of iodo-1,2,3-triazoles was applied for the first time to preorganize a cleft-type XB-based receptor system *via* intramolecular HBs. Carbazole was chosen as a rigid spacer motif between two iodo-triazoles, which simultaneously act as the XB donors as well as HB acceptors (**Figure 3.2**). In contrast to the phenyl-based receptor **1**, which was intensively studied during the diploma thesis,[99] the larger distance between the two iodine atoms in the carbazole-based receptor **2** was anticipated to enable an improved coplanarisation of the system during guest complexation, which is important for the efficient formation of intramolecular HBs in **3**.[143-144]

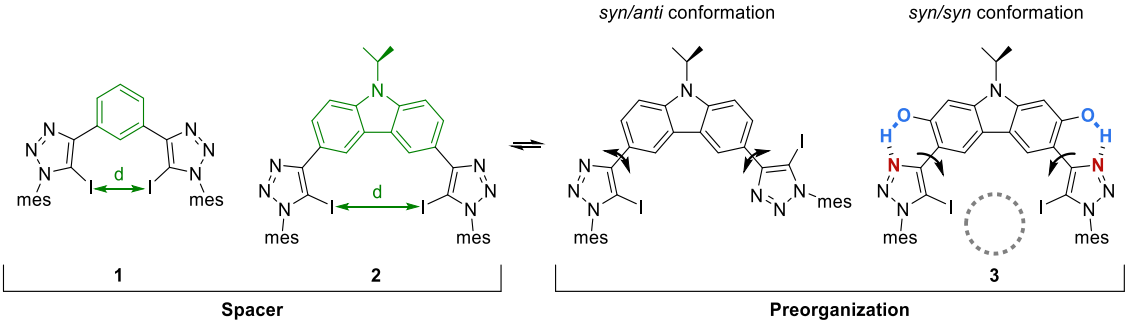

Figure 3.2: Schematic representation of studied receptors. Left): Influence of spacer unit 1,3-benzene (**1**) or 3,6-carbazole (**2**) on distance (d) between two donor moieties. Right): Preorganization *via* intramolecular HBs (**3**) and labeled conformation of the XB, guest indicated as grey dashed sphere. (Adapted with permission from ref. [36]. Copyright 2015 American Chemical Society)

The non-preorganized carbazole-based receptor **2** was prepared *via* CuAXAC reaction (see **Section 2.2.2**) directly from the corresponding iodo-alkyne (**5**) and mesityl azide in moderate yields (**Scheme 3.1**). In case of the preorganized system **3**, the 2,7-dimethoxy-carbazole core (**6**) was synthesized in a seven step synthesis. The terminal alkynes were afterwards converted into the corresponding 1,2,3-triazole moieties (**7**) by CuAAC reactions and the iodination was achieved by metalation using *n*-BuLi and subsequent treatment with iodine to obtain the methoxy-decorated precursor (**8**). The final receptor **3** was obtained in excellent yields by BBr_3-induced ether cleavage.

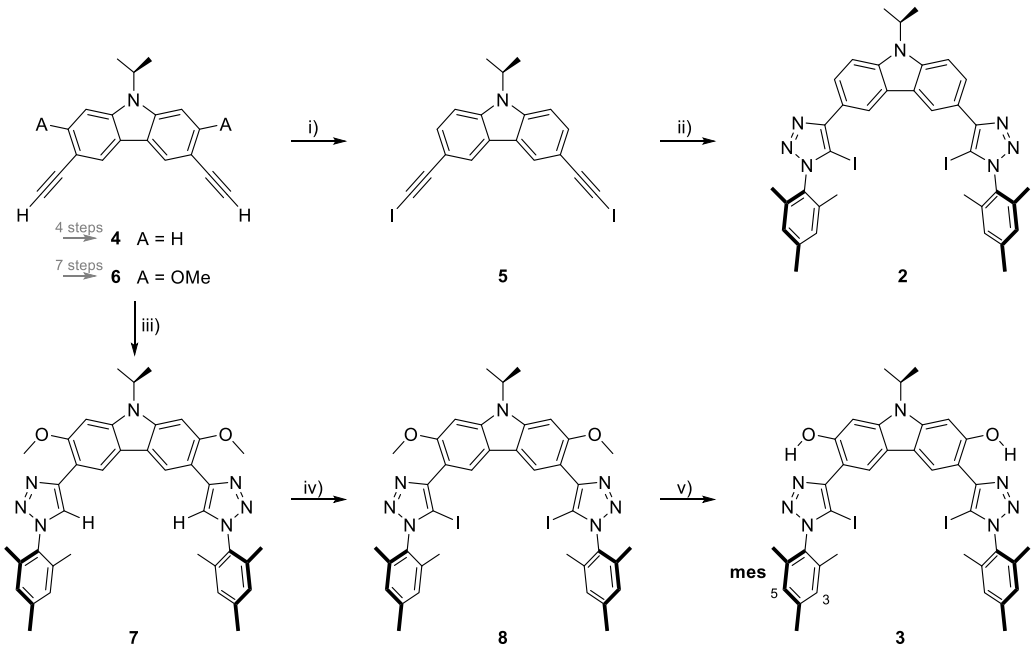

Scheme 3.1: Schematic representation of the synthesis of the non-preorganized (**2**) and preorganized (**3**) receptor: i) *N*-iodosuccinimide / $AgNO_3$, Acetone, room temperature (rt), 38%; ii) mes-N_3, CuI / TBTA, THF, rt, 53%; iii) mes-N_3, $CuSO_4$ / NaAsc., EtOH / H_2O / CH_2Cl_2 (2:1:1), 50 °C, 86%; iv) *n*-BuLi, THF, I_2 at −78 °C, then −78 °C to rt, 40%; v) BBr_3, CH_2Cl_2, −78 °C to rt, 98%. (Adapted with permission from ref. [36]. Copyright 2015 American Chemical Society)

The successful formation of the desired intramolecular HBs in solution was revealed by selective ROESY studies as well as by a clear downfield shift of the O*H* signal in the ^{1}H NMR spectrum recorded in unpolar solvents (toluol-d_8 and THF-d_8) compared to the polar and strongly competitive DMSO-d_6 (**Figure 3.3**). Moreover, the downfield shift of the aromatic proton **C** further indicates the desired preorganized form since this *syn / syn* conformation causes an adjacency of the Lewis-basic belt surrounding the XB donor atoms and this aromatic proton **C**.

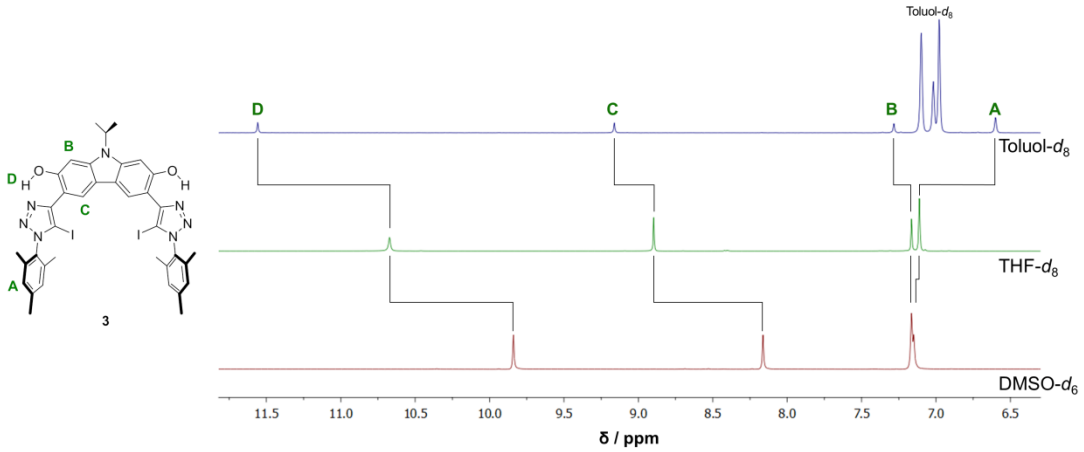

Figure 3.3: ^{1}H NMR of **3** in solvents with different polarity illustrating characteristic shifts of aromatic protons A to D.

Single crystals of free receptors (**Figure 3.4**) as well as receptors interacting with chloride (**Figure 3.5**) were grown by slow vapor diffusion of *n*-pentane into a concentrated receptor solution. Obviously, the conformational freedom of **2** allows a *anti* / *anti* conformation of the XB donors in the free receptor. In contrast, the formed intramolecular HBs in **3** limit the rotational freedom of the preorganized receptor, and thus, the essential *syn* / *syn* conformation for a bidentate complexation is already preformed.

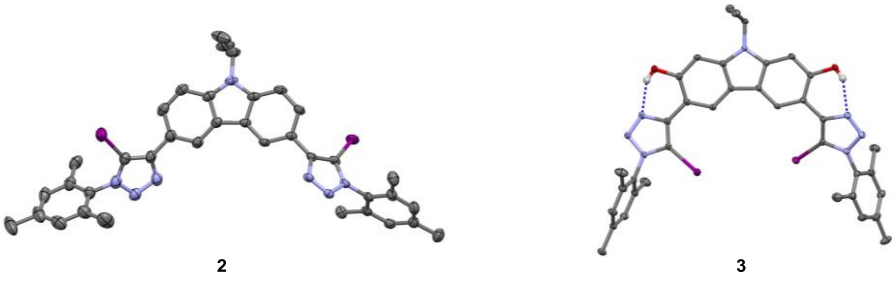

Figure 3.4: Solid-state structure of **2** in *anti / anti* conformation and **3** in *syn / syn* conformation (thermal ellipsoids at 50% probability level, hydrogen atoms and solvent molecules are omitted for clarity; key HBs to the triazole moieties are shown as dashed lines; grey: carbon, blue: nitrogen, purple: iodine, and red: oxygen). (Reprinted with permission from ref. [36]. Copyright 2015 American Chemical Society)

Furthermore, all three receptors **1** to **3** revealed the expected cleft-type complexation of the anionic guest through the formation of two nearly linear XBs (**Figure 3.5** for **1** and **2**, **Figure 3.7** for **3**), which are all significantly shorter (up to 17%) than the $\sum r_w(I\cdots Cl) = 3.73$ Å.[85] Comparing the 1:1 complexes of **1** and **2** with chloride (**Figure 3.5**), the larger distance (d) between the two iodine atoms in the carbazole-based system

(d = 4.68 Å compared to d = 3.87 Å) enables the expected improved coplanarization (dihedral angle of 13° compared to 31°). As a consequence, an increased linearity of the XBs (*C–I···Cl*⁻ XB angle of 180° compared to 170°) is enabled, which finally causes a decreased I···Cl distance (*I···Cl* XB length of 3.11 Å compared to 3.22 Å).

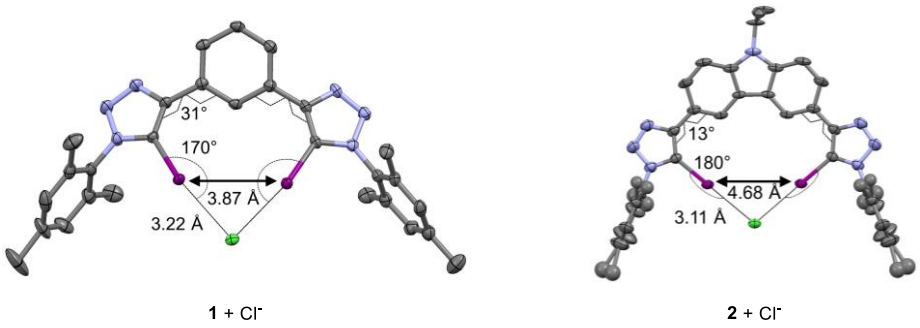

Figure 3.5: Solid-state structure of **1** and **2** interacting with chloride (thermal ellipsoids at 50% probability level, hydrogen atoms, counter ions, and solvent molecules are omitted for clarity; grey: carbon, blue: nitrogen, purple: iodine, red: oxygen, and green: chloride). (Reprinted with permission from ref. [36]. Copyright 2015 American Chemical Society)

The seminal work by Flood *et al.* concentrating on the preorganization of triazole moieties *via* intramolecular HBs to improve the anion affinity of HB-based receptors in solution already revealed the beneficial effect of this concept.[145-147] A current XB-based example, which achieved preorganization *via* the *N*-coordination of metal centers (**Figure 3.1**),[137] also indicated an improved binding behavior; however, there is no detailed thermodynamic characterization of the effect. Thus, isothermal titration calorimetry (ITC) experiments were performed with the three receptors **1** to **3** and two different tetra-*n*-butylammonium (TBA^+) halides to obtain a detailed understanding of the complex stoichiometry, the binding affinity, and the thermodynamic effect of preorganization in solution (**Table 3.1**). All titrations were performed in THF, which proved to be a good solvent for strong XB interactions in solution.[98] Normally, a guest-into-host setup was used for the titration but also inverse titrations, *i.e.*, addition of a host solution into a guest solution, were performed to confirm the reliability of the calculated values if necessary. Unfortunately, a direct comparison between **3** and the methoxy-decorated precursor **8** was not possible due to an insufficient solubility of **8** in THF.

Table 3.1: Thermodynamic parameters for the complexation of various receptors with different TBA^+ halides.

Host	Guest	K [M^{-1}]	ΔG [kJ mol^{-1}]	ΔH [kJ mol^{-1}]	TΔS [kJ mol^{-1}]	N	Host:Guest ratio
1	Br^-	2.22×10^3	−19.4	−24.5	−5.1	0.99	1:1
	Cl^-	3.52×10^3	−20.6	−22.9	−2.3	1.08	1:1
2	Br^-	1.58×10^3	−18.6	−27.4	−8.8	1.03	1:1
	Cl^-	2.34×10^3	−19.5	−24.9	−5.4	1.05	1:1
3 [a]	Br^-	3.85×10^3	−20.8	−7.2	13.6	0.52	2:1
		5.45×10^4	−27.5	−23.5	4.0	0.89	1:1
		4.18×10^4	−26.8	−22.8	4.0	1.02	1:1
		1.70×10^3	−18.7	−3.9	14.8	2.6	2:1
	Cl^-	3.17×10^3	−20.4	−15.1	5.3	0.45	2:1
		7.09×10^4	−28.1	−17.8	10.3	0.90	1:1
		8.38×10^4	−28.6	−22.0	6.6	1.06	1:1
		1.62×10^3	−18.6	−8.9	9.7	2.23	2:1

Thermodynamic parameters calculated from guest-into-host or inverse host-into-guest (marked in grey) titrations in THF at 303 K. [a] The formation of a 2:1 complex (host−guest) could be further supported by a solid-state structure and selective ROESY experiments (*vide infra*). (Adapted with permission from ref. [36]. Copyright 2015 American Chemical Society)

In line with the solid state structures, a cleft-type 1:1 complexation for **1** and **2** in solution was deduced from the stoichiometry coefficients (N = 1) obtained by ITC titration experiments. Although **2** revealed a slightly increased enthalpic contribution compared to **1**, which may be due to the optimized XB orientation (**Figure 3.5**), the entropic term is simultaneously slightly decreased, which is tentatively explained by a smaller extent of desolvation of the receptor and / or the anion upon binding. However, in total there are only subtle differences in the overall binding affinities of **1** and **2** and the effect of the spacer (**Figure 3.2**) seems to be negligible for the two flexible receptors.

Comparing the complexation of chloride and bromide, the trend for the K values (**Table 3.1**) shows a general preference for the more charge-dense / basic chloride, which allows a stronger electrostatic interaction.[98] For the same reason, the competitive interaction with solvent molecules is more pronounced for chloride, resulting in a reduced enthalpic contribution toward the host–guest complexation. However, this effect is overcompensated by a more favorable entropic term, which is assigned to an enhanced desolvation of chloride upon complexation.[25]

When comparing **2** and the preorganized system **3**, the tendency to form a 1:1 complex with chloride is enhanced by a factor of about 30 (K_1(**2**) = 2.34 × 10^3 M^{-1} and K_1(**3**) = 7.09 × 10^4 M^{-1}). As a result of this strongly increased anion affinity, even a second preorganized receptor wraps around the guest forming a 2:1 complex in solution as indicated by ITC and selective ROESY experiments (**Figure 3.6** and **3.7 B**, respectively) as well as by the solid state structure analysis (**Figure 3.7 A**).

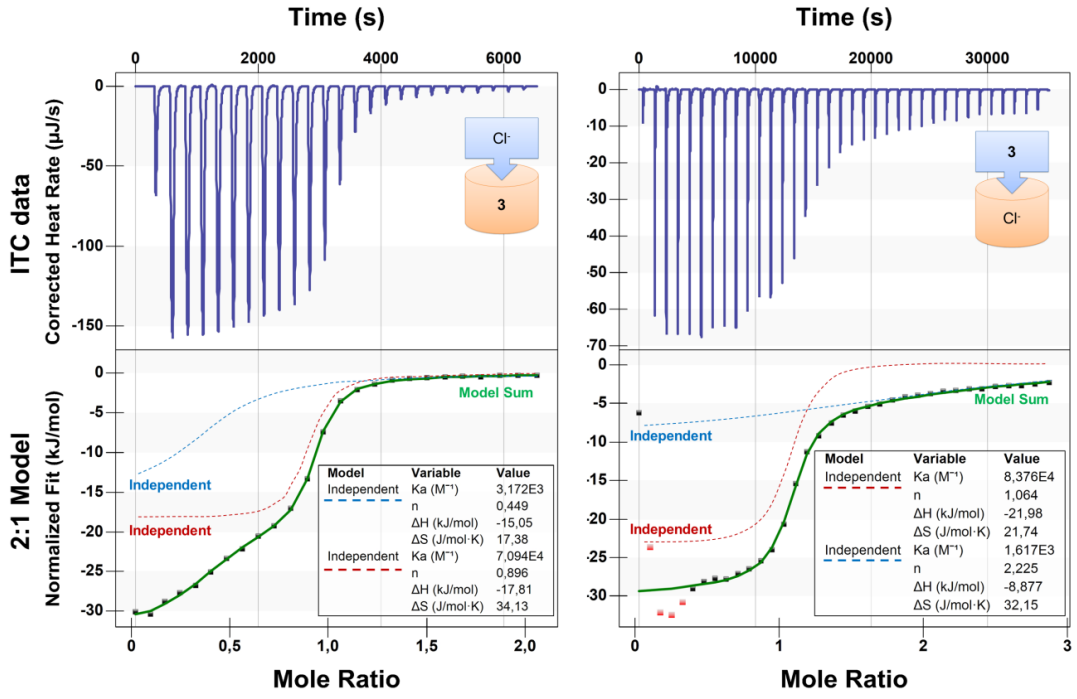

Figure 3.6: ITC titration data of receptor **3** with TBACl in guest-into-host (left) or inverse host-into-guest setup (right), red marked data points were excluded from fitting. (Reprinted with permission from ref. [36]. Copyright 2015 American Chemical Society)

The preliminary formation of a weaker 2:1 complex followed by the stepwise conversion into the predominant 1:1 complex is clearly indicated by the measured slope between 0 and 0.7 eq. of added guest in the guest-into-host ITC titration (**Figure 3.6 left**). In line with this, also the inverse titration (**Figure 3.6 right**) indicates the formation of a weak 2:1 complex since there is a significant amount of heat still released after the addition of one equivalent of **3**. To calculate the overall chloride affinity, the accumulated binding constant has to be considered, which even amounts to K_1 K_2 = 2.24 × $10^8 M^{-2}$ and represents one of the leading anion affinities for neutral bidentate XB donor systems.[65] While neutral XB donors normally suffer from an unfavorable entropic penalty as for **2** (see **Section 2.2.1**), the preorganized receptor **3** is characterized by a positive entropic term, which is the main reason for the strongly

improved binding affinity. This striking difference is attributed to the formation of intramolecular HBs and the associated restriction of rotational freedom already in the uncomplexed form of **3**. Consequently, the entropy penalty for the complexation is screened in the preorganized receptor[145] and the desolvation of host and guest give rise to a positive entropic term. Additionally, the polarization of the triazole rings may be slightly enhanced due to the formation of intramolecular HBs (dipole moment of 4.1 D and 6.1 D[145] for the flexible and preorganized triazole, respectively).

To underline the obtained ITC results and to further prove the formation of a 2:1 complex in solution, selective ROESY experiments of the free and complexed receptor were performed (**Figure 3.7 B**). For this purpose, **3** as well as a 2:1 mixture of **3** and TBACl were dissolved in THF-d_8 and the NOE signals after excitation of the methyl group of the mesityl substituent (CH_3-4^{mes}) were recorded, respectively. Both solutions revealed the expected strong contact to the adjacent aromatic proton. However, only in case of the 2:1 mixture of **3** and the anion, additional NOE-signals to the central carbazole spacer and the hydroxyl groups were visible, which can only be explained by a nearly orthogonal arrangement of two receptors within a *bis*-bidentate complex. Moreover, this coordination mode was also supported by the solid state structure (**Figure 3.7 A**), which conformably revealed the anion complexation in a *bis*-bidentate fashion *via* four highly directional XBs (167° to 177°) all significantly shorter (17% shortening) than the $\sum r_w$. Additionally, the molecular structure exposed that the hydroxyl groups are not involved in the anion complexation and only serve as intramolecular HB donors.

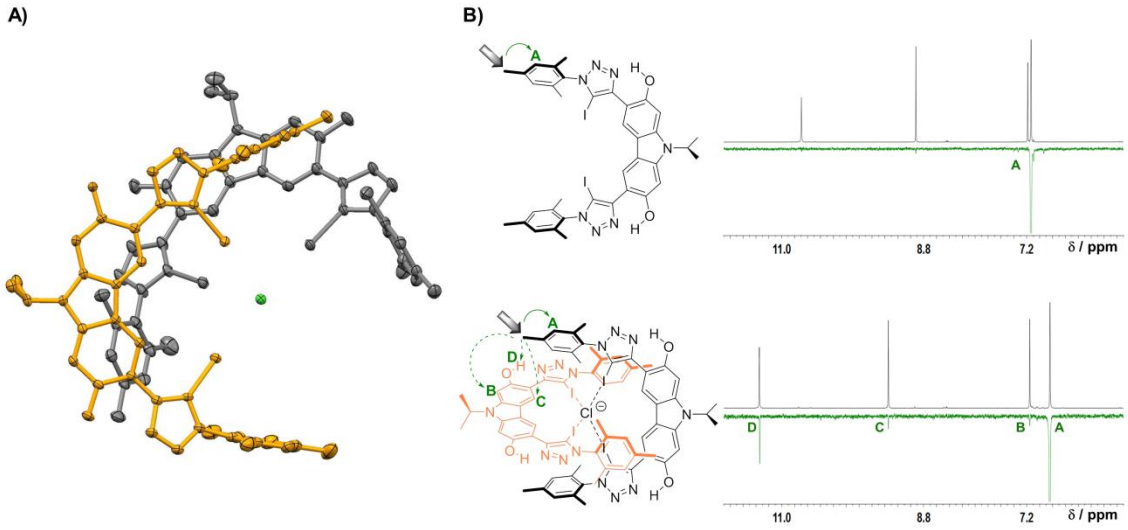

Figure 3.7: A) Solid-state structure of **3** interacting with chloride forming a 2:1 complex (thermal ellipsoids at 50% probability level, hydrogen atoms, counterions, and solvent molecules are omitted for clarity). $I^{\cdots}Cl^{-}$ XB lengths between 3.09 Å – 3.23 Å, $C–I^{\cdots}Cl^{-}$ XB angles between 167° and 177°. B) Schematic representation of the NOE contacts; the excited protons are marked with a shaded arrow and strong and medium contacts are indicated with solid and dashed arrows, respectively. ^{1}H NMR (black) and selective ROESY spectra (green) for free **3** (top) as well as for **3** in the presence of 0.5 eq. of TBACl in THF-d_8 (bottom). (Adapted with permission from ref. [36]. Copyright 2015 American Chemical Society)

In conclusion, the halide complexation ability of three different bidentate XB-based anion receptors (**1** – **3**) was characterized by ITC experiments, X-ray diffraction, and selective ROESY experiments. While the non-preorganized systems **1** and **2** showed expectable moderate association constants, a favorable entropic contribution in the rigid bidentate XB donor **3** enabled a strongly increased binding affinity. Thereby, the formation of intramolecular HBs between the central carbazole spacer and the adjacent iodo-1,2,3-triazoles was used to preorganize the system and, thus, to screen the entropic penalty of the binding event. Notably, the central carbazole is an almost ideal spacer for this assignment as it enables a bidentate complexation by a nearly planar receptor system. Following these building principles, charge-neutral, cleft-type receptors with high anion affinities can be designed. Owing to the highly directional and strong XBs as well as to the absence of isotropic Coulomb interactions, these receptors offer great potential for application as organo-catalysts in the future.

3.2 Cooperativity in ion-pair receptors

Beside the concept of preorganization, the Lewis-basic part of the triazole unit also offers the opportunity to simultaneously coordinate metal cations (see **Section 2.2.2**) and, thus, the possibility for a concurrent recognition of both cation and anion guest species in an ion-pair receptor.[148-150] Consequently, there is the opportunity to boost the anion binding affinity of triazole based receptors by a simultaneous cation complexation and the associated additional electrostatic contribution as well as enhancement of the C–I / C–H bond polarization.

In general, ion-pair receptors offer the opportunity to fine-tune the affinity as well as selectivity due to the combination of allosteric and electrostatic cooperative effects, which often enable a better control over the binding event.[151] Moreover, this receptor class has various potential application fields, such as salt solubilization / extraction, membrane transport, or sensing. However, compared with simple ion receptors, which are able to bind either a cation or an anion, the design of ditopic receptor systems is still an underexplored area.[151-154] This might be due to a combination of synthetic challenges adjusting two different binding places in an appropriate position and experimental complexities associated with the simultaneous as well as reliable quantification of different binding affinities. While the anion binding places typically involve Lewis-acidic sites (*e.g.*, boron, aluminum and uranyl), electrostatic interactions or, most frequently, HBs (*e.g.*, urea, amide, imidazolium, or hydroxyl groups),[6, 155] the cation binding sites in these ditopic systems usually take advantage of crown-ether or calixarene derivatives.[156-157]

1,2,3-Triazoles have been employed recently in ion-pair receptors as HB donors for the anion binding[148, 158] and, in few cases, also the Lewis-basic nitrogen atoms of the heterocycle were used for simultaneous cation binding (**Figure 3.8 A**, **B**).[149-150] However, there is currently no example using triazole-based XB interactions in the field of ion-pair recognition. Generally, despite considerable advantages of XBs compared to HBs in terms of affinity or selectivity, ditopic receptors based on XBs are currently very sparse (**Figure 3.8 C**).[159-160]

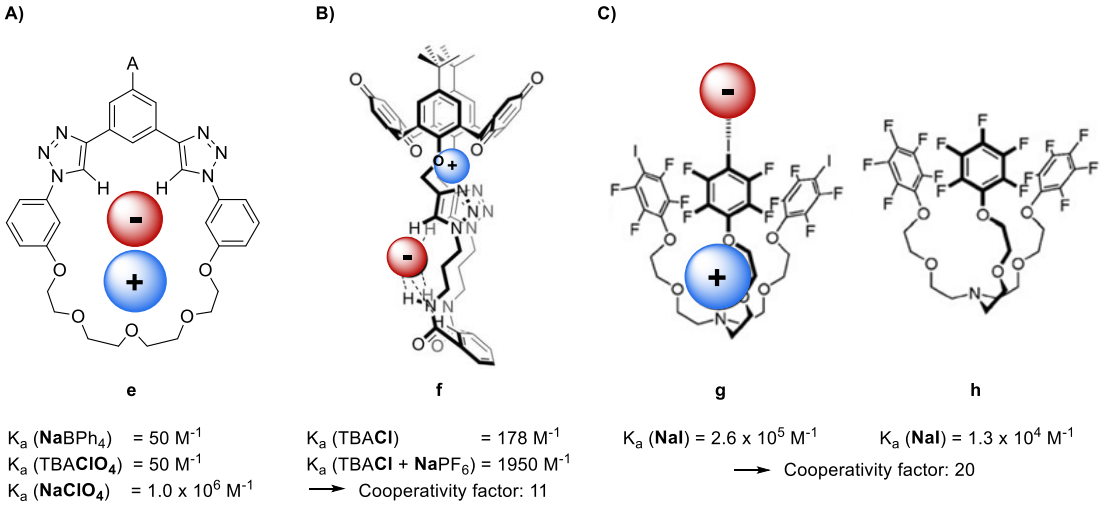

Figure 3.8: Schematic representation of exemplary ion-pair receptors based on A) HB-donating 1,2,3-triazoles, B) HB-donating as well as metal coordinating 1,2,3-triazoles or C) XB interactions.[148, 158-159] K_a values obtained by **e**: ^{1}H NMR titration in CD_2Cl_2:CD_3CN 4:1 at 298 K, **f**: ^{1}H NMR titration in 2% D_2O in CD_3CN at 293 K, **g**, **h**: ^{1}H NMR titration in $CDCl_3$.

Therefore, we decided to design a macrocyclic ion-pair receptor comprising an iodo-triazole moiety for XB-based anion recognition and a Lewis-basic cavity consisting of a triethylene glycol chain and the nitrogen atoms of the triazole motif for cation binding (**Scheme 3.2**, **right**).[37] This possible ion-pair binding mode was further demonstrated by the calculated electrostatic potential surface illustrating the heteroditopic character of the receptor (**Scheme 3.2**, **left**). The flexibility of the macrocyclic backbone should enable an adaption for the size of the cation. While the monodentate triazole-based XB interaction is known to be relatively weak,[105, 140] it should simplify the analysis of the binding affinity as well as the cooperativity effects.

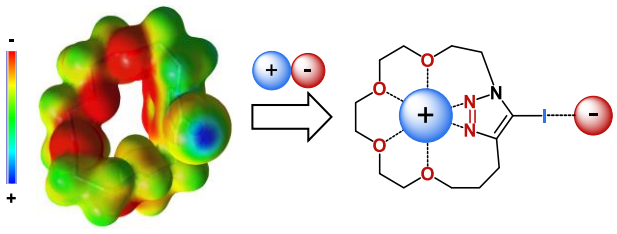

Scheme 3.2: Calculated molecular electrostatic potential surface (red: 0.00 to blue: 0.15) mapped on total density (isovalue 0.01) for the studied ion-pair system. The theoretical calculations were performed using density functional theory (DFT) (left); schematic representation of ion-pair recognition by an iodo-triazole containing crown-ether (right). (Adapted from ref. [37] with permission from The Royal Society of Chemistry)

Again, the synthesis of the desired HB- and XB-donating crown-ether-based macrocycles **12** and **13**, respectively, benefits from highly efficient CuAAC / CuAXAC-type reactions (see **Section 2.2.2**). For this purpose, unsymmetrically substituted triethylene glycols equipped with an azide as well as an alkyne (**10**) / iodo-alkyne (**11**) function were synthesized *via* a four or five step synthesis, respectively (**Scheme 3.3**). Afterwards, a diluted solution of the linear precursor (**10** or **11**) was added dropwise *via* a peristaltic pump to a heated and stirred solution containing the catalyst system ($CuSO_4$ / NaAsc. for **10** or CuI / TBTA for **11**)) required to initiate the intramolecular cyclization. Owing to a combination of a highly efficient cyclization reaction and this pseudo-high-dilution-conditions,[161] the fundamental synthetic challenge of forming well-defined monomeric macrocycles instead of larger macrocycles or linear oligomers was achieved in good yields around 75%. On the one hand, the formation of the desired products was proven by the characteristic signal shifts in the ^{1}H NMR spectra compared to the linear precursor and, ultimately, by single-crystal X-ray diffraction data (**Figure 3.9**). On the other hand, the formation of larger macrocycles or oligomers was excluded by mass spectrometry (MS).

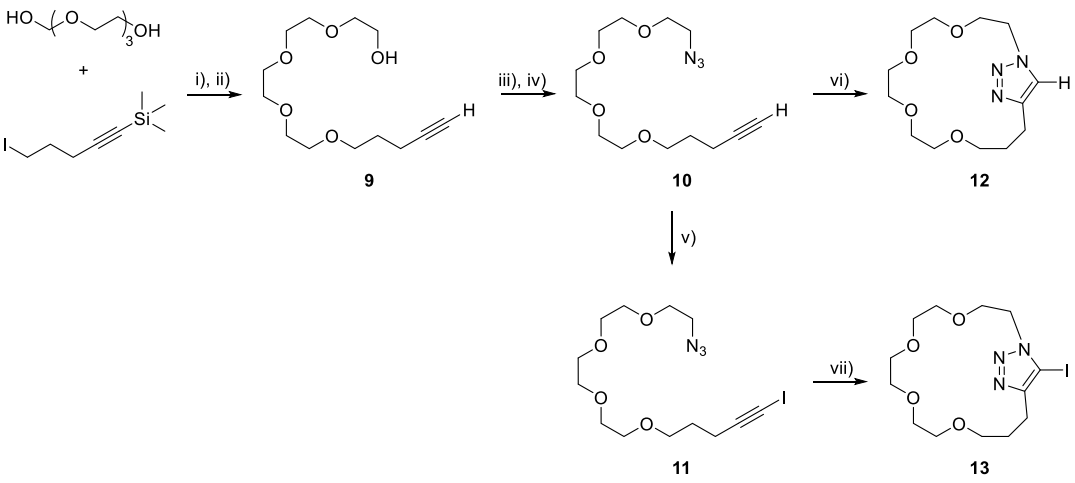

Scheme 3.3: Schematic representation of the synthesis of the HB- and XB-donating crown-ether-based macrocycles **12** and **13**: i) NaH, THF, 0 °C, 30%; ii) TBAF, THF / MeOH (2:3), rt, 99%; iii) TosCl / DMAP / Et_3N, CH_2Cl_2, 0° C, 86%; iv) NaN_3, DMSO, rt, 89%; v) *N*-iodosuccinimide / $AgNO_3$, Acetone, rt, 87%; vi) $CuSO_4$ / NaAsc., EtOH / H_2O / CH_2Cl_2 (2:1:1), 50° C, 74%; vii) CuI / TBTA, THF, 40° C, 75%. (Adapted from ref. [37] with permission from The Royal Society of Chemistry)

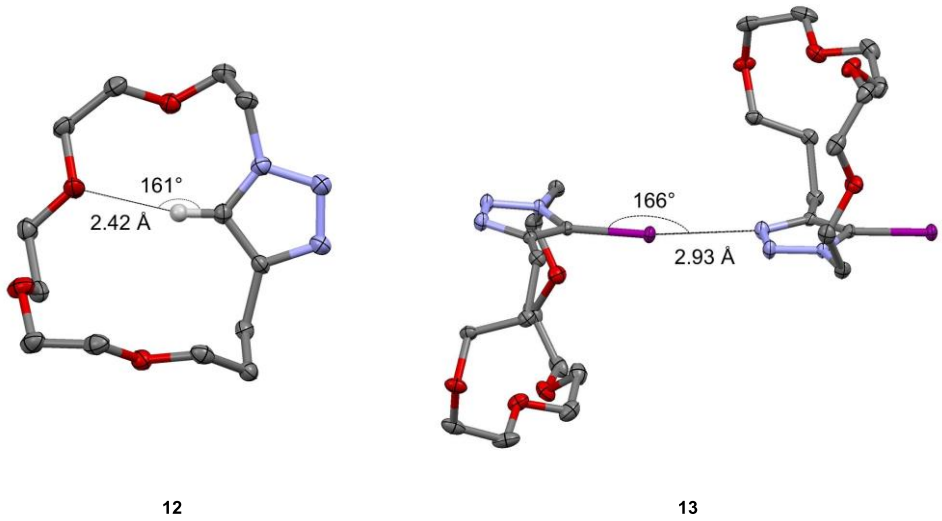

Figure 3.9: Solid-state structure of **12** (with intramolecular HB shown as dashed line) and **13** (with intermolecular XB shown as dashed line) (thermal ellipsoids at 50% probability level, hydrogen atoms and solvent molecules are omitted for clarity; grey: carbon, blue: nitrogen, purple: iodine, and red: oxygen). (Adapted from ref. [37] with permission from The Royal Society of Chemistry)

For a first proof of principle, single crystals of the macrocycles **12** and **13** interacting with sodium and a non-coordinating anion (PF_6^- or BPh_4^-) were grown by slow vapor diffusion of *n*-pentane into a concentrated receptor solution (**Figure 3.10 A** and **B**). Thereby, the anticipated simultaneous participation of the Lewis-basic nitrogen atoms of the triazole moiety and the four oxygen atoms in the cation complexation was confirmed. Nonetheless, two main points already indicated that sodium is apparently not an ideal guest for this binding cavity. At first, the binding pocket seems to be slightly strained indicated by a broad range of $Na^{+\cdots}O$ distances (2.32 Å to 2.74 Å) observed in the molecular structure (**Figure 3.10 A** and **B**). Additionally, depending on the added amount of sodium salt during the crystallization process, the stoichiometry adapts to a 1:1 as well as a 1:2 complex.

Nevertheless, the molecular structure of **13** interacting with sodium iodide finally illustrated the capability of the iodo-triazole moiety to coordinate simultaneously cationic and anionic guests (**Figure 3.10 C**). Comparable to the interaction of **12** with $NaPF_6$ (**Figure 3.10 A**), also in the XB-based macrocycle **13** the nitrogen atoms still contribute towards the cation binding forming a 1:2 complex. Simultaneously, one iodide is successfully complexed through the formation of a nearly linear XB (173°), which is significantly shorter (10% shortening) than the $\sum r_w(I\cdots I) = 3.96$ Å.[85] The second counter anion is stabilized by HBs formed between the iodide and bridging

water molecules. The close contact distances between sodium and iodide ranging from 4.6 Å to 5.1 Å falls between the $Na^{+}\cdots I^{-}$ contact ion pair distance (3.2 Å)[158] and the completely host-separated ion pair distance (5.6 Å)[159] observed for other sodium iodide complexes with organic receptor molecules.

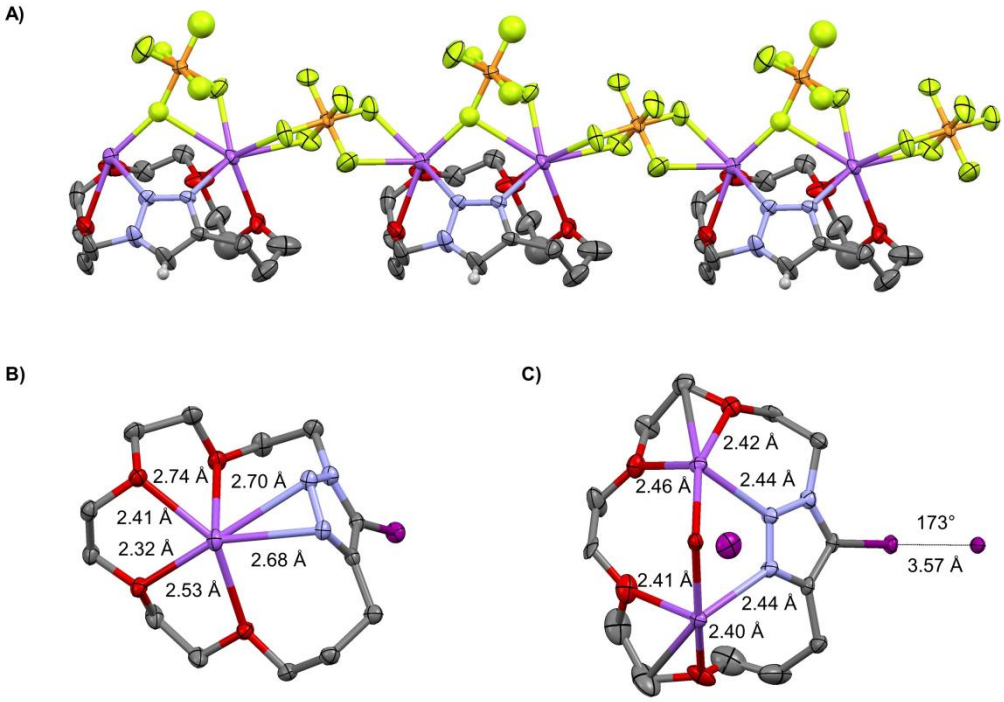

Figure 3.10: Solid-state structures of A) **12** interacting with $NaPF_6$ forming a 1:2 complex. B) **13** interacting with $NaBPh_4$ forming a 1:1 complex. C) **13** interacting with NaI forming a 1:2 complex. (thermal ellipsoids at 50% probability level, hydrogen atoms and solvent molecules are omitted for clarity; grey: carbon, blue: nitrogen, yellow: fluorine, orange: phosphor, purple: iodine, violet: sodium, and red: oxygen). (Adapted from ref. [37] with permission from The Royal Society of Chemistry)

After the heteroditopic character of the macrocycles were visualized in the solid state, detailed binding studies in solution were performed to quantify the cooperative effect of the cation complexation on the anion-binding affinity. Whereas the ITC technique, which was extensively used in **Section 3.1**, was not feasible in this case because of too small binding affinities, ^{1}H NMR and ^{13}C NMR spectroscopy was successfully applied to investigate the binding properties of the different binding places. Here, characteristic sodium- as well as iodide-induced chemical shift migrations in the ^{1}H NMR and ^{13}C NMR spectra allowed the individual characterization of cation and anion binding affinities of the macrocycle (**Figure 3.11**). A control experiment with $TBABPh_4$ verified that their respective bulky, non-coordinating counter ions (TBA^{+} in case of iodide and BPh_4^{-} in case of sodium) did not show any significant influence on the

chemical shifts. Note, the interaction of **13** with $NaBPh_4$ also causes a slight shift of the anion specific C_{17} signal, which is attributed to an increased interaction with the BPh_4^- counter ion caused by an activation of the XB *via* the cation complexation. The used solvent mixture of CD_2Cl_2 and CD_3CN (3:1) can be seen as a compromise between a sufficient solubility for both the receptor and all titrated salts (in particular sodium iodide) and on the other hand a still measurable anion binding affinity (*vide infra*). A more polar / competitive solvent would have enabled a better salt solubility but at the same time would have strongly reduced the efficiency of the XB / HB interaction.[37] In general, the analysis of the anion affinity represents the basic experimental challenge in this study. Due to the general structure of the receptor and large steric demand of the XB donor iodine, the distance between the XB-based anion-binding place and adjacent hydrogen atoms is too large to see any significant chemical shift migrations in the ^1H NMR spectrum upon anion complexation. Moreover, common alternative techniques to quantify binding affinities like *e.g.*, UV / Vis, ^{19}F NMR or ITC titrations[63, 162] were excluded due to the absence of a chromophore, the NMR active nucleus or too small binding affinities, respectively.

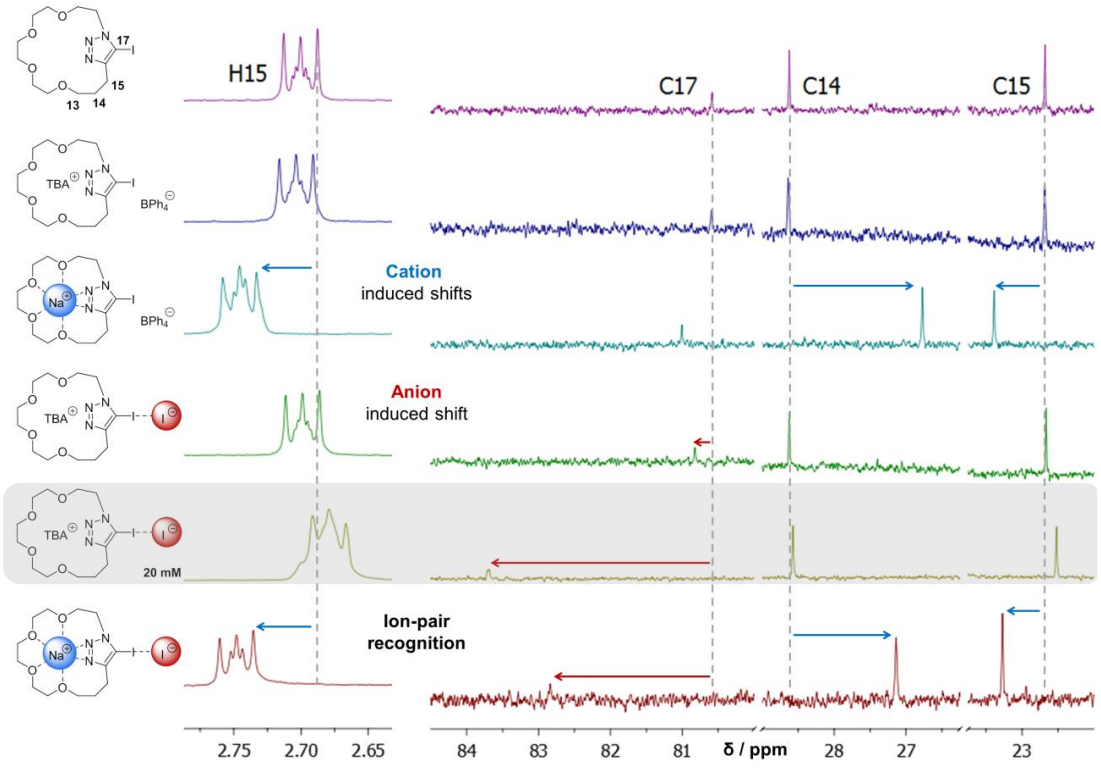

Figure 3.11: Schematic representation of the ^1H / ^{13}C NMR (500 / 126 MHz, CD_2Cl_2:CD_3CN 3:1) of host **13** [generally 1 mM or 20 mM as depicted in grey] with 8 eq. of different guests illustrating the chemical shifts used for the calculation of the cation or anion binding affinities. (Adapted from ref. [37] with permission from The Royal Society of Chemistry)

Consequently, the quaternary carbon atom C_{17} directly connected to the XB-donating iodine had to be used for the quantification of the anion affinity (K_I). Here, a downfield shift of the C_{17} signal (0.24 ppm for [Host] = 1 mM) was clearly visible upon the addition of eight equivalents of TBAI; however, this chemical shift was still insufficient for a reliable quantification of the association constant (**Figure 3.11**). Finally, by increasing the host concentration from 1 to 20 mM, the chemical shift of the C_{17} atom could be raised by 3.41 ppm, which allowed a reliable quantification of the pure anion affinity. Noteworthy, the chemical shift of C_{14}, used for the calculation of the cation binding affinity, showed no significant shift verifying the non-coordinating behavior of the TBA counter ion even at higher concentrations (**Figure 3.11**). Nevertheless, the limited solubility of sodium iodide in organic solvents dictated the use of a 1 mM host solution for the analysis of the ion-pair affinity (**Table 3.2**), which causes very long ^{13}C NMR acquisition times and a cryogenic NMR probe to reliably detect the quaternary carbon atom in the end.

As the solid state analysis indicated the possible simultaneous complexation of two cations within the crown-ether (*vide supra*), a potential contribution of this 1:2 complex also in solution was consequently checked exemplarily for the interaction of **13** with $NaBPh_4$ by assuming a 1:2 binding model to fit the binding isotherm (**Figure 3.12 A**).

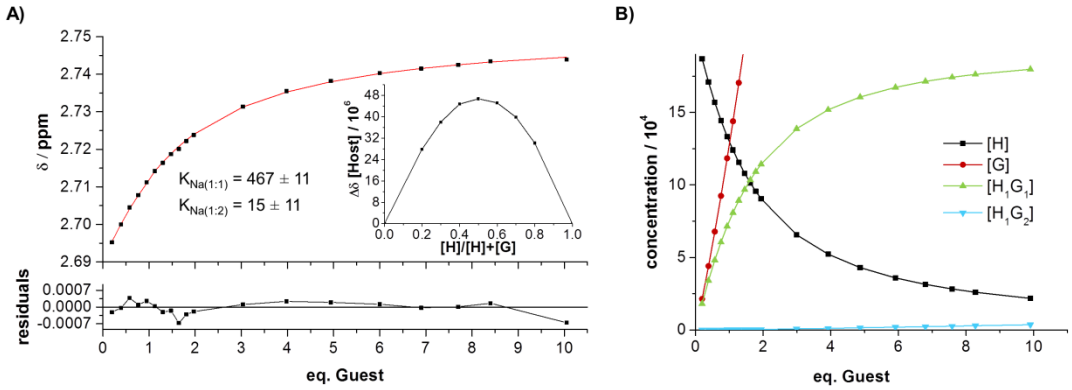

Figure 3.12: A) Analysis of the binding isotherm (H_{15}) of **13** (2 mM) and $NaBPh_4$ in CD_2Cl_2:CD_3CN (3:1) assuming a 1:2 (host:guest) binding model and (inset) corresponding Job plot analysis (H_{15}). B) Speciation curves for all of involved species (H = host, G = guest).

However, a comparable cation binding affinity for the formation of the 1:1 complex was calculated ($K_{Na(1:1)} = 434 \pm 6$ assuming a 1:1 binding model (**Table 3.2**) *vs.* $K_{Na(1:1)} = 467 \pm 11$ assuming a 1:2 binding model) followed by the subsequent formation into a negligible 1:2 complex ($K_{Na(1:2)} = 15 \pm 11$) as also illustrated by the speciation curves (**Figure 3.12 B**). Moreover, this predominant formation of the 1:1

complex was also underlined by a Job plot analysis, which is a general tool to characterize the stoichiometry of a complexation in solution (**Figure 3.12 A, inset**).[162-163] Consequently, the 1:1 binding model was applied for the analysis of all the binding isotherms, since it should describe the complexation in solution most properly (**Table 3.2**).

Table 3.2: Overview of the binding constants calculated from NMR titration data for **12** and **13** with different guests applying a 1:1 binding model (sodium added as $NaBPh_4$ and iodide added as TBAI, measurements at 297 K in a CD_2Cl_2:CD_3CN (3:1) solvent mixture).

Host	Guest	NMR	[Host]	K_{Na} [M^{-1}]	K_I [M^{-1}]
13	Na^+	^1H	2 mM	434 ± 6 [a]	-
	I^-	^{13}C	20 mM	-	4.7 ± 0.4 [d]
	NaI	^1H	1 mM	394 ± 14 [a]	N/S
		^{13}C	1 mM	406 ± 60 [b]	135 ± 17 [d]
12	Na^+	^1H	2 mM	126 ± 6 [c]	-
	I^-	^{13}C	20 mM	-	N/D
	NaI	^1H	1 mM	155 ± 19 [c]	N/S
		^{13}C	1 mM	174 ± 30 [b]	N/D

Signal used for the calculation of the corresponding association constant: *a* = H_{15}, *b* = C_{14}, *c* = H_{13}, *d* = C_{17}; N/S = no shift; no anion induced shift observable in the ^1H NMR, which is tentatively assigned to the large distance between the anion binding place and the adjacent hydrogen atoms; N/D = not determined, no reliable quantification of K_I due to an insufficiently large chemical shift. (Adapted from ref. [37] with permission from The Royal Society of Chemistry)

In line with the non-ideal geometry of the cation binding place for the sodium ion as already indicated by the X-ray analysis (**Figure 3.10**), a comparatively weak cation-binding affinity of the macrocycles was quantified in solution ($K_{Na} < 10^3\ M^{-1}$ compared to $K_{Na} > 10^4\ M^{-1}$ for optimized crown-ether systems).[164] Furthermore, the combination of a monodentate interaction without charge-assistance dictated by the general receptor design and the rather low charge density / basicity of the guest iodide led to the expected very weak binding affinity of **13** towards mere iodide ($K_I = 4.7 \pm 0.4\ M^{-1}$). Accordingly, the reliable quantification of the anion affinity was rather challenging and required a higher host concentration (*vide supra*); however, comparable monodentate iodo-triazole-based receptors gave very similar results.[105, 140, 165]

Finally, **13** was directly treated with sodium iodide and analyzed by ^1H NMR and ^{13}C NMR regarding the cooperativity of the ion-pair recognition. Therefore, the comparability between the different NMR titration experiments was proven initially.

Despite changing the atom position used for the calculation (H_{15} *vs.* C_{14}), the cation binding affinities calculated by ^{1}H NMR ($K_{Na} = 394 \pm 14\ M^{-1}$) show a very good coincidence with the one calculated by ^{13}C NMR ($K_{Na} = 406 \pm 60\ M^{-1}$). The larger error in case of the latter is attributed to the fewer data points that were accessible for the fitting process, which is accounted by the very long acquisition time of nearly one day for one data point. Comparing the cation binding affinity calculated by the titration of **13** with $NaBPh_4$ ($K_{Na} = 434 \pm 6\ M^{-1}$) with the titration of **13** with NaI ($K_{Na} = 394 \pm 14\ M^{-1}$), the similar binding affinities indicated an independence of the cation binding place from the anion. Thus, the cation binding is clearly dominated by the multidentate coordination within the macrocycle and is not decisively influenced by cooperative effects (*e.g.*, an additional Coulomb attraction and a cooperative polarization of the 1,2,3-triazole ring) of the simultaneously coordinated iodide. In contrast, the presence of the coordinated cation significantly enhanced the monodentate XB interaction of **13** to the anion ($K_I = 4.7 \pm 0.4\ M^{-1}$ *vs.* $K_I = 135 \pm 17\ M^{-1}$ by simultaneous sodium complexation). This cooperative effect is ascribed to an additional electrostatic contribution and, in particular, an enhancement of the C–I bond polarization as visualized by the electrostatic potential calculations (**Figure 3.13**). Thereby, the data of the free (**Figure 3.13 left**) and the sodium complexed (**Figure 3.13 right**) form of **13** revealed a significantly increased size of the σ-hole due to the additional electrostatic force as well as an increased polarization of the 1,2,3-triazole moiety.

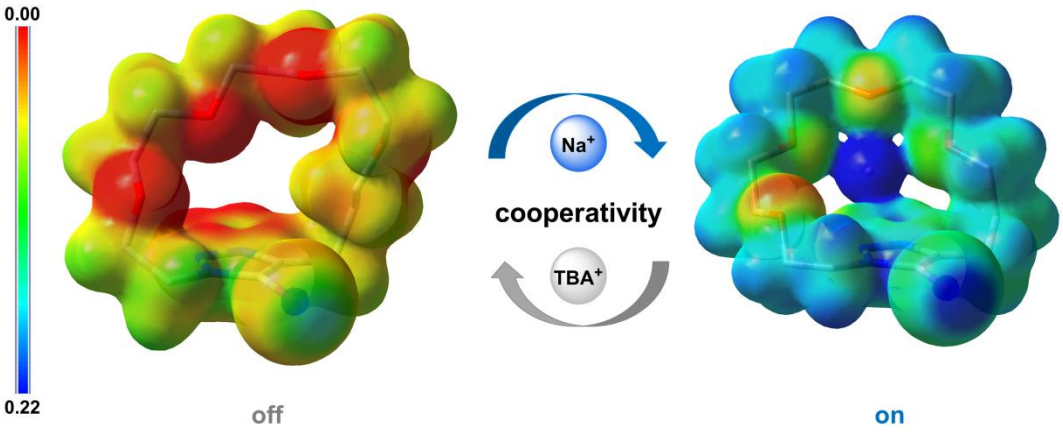

Figure 3.13: Calculated molecular electrostatic potential surface (red: 0.00 to blue: 0.22) mapped on total density (isovalue 0.012) for **13** in the free (left) and sodium complexed form (right). Note that both electrostatic potential surfaces are plotted with the same parameters to warrant comparability. (Adapted from ref. [37] with permission from The Royal Society of Chemistry)

The expected decrease of the binding affinity by changing from the XB- to the analogous HB-based interaction[99] led to an insufficient chemical shift of the C_{17} atom during the NMR titration. Thus, a reliable quantification of the anion affinity of **12** was precluded for both the mere anion (even at a host concentration of 20 mM) as well as for the ion-pair study. In case of the latter, the addition of significantly larger amounts of sodium iodide would have been necessary to achieve a reliable analysis of the binding isotherm, which was excluded due to solubility issues of the sodium salt. Moreover, comparing the cation-binding affinities of the XB- ($K_{Na} = 434 \pm 6\ M^{-1}$) and the HB-based receptor ($K_{Na} = 126 \pm 6\ M^{-1}$), also a significantly decreased K_{Na} value was observed for the latter. In line with the solid-state structure (**Figure 3.9**), this lowered cation-binding affinity was attributed to a possible competing intramolecular HB formation of **12**, which would negatively influence the cation complexation of the crown-ether.

Thus, detailed selective ROESY experiments of **12** were performed to prove the existence of this intramolecular HB in a CD_2Cl_2:CD_3CN (3:1) solvent mixture (**Figure 3.14**). After selective excitation of the triazole proton (H_{17}) in the free macrocycle **12**, strong NOE signals of all protons of the crown-ether binding pocket indicated a freely rotatable triazole moiety. Accordingly, the formation of an intramolecular HB between H_{17} and one of the oxygen atoms of the crown-ether was indicated. In contrast, upon the addition of the sodium salt, the nitrogen atoms of the triazole unit got involved in the cation complexation and, thus, the possibility of an intramolecular HB formation was lowered. Consequently, the NOE signals to all protons located at the cation-binding place decreased (H_2 to H_{14}).

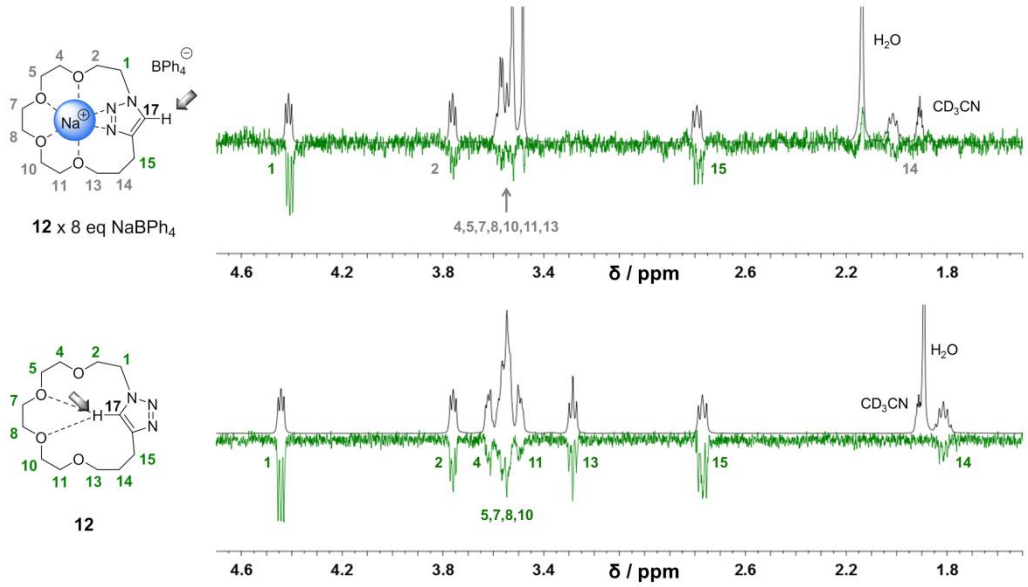

Figure 3.14: NMR spectra and schematic representation of the NOE contacts; the selectively excited proton (H_{17}) is marked with a shaded arrow and strong as well as weak contacts are indicated with green and grey numbers, respectively. ^{1}H NMR (black) and selective ROESY spectra (green) for **12** [20mM] in the absence (bottom) as well as in the presence of 8 eq. of $NaBPh_4$ (top) in a CD_2Cl_2:CD_3CN (3:1) solvent mixture. (Adapted from ref. [37] with permission from The Royal Society of Chemistry)

In conclusion, highly efficient CuAAC-type reactions executed under pseudo-high-dilution-conditions simultaneously enabled the synthesis of well-defined macrocycles (**12** and **13**) as well as the installation of a triazole moiety for simultaneous cation–anion binding through Lewis-basic nitrogen atoms and monodentate HB / XB interactions. Subsequently, this heteroditopic character was proven by solid-state analysis and was further supported by quantum chemical calculations of **13** visualizing the size dependence of the σ-hole on the cation binding. Afterwards, this cooperative effect of the cation complexation on the anion-binding affinity was quantified by detailed ^{1}H and ^{13}C NMR titration experiments in solution with sodium iodide as representative ion pair. Despite a comparatively weak cation-binding affinity of the macrocycle due to the non-ideal fit of the cation with the cavity, a cooperativity factor of about 28 could be achieved (**Figure 3.8**), which successfully demonstrated the huge potential of the iodo-triazole moiety for simultaneous metal coordination and XB-based anion recognition. In contrast, the combination of an intramolecular HB interfering with the cation binding place and the generally lower anion affinity of the HB-based analogue precluded the analysis of the cooperativity in **12**.

4 Application of halogen bond donors in polymeric architectures – bridging solution and solid state

Parts of this chapter have been published in P4) R. Tepper, S. Bode, R. Geitner, M. Jäger, H. Görls, J. Vitz, B. Dietzek, M. Schmitt, J. Popp, M. D. Hager, U. S. Schubert, *Angew. Chem. Int. Ed.* **2017**, *56*, 4047-4051; *Angew. Chem.* **2017**, *129*, 4105-4110; P5) J. Dahlke, R. Tepper, R. Geitner, S. Zechel, J. Vitz, R. Kampes, J. Popp, M. D. Hager, U. S. Schubert, *Polym. Chem.* **2018**, *9*, 2193-2197.

Recently, also the combination of XBs with polymeric architectures has attracted growing interest. In particular, the high interaction strength, the directionality as well as the tendency to be less sensitive to polar / aqueous environments made XBs suitable for the design of functional supramolecular materials (*e.g.*, macromolecular self-assembly into higher-order structures like micelles, formation of hydrogels, construction of polymeric liquid crystallinity).[38-39, 100, 166-170]

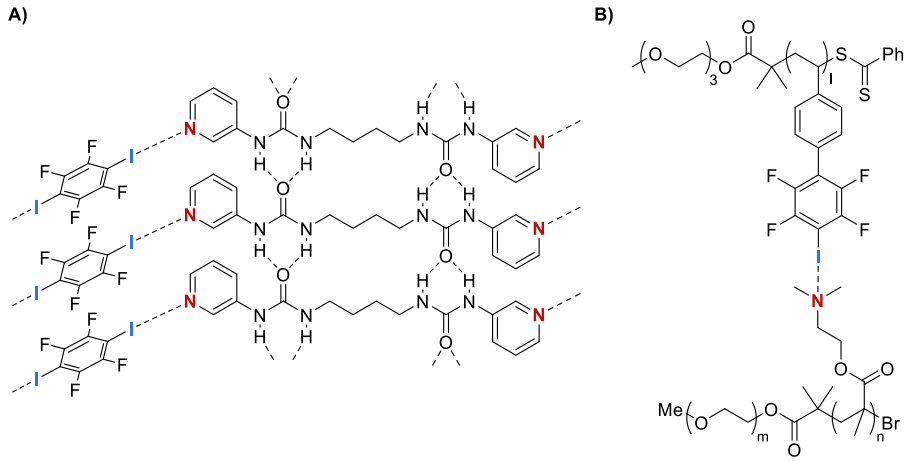

Figure 4.1: Schematic representation of two XB-based polymeric architectures.[167, 169]

The combination of XBs and polymer science is still in its infancy and is by now mainly concentrated on halogenated perfluoroarenes and perfluoroalkanes as readily accessible XB donors interacting with different pyridine as well as amine derivatives (**Figure 4.1**).[38] However, there is a much larger variety of conceivable XB donor / acceptor pairs featuring a broad range of interaction strengths as well as complex stoichiometries as already examined in more detail in solution phase applications. Hence, transferring the knowledge from solution to polymeric systems could allow the design of novel functional materials with on demand properties.

4.1 Motivation and synthesis

Due to the strong but yet reversible character of XB interactions, we thought of a great potential of a reversible XB-induced crosslinking of polymeric systems (**Figure 4.2 A**) and, thus, of designing a new class of intrinsic self-healing polymer networks (**Figure 4.2 C**). These systems are in general able to heal, for example, a mechanical damage and to restore the mechanical properties.[171-172] Although, different supramolecular interactions,[173] *e.g.*, HBs,[174-175] ionic interactions,[176-177] π-π-interactions[178] or metal-ligand interactions[179-180] have already been utilized to prepare such self-healing polymer networks, XB interactions were overlooked for this kind of application up to now.

To gain a profound knowledge of the general binding behavior of polymeric donor systems, initially, a systematic series of cleft-type anion receptors were embedded into a polymeric architecture and were comprehensively characterized by ITC experiments in solution. Thereby, the dependence of the anion affinity on different key parameters, namely, monomeric *vs.* polymeric receptor, XB- *vs.* HB-based interaction as well as the effect of charge assistance was analyzed (**Figure 4.2 B**). Afterwards, due to the combination of these donor systems with a copolymer bearing accepting carboxylate groups supramolecular cross-linked polymer networks were obtained, which were subsequently analyzed regarding their intrinsic self-healing behavior (**Figure 4.2 C**).

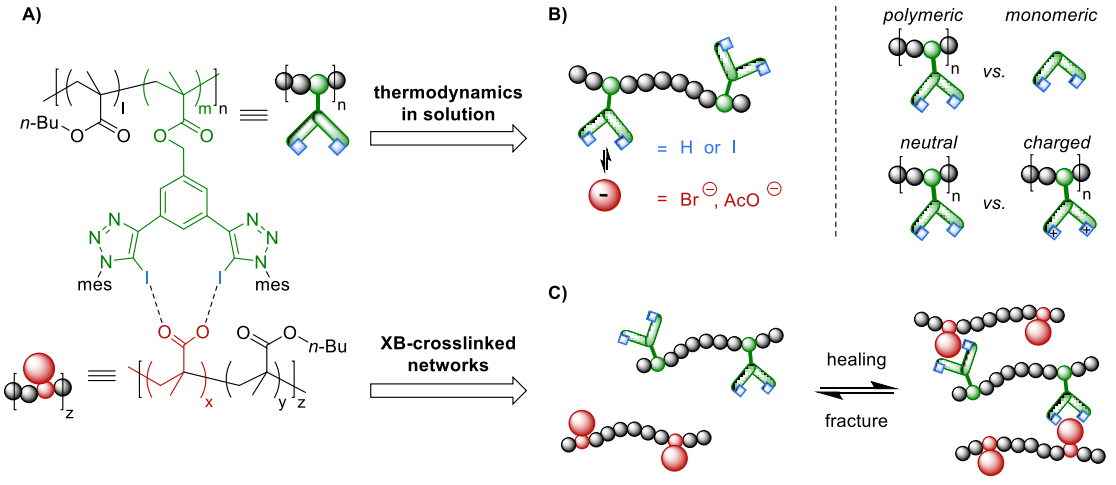

Figure 4.2: A) Schematic representation of studied polymeric donor / acceptor pair, which was analyzed B) regarding the key parameters influencing the thermodynamic behavior in solution as well as C) regarding the self-healing behavior of XB-crosslinked networks.

For the general donor motif, the well-established and easily accessible phenyl-based system **1** was utilized, which has been extensively studied in its monomeric form[36, 99] and in this context already revealed an efficient binding behavior in particular to oxo-anions like acetate.[99] To introduce a polymerizable group, a benzyl alcohol derivative was chosen as starting material for this project ensuring the simple introduction of a methacrylate group in the end (**Scheme 4.1**). Thus, comonomers containing HB (**20**) or XB (**21**) based receptor units were synthesized, which were subsequently polymerized by the reversible addition-fragmentation chain transfer polymerization (RAFT) to prepare well-defined copolymers (**p1** and **p2**) with a low dispersity and precise molar masses (M_n(**p1**) = 26,500 g/mol, Đ = 1.1; M_n(**p2**) = 30,100 g/mol, Đ = 1.2).[181] In all cases, butyl methacrylate (BMA) was chosen as second comonomer due to its low glass transition temperature (around 20 °C), which already proofed beneficial for self-healing applications.[182]

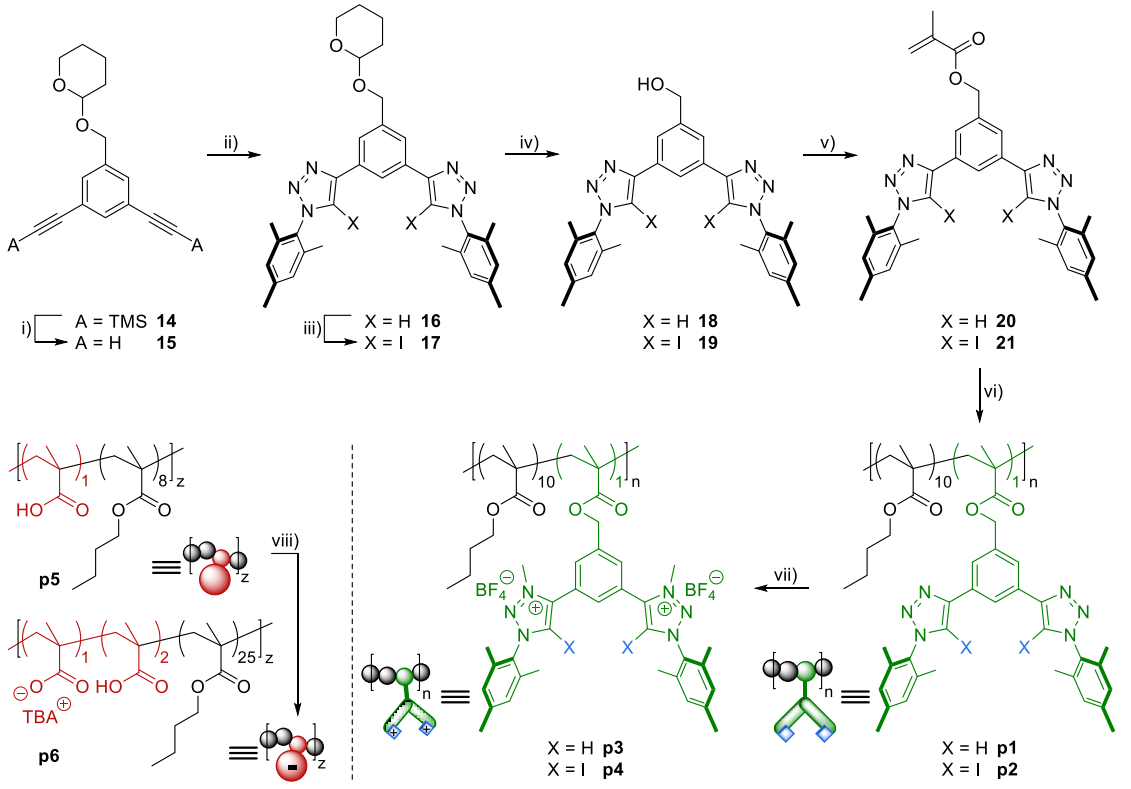

Scheme 4.1: Schematic representation of the synthesis of the HB- and XB-donor containing copolymers **p1** to **p4** (green, blue) as well as acceptor copolymers **p5** and **p6** (red): i) KOH, MeOH, rt, 99%; ii) mes-N_3, $CuSO_4$ / NaAsc., EtOH / H_2O / CH_2Cl_2 (2:1:1), 50° C, 85%; iii) *n*-BuLi, THF, I_2 at −78 °C, then −78 °C to rt, 64%; iv) TosOH, MeOH / CH_2Cl_2 (1:1), rt, 99% (X = H), 97% (X = I); v) methacrylic anhydride, DMAP / Et_3N, CH_2Cl_2, rt, 89% (X = H), 90% (X = I); vi) RAFT-polymerization with BMA, CPDB / AIBN (4:1), DMF, 70 °C; vii) Me_3OBF_4, CH_2Cl_2, rt, 95% (X = H), 97% (X = I); viii) TBAOH, DMF, rt. (Adapted with permission from ref. [183]. Copyright 2017 WILEY-VCH Verlag GmbH & Co. KGaA, Weinheim)

Also in polymeric donor systems, the alkylation of the triazole moieties worked quantitatively and enabled the formation of the corresponding triazolium salts (**p3** and **p4**). While these triazolium systems are characterized by an increased C–H / C–I polarization as well as an additional charge-assistance,[99] this post-functionalization simultaneously guarantees the same BMA / receptor ratio (**Scheme 4.1**) in the neutral and positively charged form of the copolymers (**p1** *vs.* **p3** and **p2** *vs.* **p4**) and, thus, ensures comparability. For the polymeric acceptor systems (**p5** and **p6**), BMA was copolymerized with methacrylic acid (MAA) and the resulting copolymer **p5** (M_n(**p5**) = 33,300 g/mol, Đ = 1.1) was subsequently treated with an excess of TBAOH to obtain the analogous partially anionic system **p6** (**Scheme 4.1**).

4.2 ITC investigations in solution

The general binding behavior of the polymeric donor systems (**p1** to **p4**) and in particular the dependence of the anion affinity on the key parameters (*i.e.*, monomeric *vs.* polymeric receptor, XB- *vs.* HB-based interaction as well as effect of charge assistance) was analyzed by comprehensive ITC experiments in solution (**Table 4.1**).

Table 4.1: Thermodynamic parameters for the complexation of various donor systems with different TBA^+ halides.

Host	Guest	K [M−1]	ΔG [kJ mol−1]	ΔH [kJ mol^{-1}]	TΔS [kJ mol^{-1}]	N	Host:Guest ratio
p1 [a]	Br^-	-	-	-	-	-	
p3	Br^-	3.55×10^3	−20.7	−13.9	6.8	1.06	1:1
1	Br^-	2.22×10^3	−19.4	−24.5	−5.1	1.00	1:1
p2	Br^-	2.36×10^3	−19.6	−28.4	−8.8	0.79	1:1
p4	Br^-	2.87×10^4	−25.9	−31.8	−5.9	1.05	1:1
p4	AcO^-	4.17×10^5	−32.6	−12.9	19.7	0.96	1:1
		2.11×10^3	−19.3	−22.8	−3.5	1.50	1:2
		7.97×10^3	−22.7	−28.6	−5.9	0.70	1:2
		5.17×10^5	−33.2	−11.9	21.3	1.06	1:1

Thermodynamic parameters calculated from guest-into-host or inverse host-into-guest (marked in grey) titrations in THF at 303 K. [a] No sufficient heat effect was observed in the ITC measurement. (Adapted with permission from ref. [183]. Copyright 2017 WILEY-VCH Verlag GmbH & Co. KGaA, Weinheim)

First, to allow a classification of the polymeric donors with respect to literature[98-99] and to evaluate the different key parameters on the binding behavior, a systematic analysis of all prepared systems (**p1** to **p4** and **1**) with a simple spherical guest (bromide) was performed. As expected, the HB-based host systems (**p1** and **p3**) revealed significantly smaller association constants compared to the XB-based analogous (**p2** and **p4**). In the case of the uncharged HB system **p1**, the anion affinity to bromide was even too low to be determined by ITC (**Table 4.1**).

Comparing the polymeric XB-based system **p2** with the analogous monomeric reference system **1** from **Section 3.1**, only minor influences of the polymer backbone on the complexation behavior of the receptor unit can be observed. In both cases, ITC experiments revealed 1:1 complexes with nearly the same binding affinities (**Table 4.1**), indicating the anticipated cleft-type complexation of the anion (**Figure 3.5**). In case of **p2**, a slightly more unfavorable entropic term towards the binding was determined, which may have two reasons: Firstly, a tentatively weaker solvation of the receptor in the polymer system may lead to less desolvation during the complexation. Secondly, the uncharged polymer entangles and forms a random coil, which needs to be unknot before the binding sites become accessible for anions. As a result, the conformational freedom is restricted leading to a smaller entropic contribution compared to the monomeric system. Furthermore, the formation of a random coil is also in line with the slightly decreased stoichiometric value (N(**p2**) = 0.79), which could be indicative for some blocked / unavailable receptor units in the polymer chain of **p2**.

When comparing the charge-neutral (**p1** and **p2**) and the doubly positive charged systems (**p3** and **p4**), the bromide affinity is enhanced by about one order of magnitude for the charged receptor systems (K(**p2**) = 2.36×10^3 M^{-1} and K(**p4**) = 2.87×10^4 M^{-1}). In particular, in line with previous results the enhanced enthalpic term can be explained by the additional Coulomb interaction as well as by a stronger C–H / C–X bond polarization of the triazolium moiety compared to the charge-neutral triazole moiety.[99] Furthermore, as already explained in **Section 2.2.1**, the solvent interaction is more pronounced for charged receptors causing an enhanced desolvation during complexation and, as a net result, a more favorable entropic contribution.[25] At the same time, the increased stoichiometric value for **p4** compared to **p2** (N(**p4**) = 1.05 and N(**p2**) = 0.79) indicated a better accessibility of the receptor units, which could be explained by the

rejection of adjacent positively charged receptor units and, consequently, by a less entangled polymer chain.

For a descriptive transfer of the knowledge from solution investigations to the polymeric network, initially, the interaction of the strongest donor system (**p4**) was exemplarily studied with the polyatomic acetate, which mimics the carboxylate group of the polymeric acceptor system **p6**. As expected from previous experiments of the monomeric receptor system **1**, a preference of **p4** for acetate over bromide was observed (**Table 4.1**) and is rationalized by the higher basicity of the oxo-anion.[99] As a result of the increased binding affinity even the tendency to form a weak 1:2 complex (N_2(**p4**) = 1.50) was observed for acetate, which was underlined by inverse titration experiments. Finally, ITC experiments with complete polymer-based donor / acceptor pairs (**p4** with **p5** as well as **p4** with **p6**) display exothermic signals and, consequently, revealed an attractive interaction between the two polymeric systems. Moreover, the titration of **p4** with a pure BMA-based reference polymer revealed no significant heat change, which further indicates that the formation of XBs between the receptor unit and the acid function of the MAA comonomer is responsible for the observed attractive interaction of **p4** with **p5** and **p6**. Unfortunately, a reliable quantification of the thermodynamic parameters is precluded due to the unknown degree of accessible donor and / or acceptor sites. In particular, steric hindrances in the entangled polymer system and / or entropic penalties associated with the restricted flexibility upon arranging the two polymers could tentatively block some binding places.

4.3 Material properties in thin films

Nevertheless, with the knowledge of the binding behavior of polymeric XB / HB-donor systems in solution in hand, material properties in films were studied next. For this purpose, solutions of the polymeric donor / acceptor pairs were mixed in stoichiometric amounts according to the degree of functionality and the desired network (*e.g.*, **p46** from **p4** and **p6**, see **Figure 4.3 A**) precipitated during slow solvent evaporation and was finally dried under reduced pressure. Subsequently, the successful XB-based crosslinking was demonstrated by the help of nanoindentation measurements, FT-Raman spectroscopy as well as X-ray diffraction studies. Finally, the applicability of these networks as self-healing films was investigated as described in the next sections.

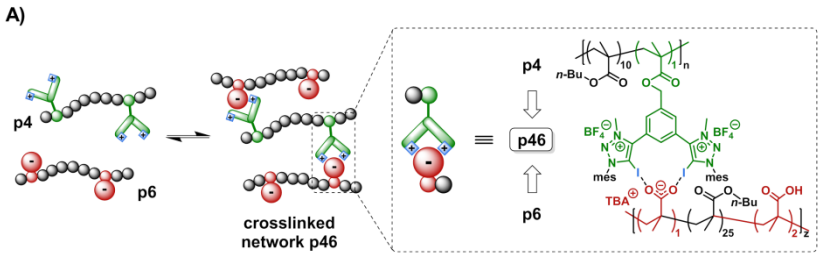

B)

Polymer Network	Stiffness E_i [GPa]	Hardnes s [MPa]
p25	1.82	60
p26	1.50	50
p36	1.55	55
p45	1.55	55
p46	1.71	62
BMA ref.	0.98	23

Figure 4.3: A) Schematic representation of the exemplary polymer network **p46** crosslinked *via* XB formation. B) Summary of indentation moduli (E_i) as well as hardness of the polymer networks. (Adapted with permission from ref. [183]. Copyright 2017 WILEY-VCH Verlag GmbH & Co. KGaA, Weinheim)

Nanoindentation experiments represent a standard technique to determine the mechanical properties, even in case of very little amounts of available material.[179, 184-185] The measurements revealed that the non-crosslinked pure BMA-based reference polymer exhibit a significantly lower stiffness compared to the donor / acceptor-based networks (**Figure 4.3 B**). These enhanced mechanical properties of the networks with indentation moduli (E_i) up to 1.82 GPa were assigned to the embedded bidentate receptor units, which enable a crosslinking due to the possible formation of 1:1 and 1:2 complexes between the donor units and the carboxylate groups of the polymers (*vide supra*). In line with the detected higher binding affinity of the XB interactions in solution (**Table 4.1**), also a slightly increased stiffness and hardness of the XB-based network (**p46**) compared to the HB-based analogue (**p36**) was observed.

Simultaneously, FT-Raman spectroscopy[186-188] was applied to prove the XB-based crosslinking of **p4** (charge-assisted donor) as well as **p2** (neutral donor) in their corresponding donor / acceptor networks **p46** and **p26** (**Figure 4.4 A** for **p46**). Thereby, the C–I stretching vibration as well as the triazolium ring vibration reacted sensitively to the formation of the XB interaction. Comparing the C–I stretching vibration in **p4** (295 cm^{-1}) with the one in the network **p46** (285 cm^{-1}), the wavenumber shift of 10 cm^{-1} represents a clear indication for a C–I bond lengthening[189-190] and, thus, is consistent with the expected charge transfer and partial population of the σ*(C–I) orbital upon XB formation.[72] In line with the expected weaker XB formation of the neutral donor system **p2** compared to **p4**, the corresponding network **p26** showed a smaller wavenumber shift of the C–I band (5 cm^{-1}).

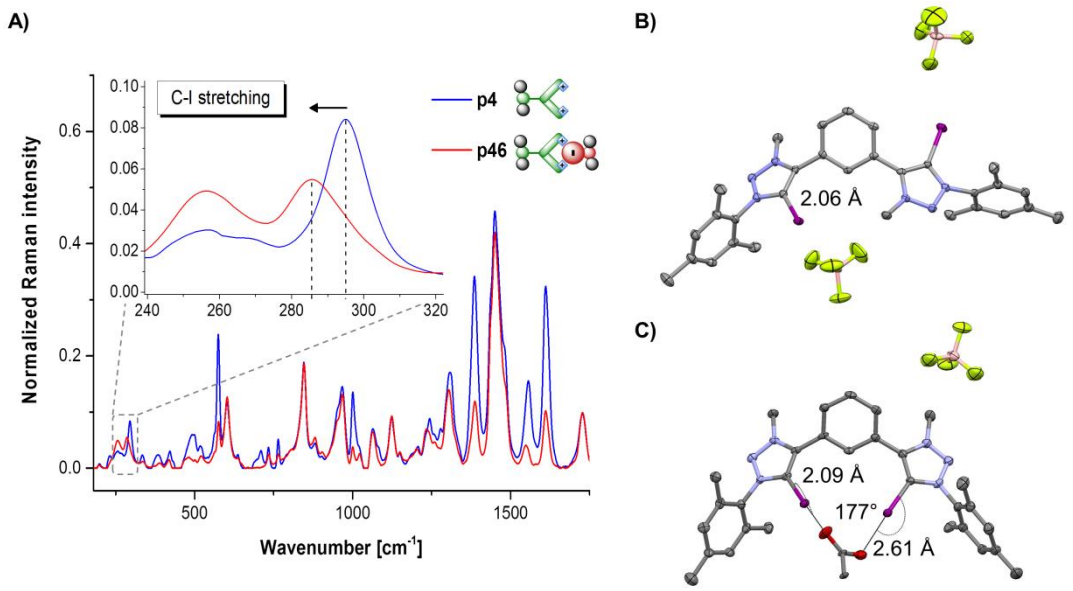

Figure 4.4: A) Normalized and background corrected FT-Raman spectrum of the copolymer **p4** (blue line) and the polymer network **p46** (red line) as well as (inset) the shift of the C–I bond from **p4** (295 cm^{-1}) to **p46** (285 cm^{-1}), which proves the network formation *via* XBs. B) Solid-state structures of the free reference receptor[191] as well as C) the interaction with acetate (thermal ellipsoids at 50% probability level, hydrogen atoms and solvent molecules are omitted for clarity; grey: carbon, blue: nitrogen, purple: iodine, yellow: fluorine, red: oxygen, and pink: boron). (Adapted with permission from ref. [183]. Copyright 2017 WILEY-VCH Verlag GmbH & Co. KGaA, Weinheim)

A comparison of the C–I bond lengths in the solid state structures of the free receptor[191] (2.06 Å) with the one in the acetate complex (2.09 Å) revealed a slight bond lengthening upon XB formation towards a strongly coordinated anion (**Figure 4.4 B**, **C**) and, thus, is in line with the observed bond weakening in the FT-Raman spectroscopy. Just like spherical guests,[99] also the acetate is bound in a cleft-type complexation through the formation of two nearly linear XBs (177° to 173°), which are significantly shorter (25% shortening) than the $\sum r_w(I\cdots O) = 3.50$ Å[85] and represent one of the shortest XB interactions with an oxo-anion that has been structurally observed up to now.[76]

Finally, these hard materials were examined regarding their self-healing behavior in thin films. As already explained in the beginning (**Figure 4.2**), the proven XB formation between the polymeric donor / acceptor pair (*vide supra*) constitutes the basis for this application. Satisfactorily, scratch tests[192] revealed a self-healing behavior of all donor / acceptor networks at 100 °C (see exemplarily **Figure 4.5 A)** with slight differences regarding the shortest healing time and the lowest healing temperature (**Figure 4.5 B)**. The sufficient thermal stability of all polymer networks ($T_d > 220$ °C)

was indicated by differential scanning calorimetry (DSC) and thermogravimetric analysis (TGA) investigations confirming no degradation at self-healing temperature. Interestingly, the combination of a XB-based donor with the partially anionic acceptor (**p26** and **p46**) required slightly higher temperatures for complete scratch healing, which is assigned to a stronger crosslinking and, thus, is in line with the detected stronger host-guest interaction in solution.

A)

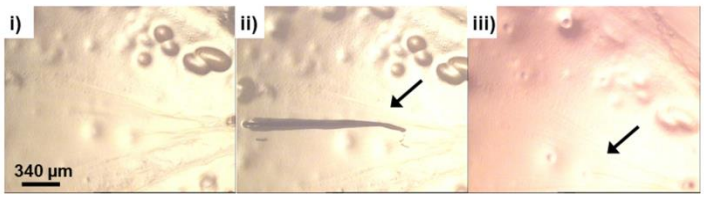

B)

Polymer Network	XB-based p25	p26	p45	p46	HB-based p36
lowest temp. [°C]	80	100	80	100	100
shortest time at 100 °C [h]	4	17	4	17	4

Figure 4.5: A) Self-healing behavior of the copolymer network **p46**. i) Film, ii) first scratch, iii) healing after 17 h at 100 °C. B) Summary of self-healing abilities of the polymer networks. (Adapted with permission from ref. [183]. Copyright 2017 WILEY-VCH Verlag GmbH & Co. KGaA, Weinheim)

In conclusion, although the familiar HB interaction has been extensively used in self-healing polymers, XBs were overlooked up to now and were for the first time comprehensively analyzed as driving force in healable polymeric networks. In this context, also the first systematic ITC study of polymeric XB donors was performed providing detailed information concerning their complexation behavior in solution. This knowledge from solution phase behavior in combination with a X-ray diffraction analysis, FT-Raman measurements as well as the information from nanoindentation experiments, gave insight towards a XB-based crosslinking in polymeric networks and, as a net result, helped to rationalize the thermally induced self-healing behavior.

4.4 Subsequent work using *bis*-bidentate linkers for formation of networks

Having established the first XB-based self-healing network based on a polymeric donor / acceptor pair, subsequent work concentrated on a flexible *bis*-bidentate linker unit between copolymers bearing accepting phosphate groups (**Scheme 4.2**).[193] In this context, the change from acetate to phosphate enabled the introduction of a stronger double negatively charged acceptor part,[99] which is linked by a flexible ethyl bridge to the polymer backbone to enhance the accessibility for the crosslinker. In addition, the two cleft-type receptor units of the linker are connected *via* an octanoic diester chain to increase the flexibility and, thus, to enable an efficient crosslinking in the later polymer network.

The bifunctional donor systems (**22** and **23**) were readily accessible exploiting the modular character of the respective benzyl alcohol derivatives (**18** and **19**) (**Scheme 4.1**) in a one-step synthesis with octanedioyl dichloride (**Scheme 4.2**). The polymeric acceptor **p7** (M_n(**p7**) = 15,100 g/mol, Đ = 1.2) was obtained by RAFT-polymerization of BMA with a phosphate-based functional comonomer and was afterwards treated with an excess of TBAOH to obtain the analogous anionic system **p8**.

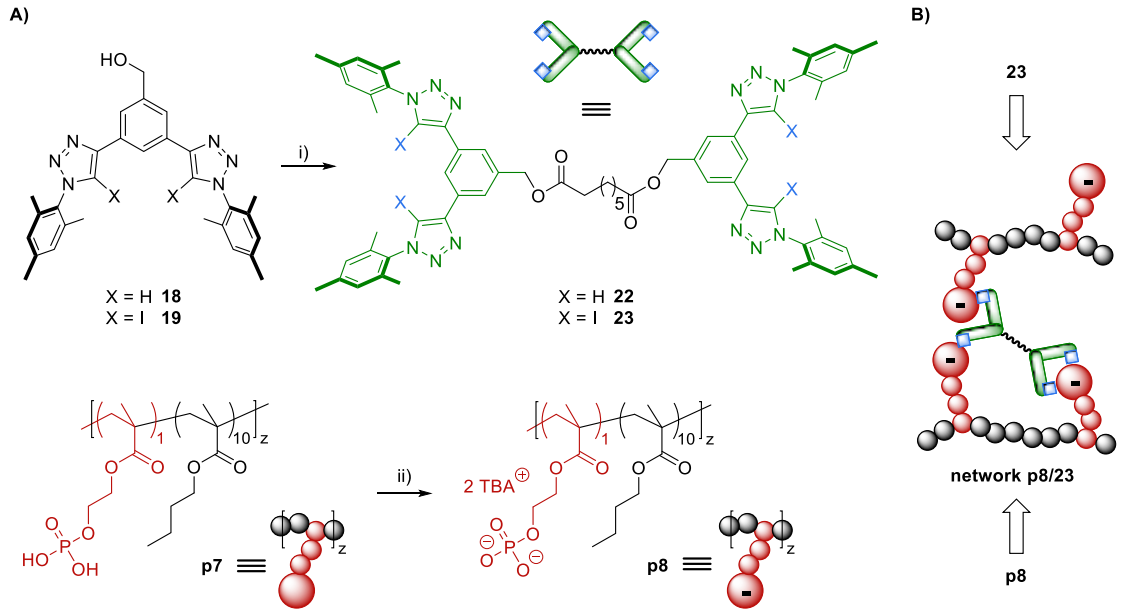

Scheme 4.2: A) Schematic representation of the synthesis of the *bis*-bidentate HB- and XB-based linker systems **22** and **23** (green, blue) as well as acceptor copolymers **p7** and **p8** (red). i) Octanedioyl dichloride, DMAP / Et_3N, CH_2Cl_2, rt, 97% (X = H), 92% (X = I); ii) TBAOH, $CHCl_3$, rt. B) Exemplary formation and nomenclature of polymer network **p8/23**. (Adapted from ref. [193] with permission from The Royal Society of Chemistry)

In analogy to the polymeric donor systems, ITC investigations were performed in solution first. Comparing the bromide affinity of the XB-based linker ($K(\mathbf{23}) = 2.76 \times 10^3\ M^{-1}$) with the analogous mono-functional reference compound ($K(\mathbf{1}) = 2.22 \times 10^3\ M^{-1}$, **Table 4.1**), nearly the same association constant was determined indicating only minor interactions between the two adjacent binding sites of linker **23**. Furthermore, the aimed *bis*-bidentate complexation mode of the linker was supported by a measured complex stoichiometry of $N(\mathbf{23}) = 1.78$ indicating two bound anions (one in each bidentate binding site). Afterwards, crosslinked polymer networks were prepared and again validated by FT-Raman measurements, which supported the desired XB-based crosslinking by the wavenumber shift of the triazole ring vibration (1524 cm^{-1} for **23** and 1520 cm^{-1} for network **p8/23**). This shift of 4 cm^{-1} is slightly smaller than the one observed in the previous project (8 cm^{-1} for **p46**) attributed to the missing charge-assistance of the donors and the consequently weaker XB interaction.

The beneficial effect of the XB-based crosslinker can be best explained by comparing the mechanical properties as well as the self-healing behavior of **p8** with the network **p8/23**. While **p8** already revealed a good healing behavior at 100 °C due to its ionomeric character and the associated intrinsic self-healing ability,[177, 194] the polymer simultaneously suffered from a low mechanical stability ($E_i(\mathbf{p8}) = 0.27$ GPa). The XB crosslinked network in contrast convinced with a significantly increased mechanical stability ($E_i(\mathbf{p8/23}) = 1.34$ GPa) by simultaneously maintaining the very good healing abilities at 100 °C. Noteworthy, the HB-based network only showed a minimal improvement of the mechanical stability ($E_i(\mathbf{p8/22}) = 0.40$ GPa) indicating a much weaker crosslinking compared to the XB-based interaction, which is in line with the expected weaker HB interaction observed in solution.[195]

5 Summary

The XB is a highly directional supramolecular interaction in which a covalently bound halogen X is polarized by an electron-withdrawing group R and, thus, is able to act as the electrophilic species (XB donor) in the presence of a Lewis base (XB acceptor).[26] Accordingly, the polarizability of X (I > Br > Cl > F) as well as the electron-withdrawing ability of R are key factors influencing the strength of the interaction.[68] While there are several similarities to the better known HB, in particular, the characteristic differences regarding the greater preference for linearity[71] combined with the potential tunability[55, 74] of the interaction strength as well as the better solvent resistance[92, 196] gives rise to the construction of highly functional and very selective XB-based binding sites.[27-28]

This thesis details on the design of anion receptors based on 1,2,3-triazole derivatives, which are readily prepared and functionalized by making use of azide–alkyne cycloaddition reactions. The obtained heterocycle convinced by its sufficient electron-withdrawing behavior to create strong XB or HB interactions to a Lewis base as well as its intrinsic heteroditopic character allowing additional supramolecular interactions with an electrophilic partner.[34-35] In order to allow XBs with maximum strength,[68] iodine-based XB donors were chosen and continuously compared to their HB-based analogous (see **Chapter 2** and **Scheme 5.1 blue frames**).

Chapter 3 describes the utilization of the intrinsic heteroditopic character of the triazole moiety in two different concepts to strongly improve the anion binding affinity of XB-based donor systems in solution (**Scheme 5.1 green frames**).

In a first attempt, intramolecular HBs formed between hydroxyl substituents of the central spacer unit and a nitrogen atom of adjacent iodo-1,2,3-triazoles were used to create a more rigid bidentate XB donor system (**Chapter 3.1**).[36] Hence, a relaxation of the receptor was already prevented in its uncomplexed form, *i.e.*, the preorganized receptor is spring-loaded for complexation, and, thus, a strongly improved halide complexation without entropic penalty (reorganization of the system) was enabled.

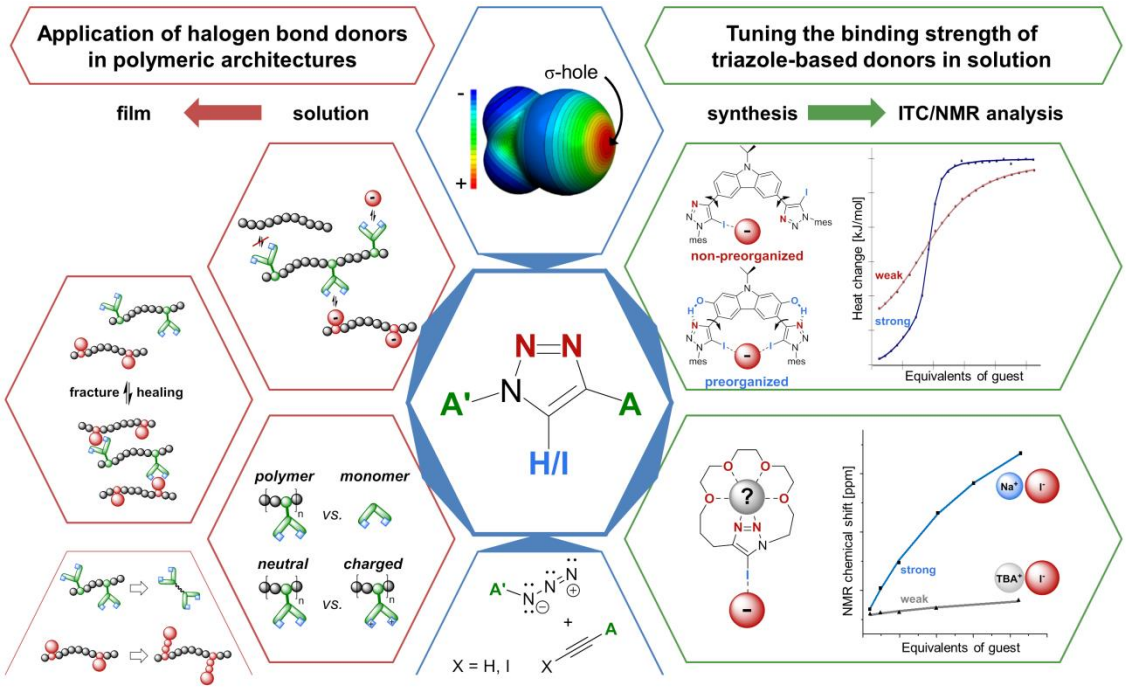

Scheme 5.1: Schematic representation of the 1,2,3-triazole unit as central building block for anion receptors with Lewis-basic nitrogen atoms (red), Lewis-acidic XB / HB donor atom (blue) and substituents A and A' (green) demonstrating modular synthetic character (blue frame). The anion binding affinity was tuned by taking advantage of the heteroditopic character of the heterocycle and was analyzed by NMR or ITC titration experiments in solution (green frame). Implementation of anion receptor units in a polymer backbone and their key parameters studied in solution as well as their application in crosslinked networks showing self-healing in thin films (red frame).

Following these building principle, charge-neutral receptors with high binding affinities can be designed.[145] Owing to the highly directional and strong XBs as well as to the absence of isotropic Coulomb interactions, these receptors offer great potential for applications as (enantio-) selective organo-catalysts in the future.[62, 102] In the second attempt, the iodo-1,2,3-triazole moiety was embedded into a crown-ether structure for simultaneous cation–anion binding through Lewis-basic nitrogen atoms and the XB-donating iodine atom (**Chapter 3.2**).[37] Here, the cation complexation induced cooperative effects, namely an additional Coulomb attraction and, in particular, the enhancement of the C–I bond polarization, strongly boosted the anion affinity of the macrocycle. While ITC titration experiments used in the first project enabled a detailed understanding of the complex stoichiometry, the binding affinity, and the thermodynamic effect of preorganization in solution by only one experiment, the ^{1}H and ^{13}C NMR titration experiments of the second project guaranteed a consistent and reliable analysis of two different binding places within one molecule to determine weak individual binding affinities as well as the cooperative effect.[162] Moreover, in both

projects the titration experiments in solution were supported by comprehensive solid-state analyses, selective ROESY experiments, and theoretic calculations.

Aiming at the design of functional supramolecular materials, bidentate receptor units were embedded into a polymeric architecture and were initially analyzed concerning their binding behavior in solution and finally also evaluated regarding the material properties in thin films as described in **Chapter 4** (**Scheme 5.1 red frames**).[183]

Therefore, comonomers containing cleft-type receptor units based on (partly charge-assisted) XB and HB interactions were copolymerized with BMA *via* RAFT to obtain polymeric donor systems. Noteworthy, despite a slight variation of the entropic contribution, the binding site of the polymeric donor behaved very similar compared to the monomeric reference system, indicating only minor influences of the polymer backbone on the complexation behavior in solution. The ITC studies additionally aided to reveal the significantly reduced binding affinity of analogous HB-based systems, the strong influence of charge-assistance boosting the anion affinity by about one order of magnitude as well as to confirm an attractive interaction even between completely polymer-based donor / acceptor pairs, which represents the basis to establish crosslinked polymer films. Upon film preparation, very hard materials with E_i up to 1.82 GPa were obtained representing the first indication for the desired network formation. In case of XB-based systems, a C–I bond lengthening, which is indicative for a partial population of the σ*(C–I) orbital upon XB formation,[72] was revealed by Raman spectroscopy and, consequently, further supports the XB-induced crosslinking. Finally, this strong but still reversible network formation constitutes the basis for the observed intrinsic self-healing behavior of the material, which enabled the thermally triggered correction of a mechanical damage.[192] Moreover, subsequent work concentrating on *bis*-bidentate linkers for network formation further impressively showed the benefits of strong XBs compared to the better known but weaker HB interaction by providing self-healing materials with a significantly increased mechanical stability (E_i(XB-based) = 1.34 GPa compared to E_i(HB-based) = 0.40 GPa). Thus, the combination of a XB-based crosslinker with a copolymer bearing accepting groups allowed the design of functional materials with good healing ability and simultaneously excellent mechanical performance required for later applications like coating materials. These first results may aid in the exploitation of the rich application potential of XB-

based supramolecular polymer architectures (*e.g.*, stimulus-responsive materials, stabilization of polymer blends).[38]

Ultimately, by employing iodo-1,2,3-triazole and iodo-1,2,3-triazolium units as XB-donors, a rapid synthetic access to highly functionalizable anion receptors with excellent binding affinities, which are suitable for applications as *e.g.*, sensor units, organo-catalysts or building blocks for supramolecular functional materials, is provided.

6 Zusammenfassung

Die XB beschreibt eine attraktive supramolekulare Wechselwirkung mit hoher Direktionalität, in der ein kovalent gebundenes Halogen X durch eine elektronenziehende Gruppe R polarisiert wird und somit in Gegenwart einer Lewis-Base (XB-Akzeptor) als Elektrophil (XB-Donor) fungieren kann.[26] Demzufolge sind die Polarisierbarkeit von X (I > Br > Cl > F) sowie die elektronenziehende Eigenschaften von R Schlüsselfaktoren für die Stärke dieser Wechselwirkung.[68] Es gibt zwar einige Analogien zu den bekannteren HB, jedoch ermöglichen besonders die charakteristischen Unterschiede hinsichtlich einer höheren Direktionalität[71] in Kombination mit einer leichteren Variation der Wechselwirkungsstärke[55, 74] sowie einem geringeren Lösungsmitteleinfluss[92, 196] die Konstruktion hochselektiver und funktioneller XB-basierter Bindungsstellen. [27-28]

Ziel dieser Arbeit war es, Anionenrezeptoren basierend auf 1,2,3-Triazolderivaten zu entwickeln, die mittels Cycloadditionsreaktionen zwischen organischen Aziden und Alkinen sehr leicht zugänglich und funktionalisierbar sind. Der so erhaltene Heterozyklus ermöglicht durch seine elektronenziehende Wirkung zum einen die Ausbildung starker XB- oder HB-Wechselwirkungen zu einer Lewis Base und gestattet zum anderen durch seinen intrinsischen heteroditopen Charakter zusätzliche supramolekulare Wechselwirkungen mit einem elektrophilen Partner.[34-35] Um möglichst große Wechselwirkungsstärken zu erzielen konzentrierte sich diese Arbeit auf Iod-basierte XB-Donoren,[68] welche kontinuierlich mit ihren analogen HB-basierten Systemen verglichen wurden (siehe **Kapitel 2** und **Schema 6.1 blaue Rahmen**).

Kapitel 3 beschreibt in zwei verschiedenen Konzepten die Verwendung des intrinsischen heteroditopischen Charakters der Triazoleinheit, mit dem Ziel, die Anionenbindungsaffinität von XB-basierten Donorsystemen in Lösung zu verbessern (**Schema 6.1 grüne Rahmen**).

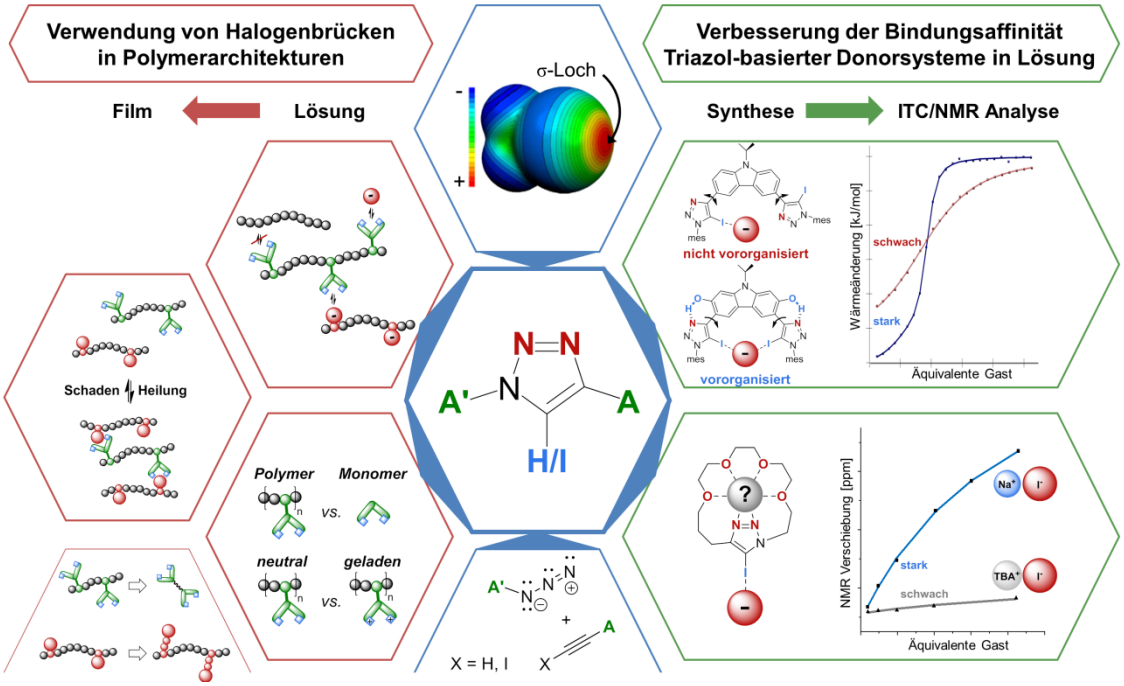

Schema 6.1: Schematische Darstellung der 1,2,3-Triazoleinheit als zentraler Baustein der Anionenrezeptoren mit Lewis-basischen Stickstoffatomen (rot), Lewis-saurem XB / HB-Donoratom (blau) und den modular variierbaren Substituenten A und A' (grün) (blaue Rahmen). Durch gezielte Nutzung des heteroditopischen Charakters des Heterozyklus konnte die Anionenaffinität der Systeme verbessert und anschließend mittels NMR- oder ITC-Titrationsexperimenten in Lösung analysiert werden (grüne Rahmen). In ein Polymergerüst eingebettete Rezeptoreinheiten wurden zunächst auf ihre ausschlaggebenden Parameter in Lösung und anschließend auf ihre selbstheilenden Eigenschaften in vernetzten Polymerfilmen untersucht (rote Rahmen).

Im ersten Abschnitt wurden intramolekulare HBs zwischen Hydroxylgruppen der zentralen Einheit und einem Stickstoffatom benachbarter Iod-1,2,3-triazole verwendet, um ein versteiftes zweizähniges XB-Donorsystem zu erhalten (**Kapitel 3.1**).[36] Somit konnte die Beweglichkeit des Rezeptors bereits in seiner freien Form stark eingeschränkt und das System für die Komplexierung vororientiert werden. Ein entropisches Hemmnis (Reorganisation des Systems) wurde somit in dem vororganisierten Rezeptor vermieden und folglich eine stark erhöhte Bindungsaffinität zu Halogeniden ermöglicht. Diesem Konzept folgend können ladungsneutrale Rezeptoren mit hohen Bindungsaffinitäten entworfen werden,[145] welche aufgrund der hohen Direktionalität und Stärke von XBs sowie der Abwesenheit isotroper Coulomb-Wechselwirkungen ein großes Potenzial für mögliche zukünftige Anwendungen als (enantio-) selektive Organokatalysatoren aufweisen.[62, 102] Im zweiten Abschnitt wurde die Iod-1,2,3-triazoleinheit in eine Kronenether-Struktur eingebettet. Die Kombination aus Lewis-basischen Stickstoffatomen und Lewis-saurem XB-Donor eröffnete dabei die

Möglichkeit einer simultanen Bindung von Kation und Anion in einem Ionenpaar-Rezeptor (**Kapitel 3.2**).[37] Die durch die Kationenkomplexierung induzierten kooperativen Effekte (das heißt eine zusätzliche Coulomb-Anziehung und insbesondere eine Verstärkung der Polarisation der C–I Bindung) bewirkten dabei eine enorme Verstärkung der Anionenaffinität des Makrozyklus. Dabei ermöglichten die im ersten Projekt verwendeten ITC Titrationsexperimente ein schnelles und detailliertes Verständnis bezüglich Komplex-Stöchiometrie, Bindungsaffinität und thermodynamischer Effekte der Vororganisation in Lösung. ^{1}H und ^{13}C NMR Titrationsexperimente des zweiten Projekts garantierten dagegen eine konsistente sowie zuverlässige Analyse von zwei individuellen Bindungsstellen innerhalb eines Moleküls, um zum einen die relativ schwachen individuellen Bindungsaffinitäten und zum anderen den finalen kooperativen Effekt zu bestimmen.[162] Darüber hinaus wurden die durchgeführten Titrationsexperimente in beiden Projekten durch selektive ROESY-Experimente sowie umfassende Kristallstrukturanalysen und theoretische Berechnungen unterstützt.

Für die Anwendung in funktionalen supramolekularen Materialien wurden zweizähnige Rezeptoreinheiten in eine polymere Architektur eingebettet und zunächst hinsichtlich ihres Bindungsverhaltens in Lösung bewertet, um anschließend ebenfalls ihre Materialeigenschaften in dünnen Filmen besser zu verstehen (siehe **Kapitel 4** und **Schema 6.1 rote Rahmen**).[183]

Um entsprechende polymerbasierte Donorsysteme zu erhalten, wurden (teilweise ladungsunterstützte) XB- und HB-basierende Rezeptoreinheiten als Comonomer verwendet und zusammen mit BMA mittels RAFT copolymerisiert. Bemerkenswert war, dass bis auf einen leicht veränderten entropischen Beitrag die Bindungseigenschaften des polymerbasierten Donors sehr gut mit denen des monomeren Referenzsystems übereinstimmten und somit nur ein sehr geringer Einfluss des Polymerrückgrats auf das Komplexierungsverhalten in Lösung zu beobachten war. ITC-Studien zeigten außerdem neben den stark reduzierten Bindungsaffinitäten analoger HB-basierter Systeme noch den starken Einfluss der zusätzlichen Coulomb-Wechselwirkung (Ladungsassistenz) an, welche die Anionenaffinität der Donoren um etwa eine Größenordnung erhöhte. Weiterhin wurde die attraktive Wechselwirkung zwischen vollständig polymerbasierten Donor / Akzeptor-Paaren bestätigt und somit die

Grundlage für die anschließende Herstellung vernetzter Polymerfilme gelegt. Bei der Filmherstellung wurden sehr harte Materialien mit einem E_i-Modul von bis zu 1,82 GPa erhalten, was einen ersten Hinweis auf die gewünschte Netzwerkbildung darstellte. Im Fall der XB-basierten Systeme wurde mittels Raman-Spektroskopie eine Verlängerung der C–I Bindung festgestellt, welche auf eine partielle Population des σ*(C–I) Orbitals durch Ausbildung einer XB hindeutete,[72] und somit ein weiteres Indiz der XB-induzierten Vernetzung gefunden. Letztendlich bildete diese starke, aber dennoch reversible Vernetzung die Grundlage für das beobachtete intrinsische Selbstheilungsverhalten des Materials, welches ihm eine thermisch induzierte Korrektur eines mechanischen Schadens ermöglichte.[192] Darüber hinaus unterstrichen nachfolgende Arbeiten mit bifunktionellen Linkern zur Netzwerkbildung eindrucksvoll die Vorteile der XB. Im Vergleich zu den zwar bekannteren, aber deutlich schwächeren HB-Wechselwirkungen ermöglichten die XB die Herstellung selbstheilender Materialien mit signifikant erhöhter mechanischer Stabilität (E_i(XB-basiert) = 1,34 GPa im Vergleich zu E_i (HB-basiert) = 0,40 GPa). Auf diese Weise konnte gezeigt werden, dass die Kombination eines XB-basierten Vernetzers mit einem Akzeptorgruppen tragenden Copolymer die Entwicklung funktioneller Materialien mit guten Selbstheilungsfähigkeiten und gleichzeitig ausgezeichneten mechanischen Stabilitäten eröffnete, welche speziell für spätere Anwendungsgebiete wie beispielsweise in Beschichtungsmaterialien interessant wäre. Diese ersten grundlegenden Ergebnisse können bei der künftigen Anwendung der XBs im Rahmen XB-basierter supramolekularer Polymerarchitekturen (z. B. schaltbare Materialien oder Stabilisierung von Polymermischungen) helfen.[38]

Letztlich wurde durch die Verwendung von Iod-1,2,3-triazol- und Iod-1,2,3-triazolium-Einheiten als XB-Donoren der Aufbau hochfunktionalisierbarer Anionenrezeptoren mit exzellenten Bindungsaffinitäten sowie einem schnellen synthetischen Zugang ermöglicht, welche sich für Anwendungen beispielsweise in Sensoreinheiten, Organokatalysatoren oder als Bausteine für supramolekulare funktionelle Materialien eignen.

7 References

[1] J. M. Lehn, E. Sonveaux, A. K. Willard, *J. Am. Chem. Soc.* **1978**, *100*, 4914-4916.
[2] E. Graf, J. M. Lehn, *J. Am. Chem. Soc.* **1976**, *98*, 6403-6405.
[3] C. H. Park, H. E. Simmons, *J. Am. Chem. Soc.* **1968**, *90*, 2431-2432.
[4] P. A. Gale, E. N. W. Howe, X. Wu, M. J. Spooner, *Coord. Chem. Rev.* **2018**, DOI: 10.1016/j.ccr.2018.1002.1005.
[5] J. Zhao, D. Yang, X.-J. Yang, B. Wu, *Coord. Chem. Rev.* **2018**, DOI: 10.1016/j.ccr.2018.1001.1002.
[6] P. D. Beer, P. A. Gale, *Angew. Chem. Int. Ed.* **2001**, *40*, 486-516.
[7] P. A. Gale, E. N. W. Howe, X. Wu, *Chem* **2016**, *1*, 351-422.
[8] P. A. Gale, C. Caltagirone, *Chem. Soc. Rev.* **2015**, *44*, 4212-4227.
[9] N. Busschaert, C. Caltagirone, W. Van Rossom, P. A. Gale, *Chem. Rev.* **2015**, *115*, 8038-8155.
[10] D. W. Schindler, *Science* **1974**, *184*, 897-899.
[11] R. Vilar, *Angew. Chem. Int. Ed.* **2003**, *42*, 1460-1477.
[12] N. Gimeno, R. Vilar, *Coord. Chem. Rev.* **2006**, *250*, 3161-3189.
[13] M. J. Langton, P. D. Beer, *Acc. Chem. Res.* **2014**, *47*, 1935-1949.
[14] T. A. Barendt, A. Docker, I. Marques, V. Félix, P. D. Beer, *Angew. Chem. Int. Ed.* **2016**, *55*, 11069-11076.
[15] D. A. Leigh, *Angew. Chem. Int. Ed.* **2016**, *55*, 14506-14508.
[16] Z. Zhang, P. R. Schreiner, *Chem. Soc. Rev.* **2009**, *38*, 1187-1198.
[17] A. G. Doyle, E. N. Jacobsen, *Chem. Rev.* **2007**, *107*, 5713-5743.
[18] P. H.-Y. Cheong, C. Y. Legault, J. M. Um, N. Çelebi-Ölçüm, K. N. Houk, *Chem. Rev.* **2011**, *111*, 5042-5137.
[19] A. Vargas Jentzsch, A. Hennig, J. Mareda, S. Matile, *Acc. Chem. Res.* **2013**, *46*, 2791-2800.
[20] A. P. Davis, D. N. Sheppard, B. D. Smith, *Chem. Soc. Rev.* **2007**, *36*, 348-357.
[21] P. A. Gale, J. T. Davis, R. Quesada, *Chem. Soc. Rev.* **2017**, *46*, 2497-2519.
[22] S. Matile, A. Vargas Jentzsch, J. Montenegro, A. Fin, *Chem. Soc. Rev.* **2011**, *40*, 2453-2474.
[23] M. J. Langton, C. J. Serpell, P. D. Beer, *Angew. Chem. Int. Ed.* **2016**, *55*, 1974-1987.
[24] S. Kubik, C. Reyheller, S. Stüwe, *J. Incl. Phenom. Macrocycl. Chem.* **2005**, *52*, 137-187.
[25] F. P. Schmidtchen, *Chem. Soc. Rev.* **2010**, *39*, 3916-3935.
[26] G. R. Desiraju, P. S. Ho, L. Kloo, A. C. Legon, R. Marquardt, P. Metrangolo, P. Politzer, G. Resnati, K. Rissanen, *Pure Appl. Chem.* **2013**, *85*, 1711-1713.
[27] G. Cavallo, P. Metrangolo, R. Milani, T. Pilati, A. Priimägi, G. Resnati, G. Terraneo, *Chem. Rev.* **2016**, *116*, 2478-2601.
[28] L. C. Gilday, S. W. Robinson, T. A. Barendt, M. J. Langton, B. R. Mullaney, P. D. Beer, *Chem. Rev.* **2015**, *115*, 7118-7195.
[29] S. H. Jungbauer, S. Schindler, E. Herdtweck, S. Keller, S. M. Huber, *Chem. Eur. J.* **2015**, *21*, 13625-13636.
[30] M. G. Sarwar, B. Dragisic, S. Sagoo, M. S. Taylor, *Angew. Chem. Int. Ed.* **2010**, *49*, 1674-1677.
[31] N. Schulz, P. Sokkar, E. Engelage, S. Schindler, M. Erdelyi, E. Sanchez-Garcia, S. M. Huber, *Chem. Eur. J.* **2018**, *24*, 3464-3473.

[32] M. S. Taylor, in *Halogen Bonding II: Impact on Materials Chemistry and Life Sciences* (Eds.: P. Metrangolo, G. Resnati), Springer International Publishing, Cham, **2015**.
[33] J. Y. C. Lim, P. D. Beer, *Chem* **2018**, *4*, 731-783.
[34] B. Schulze, U. S. Schubert, *Chem. Soc. Rev.* **2014**, *43*, 2522-2571.
[35] Y. Hua, A. H. Flood, *Chem. Soc. Rev.* **2010**, *39*, 1262-1271.
[36] R. Tepper, B. Schulze, H. Görls, P. Bellstedt, M. Jäger, U. S. Schubert, *Org. Lett.* **2015**, *17*, 5740-5743.
[37] R. Tepper, B. Schulze, P. Bellstedt, J. Heidler, H. Görls, M. Jäger, U. S. Schubert, *Chem. Commun.* **2017**, *53*, 2260-2263.
[38] G. Berger, J. Soubhye, F. Meyer, *Polym. Chem.* **2015**, *6*, 3559-3580.
[39] F. Meyer, P. Dubois, *CrystEngComm* **2013**, *15*, 3058-3071.
[40] M. Colin, *Ann. Chim.* **1814**, *91*, 252-272.
[41] F. Guthrie, *J. Chem. Soc.* **1863**, *16*, 239-244.
[42] R. S. Mulliken, *J. Am. Chem. Soc.* **1950**, *72*, 600-608.
[43] O. Hassel, *Science* **1970**, *170*, 497-502.
[44] M. T. Messina, P. Metrangolo, W. Panzeri, E. Ragg, G. Resnati, *Tetrahedron Lett.* **1998**, *39*, 9069-9072.
[45] A. Farina, S. V. Meille, M. T. Messina, P. Metrangolo, G. Resnati, G. Vecchio, *Angew. Chem. Int. Ed.* **1999**, *38*, 2433-2436.
[46] H. Wang, W. Wang, W. J. Jin, *Chem. Rev.* **2016**, *116*, 5072-5104.
[47] M. H. Kolář, P. Hobza, *Chem. Rev.* **2016**, *116*, 5155-5187.
[48] A. Mukherjee, S. Tothadi, G. R. Desiraju, *Acc. Chem. Res.* **2014**, *47*, 2514-2524.
[49] P. Metrangolo, H. Neukirch, T. Pilati, G. Resnati, *Acc. Chem. Res.* **2005**, *38*, 386-395.
[50] Z. Han, G. Czap, C.-l. Chiang, C. Xu, P. J. Wagner, X. Wei, Y. Zhang, R. Wu, W. Ho, *Science* **2017**, *358*, 206-210.
[51] R. Bertani, P. Sgarbossa, A. Venzo, F. Lelj, M. Amati, G. Resnati, T. Pilati, P. Metrangolo, G. Terraneo, *Coord. Chem. Rev.* **2010**, *254*, 677-695.
[52] G. Resnati, E. Boldyreva, P. Bombicz, M. Kawano, *IUCrJ* **2015**, *2*, 675-690.
[53] R. W. Troff, T. Mäkelä, F. Topić, A. Valkonen, K. Raatikainen, K. Rissanen, *Eur. J. Org. Chem.* **2013**, *2013*, 1617-1637.
[54] P. Metrangolo, G. Resnati, T. Pilati, R. Liantonio, F. Meyer, *J. Polym. Sci., Part A: Polym. Chem.* **2007**, *45*, 1-15.
[55] A. Priimagi, G. Cavallo, P. Metrangolo, G. Resnati, *Acc. Chem. Res.* **2013**, *46*, 2686-2695.
[56] P. S. Ho, *Future Med. Chem.* **2017**, *9*, 637-640.
[57] E. Parisini, P. Metrangolo, T. Pilati, G. Resnati, G. Terraneo, *Chem. Soc. Rev.* **2011**, *40*, 2267-2278.
[58] R. Wilcken, M. O. Zimmermann, A. Lange, A. C. Joerger, F. M. Boeckler, *J. Med. Chem.* **2013**, *56*, 1363-1388.
[59] M. H. Kolář, O. Tabarrini, *J. Med. Chem.* **2017**, *60*, 8681-8690.
[60] T. M. Beale, M. G. Chudzinski, M. G. Sarwar, M. S. Taylor, *Chem. Soc. Rev.* **2013**, *42*, 1667-1680.
[61] A. Brown, P. D. Beer, *Chem. Commun.* **2016**, *52*, 8645-8658.
[62] D. Bulfield, S. M. Huber, *Chem. Eur. J.* **2016**, *22*, 14434-14450.
[63] M. Erdelyi, *Chem. Soc. Rev.* **2012**, *41*, 3547-3557.
[64] Y. Zhao, Y. Cotelle, N. Sakai, S. Matile, *J. Am. Chem. Soc.* **2016**, *138*, 4270-4277.

[65] R. Tepper, U. S. Schubert, *Angew. Chem. Int. Ed.* **2018**, DOI: 10.1002/anie.201707986.
[66] M. Breugst, D. von der Heiden, J. Schmauck, *Synthesis* **2017**, *49*, 3224-3236.
[67] P. Metrangolo, F. Meyer, T. Pilati, G. Resnati, G. Terraneo, *Angew. Chem. Int. Ed.* **2008**, *47*, 6114-6127.
[68] T. Clark, M. Hennemann, J. S. Murray, P. Politzer, *J. Mol. Model.* **2007**, *13*, 291-296.
[69] M. G. Chudzinski, C. A. McClary, M. S. Taylor, *J. Am. Chem. Soc.* **2011**, *133*, 10559-10567.
[70] J. Thirman, E. Engelage, S. M. Huber, M. Head-Gordon, *Phys. Chem. Chem. Phys.* **2018**, *20*, 905-915.
[71] S. M. Huber, J. D. Scanlon, E. Jimenez-Izal, J. M. Ugalde, I. Infante, *Phys. Chem. Chem. Phys.* **2013**, *15*, 10350-10357.
[72] S. V. Rosokha, C. L. Stern, J. T. Ritzert, *Chem. Eur. J.* **2013**, *19*, 8774-8788.
[73] C. Wang, D. Danovich, Y. Mo, S. Shaik, *J. Chem. Theory Comput.* **2014**, *10*, 3726-3737.
[74] P. Politzer, P. Lane, M. C. Concha, Y. Ma, J. S. Murray, *J. Mol. Model.* **2007**, *13*, 305-311.
[75] K. E. Riley, P. Hobza, *J. Chem. Theory Comput.* **2008**, *4*, 232-242.
[76] N. G. White, A. Caballero, P. D. Beer, *CrystEngComm* **2014**, *16*, 3722-3729.
[77] Z. P. Shields, J. S. Murray, P. Politzer, *Int. J. Quantum Chem* **2010**, *110*, 2823-2832.
[78] C. J. Serpell, N. L. Kilah, P. J. Costa, V. Félix, P. D. Beer, *Angew. Chem. Int. Ed.* **2010**, *49*, 5322-5326.
[79] V. Vasylyeva, S. K. Nayak, G. Terraneo, G. Cavallo, P. Metrangolo, G. Resnati, *CrystEngComm* **2014**, *16*, 8102-8105.
[80] A. R. Voth, P. Khuu, K. Oishi, P. S. Ho, *Nat. Chem.* **2009**, *1*, 74.
[81] K. E. Riley, J. S. Murray, J. Fanfrlík, J. Řezáč, R. J. Solá, M. C. Concha, F. M. Ramos, P. Politzer, *J. Mol. Model.* **2011**, *17*, 3309-3318.
[82] P. Metrangolo, J. S. Murray, T. Pilati, P. Politzer, G. Resnati, G. Terraneo, *CrystEngComm* **2011**, *13*, 6593-6596.
[83] M. Göbel, B. H. Tchitchanov, J. S. Murray, P. Politzer, T. M. Klapötke, *Nat. Chem.* **2009**, *1*, 229.
[84] D. V. Levchenkov, A. B. Kharitonkin, V. A. Shlyapochnikov, *Russ. Chem. Bull.* **2001**, *50*, 385-389.
[85] A. Bondi, *J. Phys. Chem.* **1964**, *68*, 441-451.
[86] A. J. Parker, J. Stewart, K. J. Donald, C. A. Parish, *J. Am. Chem. Soc.* **2012**, *134*, 5165-5172.
[87] E. Persch, O. Dumele, F. Diederich, *Angew. Chem. Int. Ed.* **2015**, *54*, 3290-3327.
[88] F. Zapata, A. Caballero, N. G. White, T. D. W. Claridge, P. J. Costa, V. Félix, P. D. Beer, *J. Am. Chem. Soc.* **2012**, *134*, 11533-11541.
[89] B. Pinter, N. Nagels, W. A. Herrebout, F. De Proft, *Chem. Eur. J.* **2013**, *19*, 519-530.
[90] A. V. Jentzsch, D. Emery, J. Mareda, S. K. Nayak, P. Metrangolo, G. Resnati, N. Sakai, S. Matile, *Nat. Commun.* **2012**, *3*, 905.
[91] V. Gutmann, *Coord. Chem. Rev.* **1976**, *18*, 225-255.
[92] C. C. Robertson, R. N. Perutz, L. Brammer, C. A. Hunter, *Chem. Sci.* **2014**, *5*, 4179-4183.
[93] Y. Lu, H. Li, X. Zhu, W. Zhu, H. Liu, *J. Phys. Chem. A* **2011**, *115*, 4467-4475.

[94] N. B. Wageling, G. F. Neuhaus, A. M. Rose, D. A. Decato, O. B. Berryman, *Supramol. Chem.* **2015**, *28*, 665-672.
[95] C. J. Massena, N. B. Wageling, D. A. Decato, E. Martin Rodriguez, A. M. Rose, O. B. Berryman, *Angew. Chem. Int. Ed.* **2016**, *55*, 12398-12402.
[96] R. Puttreddy, O. Jurcek, S. Bhowmik, T. Makela, K. Rissanen, *Chem. Commun.* **2016**, *52*, 2338-2341.
[97] O. Dumele, D. Wu, N. Trapp, N. Goroff, F. Diederich, *Org. Lett.* **2014**, *16*, 4722-4725.
[98] S. M. Walter, F. Kniep, L. Rout, F. P. Schmidtchen, E. Herdtweck, S. M. Huber, *J. Am. Chem. Soc.* **2012**, *134*, 8507-8512.
[99] R. Tepper, B. Schulze, M. Jäger, C. Friebe, D. H. Scharf, H. Görls, U. S. Schubert, *J. Org. Chem.* **2015**, *80*, 3139-3150.
[100] G. Cavallo, G. Terraneo, A. Monfredini, M. Saccone, A. Priimagi, T. Pilati, G. Resnati, P. Metrangolo, D. W. Bruce, *Angew. Chem. Int. Ed.* **2016**, *55*, 6300-6304.
[101] F. Pan, N. K. Beyeh, K. Rissanen, *J. Am. Chem. Soc.* **2015**, *137*, 10406-10413.
[102] S. H. Jungbauer, S. M. Huber, *J. Am. Chem. Soc.* **2015**, *137*, 12110-12120.
[103] M. Saito, Y. Kobayashi, S. Tsuzuki, Y. Takemoto, *Angew. Chem. Int. Ed.* **2017**, *56*, 7653-7657.
[104] A. Vargas Jentzsch, S. Matile, *J. Am. Chem. Soc.* **2013**, *135*, 5302-5303.
[105] L. Maugeri, E. Jamieson, D. B. Cordes, A. Slawin, D. Philp, *Chem. Sci.* **2016**, *8*, 938-945.
[106] J. Y. C. Lim, I. Marques, L. Ferreira, V. Félix, P. D. Beer, *Chem. Commun.* **2016**, *52*, 5527-5530.
[107] J. Y. C. Lim, M. J. Cunningham, J. J. Davis, P. D. Beer, *Chem. Commun.* **2015**, *51*, 14640-14643.
[108] B. T. Worrell, J. A. Malik, V. V. Fokin, *Science* **2013**, *340*, 457-460.
[109] V. V. Rostovtsev, L. G. Green, V. V. Fokin, K. B. Sharpless, *Angew. Chem. Int. Ed.* **2002**, *41*, 2596-2599.
[110] R. Huisgen, *Angew. Chem. Int. Ed.* **1963**, *2*, 565-598.
[111] H. C. Kolb, M. G. Finn, K. B. Sharpless, *Angew. Chem. Int. Ed.* **2001**, *40*, 2004-2021.
[112] M. Meldal, C. W. Tornøe, *Chem. Rev.* **2008**, *108*, 2952-3015.
[113] C. Shao, G. Cheng, D. Su, J. Xu, X. Wang, Y. Hu, *Adv. Synth. Catal.* **2010**, *352*, 1587-1592.
[114] B. F. Straub, *Chem. Commun.* **2007**, 3868-3870.
[115] M. Ahlquist, V. V. Fokin, *Organometallics* **2007**, *26*, 4389-4391.
[116] J. E. Hein, J. C. Tripp, L. B. Krasnova, K. B. Sharpless, V. V. Fokin, *Angew. Chem. Int. Ed.* **2009**, *48*, 8018-8021.
[117] T. R. Chan, R. Hilgraf, K. B. Sharpless, V. V. Fokin, *Org. Lett.* **2004**, *6*, 2853-2855.
[118] V. E. Matulis, Y. S. Halauko, O. A. Ivashkevich, P. N. Gaponik, *J. Mol. Struct. – Theochem* **2009**, *909*, 19-24.
[119] M. Juríček, K. Stout, P. H. J. Kouwer, A. E. Rowan, *Org. Lett.* **2011**, *13*, 3494-3497.
[120] B. H. M. Kuijpers, G. C. T. Dijkmans, S. Groothuys, P. J. L. M. Quaedflieg, R. H. Blaauw, F. L. van Delft, F. P. J. T. Rutjes, *Synlett* **2005**, 3059-3062.
[121] Y.-M. Wu, J. Deng, Y. Li, Q.-Y. Chen, *Synthesis* **2005**, *2005*, 1314-1318.
[122] W. S. Brotherton, R. J. Clark, L. Zhu, *J. Org. Chem.* **2012**, *77*, 6443-6455.
[123] L. Li, G. Zhang, A. Zhu, L. Zhang, *J. Org. Chem.* **2008**, *73*, 3630-3633.

[124] N. L. Kilah, M. D. Wise, C. J. Serpell, A. L. Thompson, N. G. White, K. E. Christensen, P. D. Beer, *J. Am. Chem. Soc.* **2010**, *132*, 11893-11895.
[125] F. Kniep, L. Rout, S. M. Walter, H. K. V. Bensch, S. H. Jungbauer, E. Herdtweck, S. M. Huber, *Chem. Commun.* **2012**, *48*, 9299-9301.
[126] C. Caumes, O. Roy, S. Faure, C. Taillefumier, *J. Am. Chem. Soc.* **2012**, *134*, 9553-9556.
[127] K. F. Donnelly, A. Petronilho, M. Albrecht, *Chem. Commun.* **2013**, *49*, 1145-1159.
[128] T. L. Mindt, H. Struthers, L. Brans, T. Anguelov, C. Schweinsberg, V. Maes, D. Tourwé, R. Schibli, *J. Am. Chem. Soc.* **2006**, *128*, 15096-15097.
[129] J. Y. C. Lim, I. Marques, V. Félix, P. D. Beer, *J. Am. Chem. Soc.* **2017**, *139*, 12228-12239.
[130] J. Y. C. Lim, I. Marques, V. Félix, P. D. Beer, *Angew. Chem. Int. Ed.* **2018**, *57*, 584-588.
[131] M. J. Langton, I. Marques, S. W. Robinson, V. Félix, P. D. Beer, *Chem. Eur. J.* **2016**, *22*, 185-192.
[132] B. Chowdhury, S. Sinha, P. Ghosh, *Chem. Eur. J.* **2016**, *22*, 18051-18059.
[133] L. González, F. Zapata, A. Caballero, P. Molina, C. Ramírez de Arellano, I. Alkorta, J. Elguero, *Chem. Eur. J.* **2016**, *22*, 7533-7544.
[134] J. Y. C. Lim, P. D. Beer, *Eur. J. Inorg. Chem.* **2017**, *2017*, 220-224.
[135] A. Borissov, J. Y. C. Lim, A. Brown, K. Christensen, A. L. Thompson, M. D. Smith, P. D. Beer, *Chem. Commun.* **2017**, *53*, 2483-2486.
[136] M. Kaasik, S. Kaabel, K. Kriis, I. Järving, R. Aav, K. Rissanen, T. Kanger, *Chem. Eur. J.* **2017**, *23*, 7337-7344.
[137] T. K. Mole, W. E. Arter, I. Marques, V. Félix, P. D. Beer, *J. Organomet. Chem.* **2015**, *792*, 206-210.
[138] D. Mungalpara, S. Stegmuller, S. Kubik, *Chem. Commun.* **2017**, *53*, 5095-5098.
[139] J. Y. C. Lim, T. Bunchuay, P. D. Beer, *Chem. Eur. J.* **2017**, *23*, 4700-4707.
[140] L. Maugeri, J. Asencio-Hernandez, T. Lebl, D. B. Cordes, A. Slawin, M.-A. Delsuc, D. Philp, *Chem. Sci.* **2016**, *7*, 6422-6428.
[141] F. Kniep, S. H. Jungbauer, Q. Zhang, S. M. Walter, S. Schindler, I. Schnapperelle, E. Herdtweck, S. M. Huber, *Angew. Chem. Int. Ed.* **2013**, *52*, 7028-7032.
[142] A. Matsuzawa, S. Takeuchi, K. Sugita, *Chem. Asian J.* **2016**, *11*, 2863-2866.
[143] B. R. Mullaney, B. E. Partridge, P. D. Beer, *Chem. Eur. J.* **2015**, *21*, 1660-1665.
[144] B. R. Mullaney, A. L. Thompson, P. D. Beer, *Angew. Chem. Int. Ed.* **2014**, *126*, 11642-11646.
[145] S. Lee, Y. Hua, H. Park, A. H. Flood, *Org. Lett.* **2010**, *12*, 2100-2102.
[146] K. P. McDonald, R. O. Ramabhadran, S. Lee, K. Raghavachari, A. H. Flood, *Org. Lett.* **2011**, *13*, 6260-6263.
[147] K. P. McDonald, B. Qiao, E. B. Twum, S. Lee, P. J. Gamache, C.-H. Chen, Y. Yi, A. H. Flood, *Chem. Commun.* **2014**, *50*, 13285-13288.
[148] S. C. Picot, B. R. Mullaney, P. D. Beer, *Chem. Eur. J.* **2012**, *18*, 6230-6237.
[149] H. Tomiyasu, N. Shigyo, X.-L. Ni, X. Zeng, C. Redshaw, T. Yamato, *Tetrahedron* **2014**, *70*, 7893-7899.
[150] M. a. d. C. González, F. Otón, R. A. Orenes, A. Espinosa, A. Tárraga, P. Molina, *Organometallics* **2014**, *33*, 2837-2852.
[151] A. J. McConnell, P. D. Beer, *Angew. Chem. Int. Ed.* **2012**, *51*, 5052-5061.
[152] S. K. Kim, J. L. Sessler, *Chem. Soc. Rev.* **2010**, *39*, 3784-3809.

[153] P. D. Beer, M. J. Langton, in *Macrocyclic and Supramolecular Chemistry* (Ed.: R. M. Izatt), John Wiley & Sons, Ltd, Chichester, UK, **2016**.
[154] B. D. Smith, in *Macrocyclic Chemistry: Current Trends and Future Prospectives* (Ed.: K. Gloe), Springer, Netherlands, **2005**.
[155] P. A. Gale, *Chem. Commun.* **2011**, *47*, 82-86.
[156] G. W. Gokel, W. M. Leevy, M. E. Weber, *Chem. Rev.* **2004**, *104*, 2723-2750.
[157] A. Ikeda, S. Shinkai, *Chem. Rev.* **1997**, *97*, 1713-1734.
[158] B. Qiao, A. Sengupta, Y. Liu, K. P. McDonald, M. Pink, J. R. Anderson, K. Raghavachari, A. H. Flood, *J. Am. Chem. Soc.* **2015**, *137*, 9746-9757.
[159] A. Mele, P. Metrangolo, H. Neukirch, T. Pilati, G. Resnati, *J. Am. Chem. Soc.* **2005**, *127*, 14972-14973.
[160] A. Vargas Jentzsch, D. Emery, J. Mareda, P. Metrangolo, G. Resnati, S. Matile, *Angew. Chem. Int. Ed.* **2011**, *50*, 11675-11678.
[161] S. Binauld, C. J. Hawker, E. Fleury, E. Drockenmuller, *Angew. Chem. Int. Ed.* **2009**, *48*, 6654-6658.
[162] P. Thordarson, *Chem. Soc. Rev.* **2011**, *40*, 1305-1323.
[163] K. Hirose, *J. Incl. Phenom. Macrocycl. Chem.* **2001**, *39*, 193-209.
[164] Z. Wang, S. H. Chang, T. J. Kang, *Spectrochim. Acta, Part A* **2008**, *70*, 313-317.
[165] L. Maugeri, T. Lebl, D. B. Cordes, A. M. Z. Slawin, D. Philp, *J. Org. Chem.* **2017**, *82*, 1986-1995.
[166] A. Vanderkooy, M. S. Taylor, *J. Am. Chem. Soc.* **2015**, *137*, 5080-5086.
[167] A. Vanderkooy, P. Pfefferkorn, M. S. Taylor, *Macromolecules* **2017**, *50*, 3807-3817.
[168] N. Houbenov, R. Milani, M. Poutanen, J. Haataja, V. Dichiarante, J. Sainio, J. Ruokolainen, G. Resnati, P. Metrangolo, O. Ikkala, *Nat. Commun.* **2014**, *5*.
[169] L. Meazza, J. A. Foster, K. Fucke, P. Metrangolo, G. Resnati, J. W. Steed, *Nat. Chem.* **2013**, *5*, 42-47.
[170] M. Virkki, O. Tuominen, A. Forni, M. Saccone, P. Metrangolo, G. Resnati, M. Kauranen, A. Priimagi, *J. Mater. Chem. C* **2015**, *3*, 3003-3006.
[171] M. D. Hager, P. Greil, C. Leyens, S. van der Zwaag, U. S. Schubert, *Adv. Mater.* **2010**, *22*, 5424-5430.
[172] S. J. Garcia, *Eur. Polym. J.* **2014**, *53*, 118-125.
[173] F. Herbst, D. Döhler, P. Michael, W. H. Binder, *Macromol. Rapid Commun.* **2013**, *34*, 203-220.
[174] S. Chen, N. Mahmood, M. Beiner, W. H. Binder, *Angew. Chem. Int. Ed.* **2015**, *54*, 10188-10192.
[175] P. Cordier, F. Tournilhac, C. Soulie-Ziakovic, L. Leibler, *Nature* **2008**, *451*, 977-980.
[176] R. K. Bose, N. Hohlbein, S. J. Garcia, A. M. Schmidt, S. van der Zwaag, *Phys. Chem. Chem. Phys.* **2015**, *17*, 1697-1704.
[177] S. J. Kalista, J. R. Pflug, R. J. Varley, *Polym. Chem.* **2013**, *4*, 4910-4926.
[178] L. R. Hart, N. A. Nguyen, J. L. Harries, M. E. Mackay, H. M. Colquhoun, W. Hayes, *Polymer* **2015**, *69*, 293-300.
[179] S. Bode, L. Zedler, F. H. Schacher, B. Dietzek, M. Schmitt, J. Popp, M. D. Hager, U. S. Schubert, *Adv. Mater.* **2013**, *25*, 1634-1638.
[180] M. Burnworth, L. Tang, J. R. Kumpfer, A. J. Duncan, F. L. Beyer, G. L. Fiore, S. J. Rowan, C. Weder, *Nature* **2011**, *472*, 334-337.
[181] J. Chiefari, Y. K. Chong, F. Ercole, J. Krstina, J. Jeffery, T. P. T. Le, R. T. A. Mayadunne, G. F. Meijs, C. L. Moad, G. Moad, E. Rizzardo, S. H. Thang, *Macromolecules* **1998**, *31*, 5559-5562.

[182] S. Bode, M. Enke, H. Görls, S. Hoeppener, R. Weberskirch, M. D. Hager, U. S. Schubert, *Polym. Chem.* **2014**, *5*, 2574-2582.
[183] R. Tepper, S. Bode, R. Geitner, M. Jäger, H. Görls, J. Vitz, B. Dietzek, M. Schmitt, J. Popp, M. D. Hager, U. S. Schubert, *Angew. Chem. Int. Ed.* **2017**, *56*, 4047-4051.
[184] M. L. Oyen, R. F. Cook, *J. Mech. Behav. Biomed. Mater.* **2009**, *2*, 396-407.
[185] G. M. Pharr, W. C. Oliver, *MRS Bull.* **2013**, *17*, 28-33.
[186] R. Geitner, J. Kotteritzsch, M. Siegmann, T. W. Bocklitz, M. D. Hager, U. S. Schubert, S. Grafe, B. Dietzek, M. Schmitt, J. Popp, *Phys. Chem. Chem. Phys.* **2015**, *17*, 22587-22595.
[187] L. Zedler, M. D. Hager, U. S. Schubert, M. J. Harrington, M. Schmitt, J. Popp, B. Dietzek, *Mater. Today* **2014**, *17*, 57-69.
[188] B. Dietzek, D. Cialla, M. Schmitt, J. Popp, in *Confocal Raman Microscopy* (Eds.: T. Dieing, O. Hollricher, J. Toporski), Springer, Berlin, Heidelberg, **2011**.
[189] M. T. Messina, P. Metrangolo, W. Navarrini, S. Radice, G. Resnati, G. Zerbi, *J. Mol. Struct.* **2000**, *524*, 87-94.
[190] R. Bertani, P. Metrangolo, A. Moiana, E. Perez, T. Pilati, G. Resnati, I. Rico-Lattes, A. Sassi, *Adv. Mater.* **2002**, *14*, 1197-1201.
[191] This charge-assisted triazolium derivative of receptor **1** was obtained by methylation with trimethyloxonium tetrafluoroborate during the diploma thesis.
[192] S. Bode, M. Enke, M. Hernandez, R. K. Bose, A. M. Grande, S. van der Zwaag, U. S. Schubert, S. J. Garcia, M. D. Hager, *Adv. Polym. Sci.* **2015**, 1-30.
[193] J. Dahlke, R. Tepper, R. Geitner, S. Zechel, J. Vitz, R. Kampes, J. Popp, M. D. Hager, U. S. Schubert, *Polym. Chem.* **2018**, *9*, 2193-2197.
[194] L. Zhang, N. R. Brostowitz, K. A. Cavicchi, R. A. Weiss, *Macromol. React. Eng.* **2014**, *8*, 81-99.
[195] No sufficient heat effect was observed in the ITC measurement, which precluded the quantification of thermodynamic parameters.
[196] H. Wang, Q. J. Shen, W. Wang, *J. Solution Chem.* **2017**, *46*, 1092-1103.

List of abbreviations

$\sum r_w$	sum of the van der Waals radii
[Host]	concentration of the host
ΔG	overall free energy of binding
ΔH	differences in enthalpy
ΔS	differences in entropy
Đ	dispersity
A, A’	substituents
AcO^-	acetate
AIBN	2,2’-azo-*bis*-(2-methylpropionitrile)
BMA	butyl methacrylate
CPDB	2-cyano-2-propyl benzodithioate
CuAAC	copper(I)-catalyzed azide alkyne (1,3-dipolar) cycloaddition
CuAXAC / CuAHAC	copper(I)-catalyzed cycloaddition between organic azide and halo-alkynes
δ	chemical shift
DFT	density functional theory
DMAP	*N*,*N*-dimethylpyridin-4-amine
DMF	*N,N*-dimethylformamide
DMSO	dimethyl sulfoxide
DSC	differential scanning calorimetry
E	energy
E_i	indentation moduli
eq.	equivalents
Et_3N	triethylamine
EtOH	ethanol
FT	fourier transform

G	guest
H	host
h	hour
HB	hydrogen bond
HOMO	highest occupied molecular orbital
ITC	isothermal titration calorimetry
K	binding constant, association constant
LB	Lewis base
LUMO	lowest unoccupied molecular orbital
M^+	metal center
MAA	methacrylic acid
MeOH	methanol
mes	mesityl
min	minutes
M_n	number average molar mass
MS	mass spectrometry
N	molarity, binding stoichiometry
NBO	natural bond orbital
n-BuLi	*n*-butyllithium
NMR	nuclear magnetic resonance
NOE	nuclear Overhauser effect
pK_a	negative decadic logarithm of the acid dissociation constant
ppm	parts per million
R	electron-withdrawing group
RAFT	reversible addition-fragmentation chain transfer polymerization
ROESY	rotating-frame nuclear Overhauser effect spectroscopy

rt	room temperature
r_w	van der Waals radii
TBA^+	tetra-*n*-butylammonium
TBTA	tris[(1-benzyl-1*H*-1,2,3-triazol-4-yl)methyl]amin
T_d	thermal degradation temperature
TGA	thermogravimetric analysis
THF	tetrahydrofuran
TMS	trimethylsilyl
Tos	tosyl
UV / Vis	ultraviolet-visible
X	halogen
XB	halogen bond

Curriculum Vitae

Personal Data

Date of birth:	November, 6th 1987
Place of birth:	Hohenmölsen

University Education

11/2013 – present	PhD student in the group of Prof. Dr. U. S. Schubert at the *Institute of Organic and Macromolecular Chemistry* of the *Friedrich Schiller University Jena*, Germany, thesis title: "Anion receptors based on hydrogen and halogen bonding"
09/2013	Diploma (equivalent to M.Sc., grade: 1.0, with distinction)
11/2012 – 09/2013	Diploma thesis in the group of Prof. Dr. U. S. Schubert at the *Institute of Organic and Macromolecular Chemistry* of the *Friedrich Schiller University Jena*, Germany, thesis title: "Anion receptors based on halogen interactions with triazolium halides"
10/2012 – 09/2013	German Scholarship (*Deutschlandstipendium*)
10/2008 – 09/2013	Studies of Chemistry at the *Friedrich Schiller University Jena*, Germany

Civilian Service

09/2007 – 08/2008	Civilian service at the *Deutsches Rotes Kreuz* (DRK), Weißenfels, Germany

Schooling

07/2007	Abitur (grade: 1.4) at the *Goethe-Gymnasium*, Weißenfels, Germany

Jena, den 07.05.2018

Ronny Tepper

Publication list

Peer-reviewed publications

[6] J. Dahlke, R. Tepper, R. Geitner, S. Zechel, J. Vitz, R. Kampes, J. Popp, M. D. Hager, U. S. Schubert, "A healing ionomer crosslinked by a bis-bidentate halogen bond linker: a route to hard and healable coatings", *Polym. Chem.* **2018**, *9*, 2091-2197.

[5] R. Tepper, U. S. Schubert, "Halogen bonding in solution: Anion recognition, templated self-assembly, and organo-catalysis", *Angew. Chem. Int. Ed.* DOI: 10.1002/anie.201707986; *Angew. Chem.* DOI: 10.1002/ange.201707986.

[4] R. Tepper, S. Bode, R. Geitner, M. Jäger, H. Görls, J. Vitz, B. Dietzek, M. Schmitt, J. Popp, M. D. Hager, U. S. Schubert, "Polymeric halogen-bond-based donor systems showing self-healing behavior in thin films", *Angew. Chem. Int. Ed.* **2017**, *56*, 4047-4051; *Angew. Chem.* **2017**, *129*, 4105-4110.

[3] R. Tepper, B. Schulze, P. Bellstedt, J. Heidler, H. Görls, M. Jäger, U. S. Schubert, "Halogen-bond-based cooperative ion-pair recognition by a crown-ether-embedded 5-iodo-1,2,3-triazole", *Chem. Commun.* **2017**, *53*, 2260-2263.

[2] R. Tepper, B. Schulze, H. Görls, P. Bellstedt, M. Jäger, U. S. Schubert, "Preorganization in a cleft-type anion receptor featuring iodo-1,2,3-triazoles as halogen bond donors", *Org. Lett.* **2015**, *17*, 5740-5743.

[1] R. Tepper, B. Schulze, M. Jäger, C. Friebe, D. H. Scharf, H. Görls, U. S. Schubert, "Anion receptors based on halogen bonding with halo-1,2,3-triazoliums", *J. Org. Chem.* **2015**, *80*, 3139-3150.

Poster presentations

[3] R. Tepper, B. Schulze, H. Görls, P. Bellstedt, M. Jäger, U. S. Schubert, "Preorganization in a cleft-type anion receptor featuring iodo-1,2,3-triazoles as halogen bond donors", ISXB: 2nd international symposium on halogen bonding, Gothenburg, Sweden, June 6-10 2016

[2] R. Tepper, B. Schulze, M. Jäger, C. Friebe, D. H. Scharf, H. Görls, U. S. Schubert, "Anion receptors based on halogen bonding with halo-1,2,3-triazoliums", COVESTRO, Bayreuth, Germany, September 22-24 2015

[1] R. Tepper, B. Schulze, M. Jäger, C. Friebe, D. H. Scharf, H. Görls, U. S. Schubert, "Anion receptors based on halogen bonding with halo-1,2,3-triazoliums", ORCHEM, Weimar, Germany, September 15-17 2014

Oral presentation

R. Tepper, S. Bode, R. Geitner, M. Jäger, H. Görls, J. Vitz, B. Dietzek, M. Schmitt, J. Popp, M. D. Hager, U. S. Schubert, "Polymeric halogen-bond-based donor systems showing self-healing behavior in thin films", 254th ACS National Meeting, Washington, DC, U.S., August 20-24 2017 (presentation given by U. S. Schubert)

Acknowledgement

Without the continuous help and encouragement of a lot of people, this thesis would not have been possible.

First of all, I want to express my gratitude to Prof. Dr. Ulrich S. Schubert for his continuous support and the possibility to establish a completely new research field. Thank you Uli, I highly appreciated the scientific freedom and the confidence you gave me.

Furthermore, I want to sincerely thank Dr. Benjamin Schulze for supervision during the beginning of this thesis as well as for very helpful discussions and advices during the preparation of manuscripts even after his time at the university. Your detailed knowledge was crucial for the success of the thesis. Thanks a lot Benny!

Thank you very much, Dr. Michael Jäger for the various DFT calculations and the enriching considerations regarding the preparation of manuscripts and this thesis – it was a pleasure to work with you!

Special thanks go to the NMR platform, in particular Dr. Wolfgang Günther, Dr. Peter Bellstedt as well as Gabriele Sentis and Friederike Pielenz for their excellent help with demanding NMR experiments. Also, Dr. Helmar Görls deserves my sincere gratitude for the analysis of various single-crystal structures. Both, the challenging NMR measurements as well as the X-ray structure analysis were very important for the success of this thesis.

Dr. Stefan Zechel and Jan Dahlke, thank you very much for sharing your detailed knowledge about self-healing materials with me and for the excellent cooperation. In this regards, I also thank Dr. Robert Geitner for the analysis of these materials *via* FT-Raman spectroscopy as well as Dr. Jürgen Vitz for the corresponding nanoindentation measurements and helpful discussions.

I had the pleasure to spend my PhD time not only with colleagues, but rather with very good friends. In this regard, special thanks go to Tina Schlotthauer, Robert Schroot as well as Kevin Barthelmes, Christian Friebe, and Daniel Schmidt for the great time and lots of cake during our coffee breaks – it was a pleasure to grow together as friends during the years.

Furthermore, I am highly grateful to Dr. Sarah Crotty, Nicole Fritz, Annet Urbanek, Sandra Köhn, Beate Lentvogt for discussions and their help with measurements (*e.g.*, ESI / MALDI MS, elemental analyses) to characterize new substances. In this regard, I also want to kindly acknowledge the support from Dr. Uwe Köhn, Dr. Martin D. Hager, and Dr. Andreas Winter as well as from the secretaries of the Schubert group, Syliva Braunsdorf, Simone Burchardt, and Franca Frister in organizational issues.

Furthermore, I would like to thank all the students of several organic chemistry courses, my Hiwis and lab students Jan Heidler and Jooris Beyer as well as my master student Robin Kampes who supported me in lots of interesting synthetic challenges – I really enjoyed the time with you in the lab!

Last but not least, my deepest gratitude goes to my family for the very great support and permanent understanding in the last years. Special thanks go to my beloved wife Sandra and my son Fabian for always being a reliable support for me and giving me a fulfilled life besides work.

Declaration of authorship / Selbstständigkeitserklärung

Ich erkläre, dass ich die vorliegende Arbeit selbständig und unter Verwendung der angegebenen Hilfsmittel, persönlichen Mitteilungen und Quellen angefertigt habe.

I certify that the work presented here is, to the best of my knowledge and belief, original and the result of my own investigations, except as acknowledged, and has not been submitted, either in part or whole, for a degree at this or any other university.

Jena, den 07.05.2018

_____

Ronny Tepper

Publications P1 to P5

P1) R. Tepper, U. S. Schubert, “Halogen bonding in solution: Anion recognition, templated self-assembly, and organo-catalysis”, *Angew. Chem. Int. Ed.* DOI: 10.1002/anie.201707986; *Angew. Chem.* DOI: 10.1002/ange.201707986.

P2) R. Tepper, B. Schulze, H. Görls, P. Bellstedt, M. Jäger, U. S. Schubert, ”Preorganization in a cleft-type anion receptor featuring iodo-1,2,3-triazoles as halogen bond donors“, *Org. Lett.* **2015**, *17*, 5740-5743.

P3) R. Tepper, B. Schulze, P. Bellstedt, J. Heidler, H. Görls, M. Jäger, U. S. Schubert, ”Halogen-bond-based cooperative ion-pair recognition by a crown-ether-embedded 5-iodo-1,2,3-triazole“, *Chem. Commun.* **2017**, *53*, 2260-2263.

P4) R. Tepper, S. Bode, R. Geitner, M. Jäger, H. Görls, J. Vitz, B. Dietzek, M. Schmitt, J. Popp, M. D. Hager, U. S. Schubert, “Polymeric halogen-bond-based donor systems showing self-healing behavior in thin films“, *Angew. Chem. Int. Ed.* **2017**, *56*, 4047-4051; *Angew. Chem.* **2017**, *129*, 4105-4110.

P5) J. Dahlke, R. Tepper, R. Geitner, S. Zechel, J. Vitz, R. Kampes, J. Popp, M. D. Hager, U. S. Schubert, “A healing ionomer crosslinked by a bis-bidentate halogen bond linker: a route to hard and healable coatings”, *Polym. Chem.* **2018**, *9*, 2091-2197.

Publication P1

"Halogen bonding in solution: Anion recognition, templated self-assembly, and organo-catalysis"

R. Tepper, U. S. Schubert, *Angew. Chem. Int. Ed*. DOI: 10.1002/anie.201707986; *Angew. Chem.* DOI: 10.1002/ange.201707986.

Suparmolecular Chemistry

International Edition: DOI: 10.1002/anie.201707986
German Edition: DOI: 10.1002/ange.201707986

Halogen Bonding in Solution: Anion Recognition, Templated Self-Assembly, and Organocatalysis

*Ronny Tepper and Ulrich S. Schubert**

Keywords:
anion recognition · anions
halogen bonding
host–guest systems ·
supramolecular
chemistry

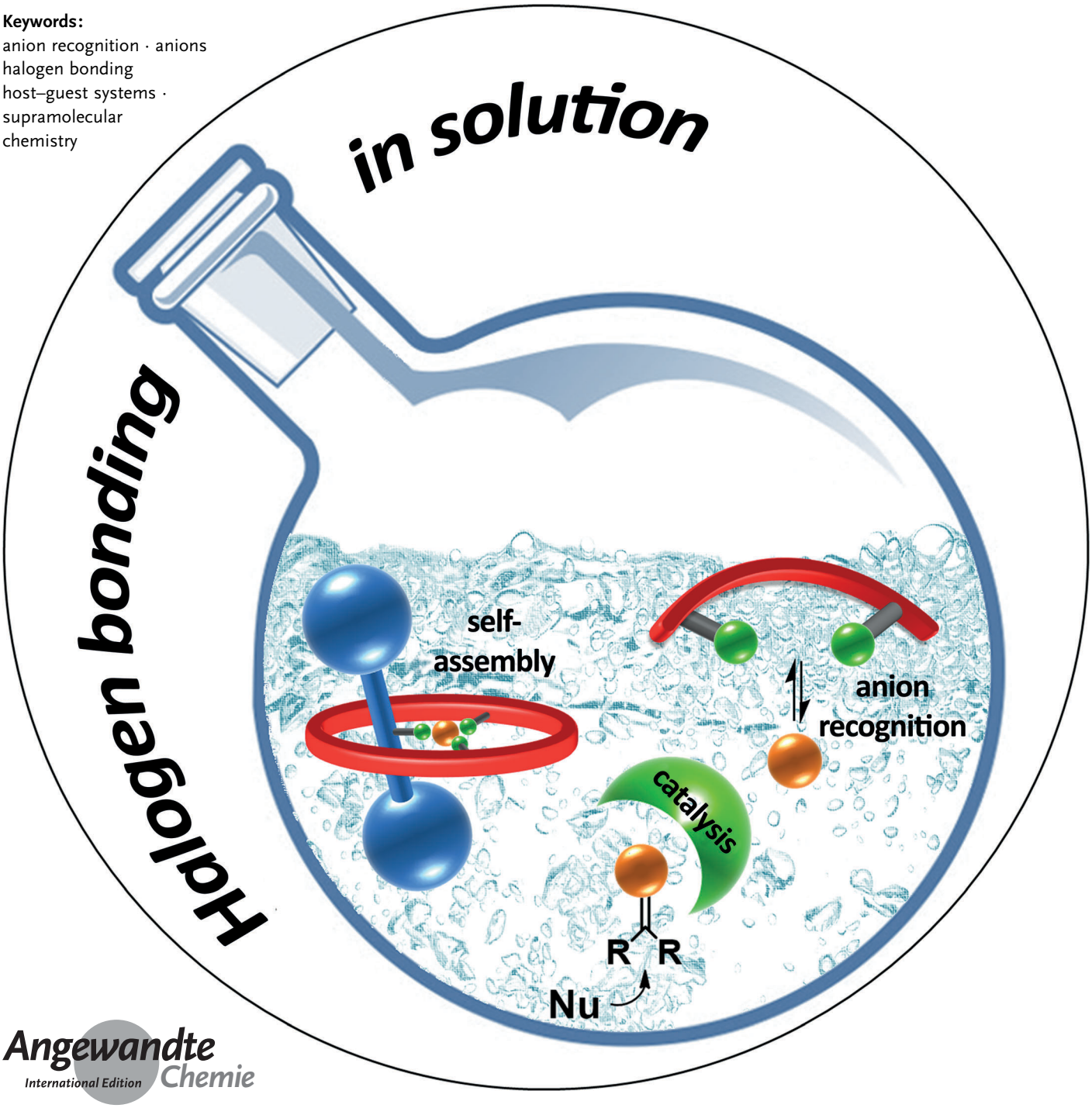

The halogen bond is a supramolecular interaction between a Lewis-acidic region of a covalently bound halogen and a Lewis base. It has been studied widely in silico and experimentally in the solid state; however, solution-phase applications have attracted enormous interest in the last few years. This Minireview highlights selected recent developments in halogen bond interactions in solution, with a focus on the use of receptors based on halogen bonds in anion recognition and sensing, anion-templated self-assembly, as well as in organocatalysis.

1. Introduction

As a consequence of the importance of anions in biological and chemical processes, anion coordination chemistry is continuously developing and new research efforts have been devoted to the design of selective anion binding sites.[1] In particular, the proposed biological and medical applications typically require aqueous conditions, but the selective recognition of anions in water remains a challenge.[2] Although selective anion recognition can be achieved by numerous supramolecular interactions, for example, hydrogen bond (HB), ion–ion, anion–π, and electrostatic interactions,[3,4] the halogen bond (XB) has long been overlooked in this context. However, in the last decade, the utility of XBs in anion coordination and supramolecular chemistry has become increasingly apparent.

The XB is a highly directional supramolecular interaction in which a covalently bound halogen in compounds of the general form R-X (X = I, Br, Cl, F) is polarized by an electron-withdrawing group R and, thus, is able to act as the electrophilic species (XB donor) in the presence of a Lewis base (XB acceptor).[5,6] Accordingly, the polarizability of X (I > Br > Cl > F) as well as the electron-withdrawing ability of R are key factors to tune the size of the electrophilic area, which is termed the σ-hole.[7] This Lewis-acidic region is surrounded by a belt of negative electrostatic potential, which also accounts for the strictly linear nature of the XB interaction.[7] In addition to this electrostatic interaction (σ-hole), the XB is also characterized by additional contributions from dispersion and charge-transfer components. The exact magnitude/importance of each contribution is controversially discussed and strongly depends on the system.[8]

Besides some studies on XBs in biological systems,[9–11] current research focuses on the theoretical[12,13] and crystallographic characterization[14–16] of XBs and their application in crystal engineering[17] and materials design.[18,19] Nevertheless, there is growing interest in the exploration of new supramolecular systems based on XBs in solution.[20–24]

Two recent reviews, which cover the literature up to mid-2015, provide a very good overview of the history and nature of XBs and demonstrate the specific advantages of XBs in quite different fields—from crystal engineering and soft materials to biomolecular recognition and functional systems in solution.[25,26] This Minireview covers recent solution-phase applications of XBs, with a focus on anion recognition and sensing processes. Furthermore, advances in XB-mediated organocatalysis as well as the XB-templated self-assembly of interlocked structures are also highlighted.

2. Anion Recognition and Sensing with Cationic Receptors

In general, anions are excellent XB acceptors due to their electron-rich nature; however, the design of strong and selective anion receptors is often complicated by certain intrinsic challenges of negatively charged species, for example, anions are larger than their isoelectronic cations, they are pH-sensitive, exhibit a wide range of geometries, and suffer from high solvation enthalpies. To meet these intrinsic challenges, a combination of strategies, such as charge-assistance, multidentate binding motifs, preorganization as well as cooperativity effects, is usually used, which will be explained and discussed in more detail in the following subchapters.

The use of positively charged receptors that benefit from a Coulombic attraction to anions (charge assistance) was identified early on as a general strategy to boost binding affinities. These cationic XB donors generally contain five- or six-membered nitrogen heterocycles as electron-withdrawing groups (R), in which one of the nitrogen atoms is quaternized to create a charge and to strongly polarize the covalently bound halogen.[25,26] The charge not only boosts the binding affinity, it also modifies the entropy ($T\Delta S$)/enthalpy (ΔH) distribution of these receptors compared to analogous neutral ones. Whereas the binding of anions by cationic receptors is more entropically driven by the release of polar-bound solvent molecules during the binding event,[27] neutral receptors benefit from negative enthalpy changes and suffer from an unfavorable entropic penalty.[28,29]

2.1. Mono-, Bi-, and Tridentate Cationic Receptors

The Ghosh research group designed the bis-heteroleptic ruthenium(II) complex **1** in which the XB subunit is directly attached to the metal center (Figure 1).[30] Detailed ^{1}H NMR and ^{31}P NMR spectroscopic measurements as well as UV/Vis titration studies in solution revealed selective phosphate recognition as well as higher binding affinities, lower detection limits, and greater changes in the lifetime of the XB-based complex in the presence of phosphate compared to the

[*] R. Tepper, Prof. U. S. Schubert
Laboratory of Organic and Macromolecular Chemistry (IOMC)
Friedrich Schiller University Jena
Humboldtstrasse 10, 07743 Jena (Germany)
and
Jena Center for Soft Matter (JCSM), Friedrich Schiller University Jena
Philosophenweg 7, 07743 Jena (Germany)
E-mail: ulrich.schubert@uni-jena.de
The ORCID identification number for the author of this article can be found under:
https://doi.org/10.1002/anie.201707986.

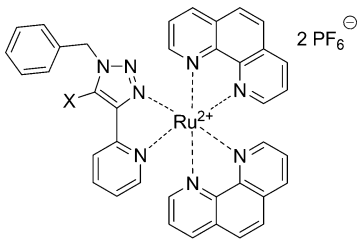

1 X = H, I

X = I $K_a(H_2PO_4^-) = 1.9 \cdot 10^5\ M^{-1}$

Figure 1. A monodentate XB/HB-based triazole system incorporated in a bis-heteroleptic ruthenium(II) complex. **1**: K_a value obtained by UV/Vis titration in CH_3CN at 298 K.[30]

analogous HB-based system. The obtained association constant of up to $10^5\ M^{-1}$ is one of the highest binding affinities for monodentate charged systems reported to date (see Table 1), which might be explainable by the very strong interconnection of the XB donor and the metal complex.

Berryman and co-workers used HB- and XB-based bidentate imidazolium (X = H, I; **2**) systems to quantify the effect of water on the halide binding (Figure 2).[31] Besides a general stronger anion affinity, the organic XB system showed an improved water resistance compared to the analogous HB-based system. Whereas a 46% reduction in the binding strength of **2** (X = H) was found on changing the

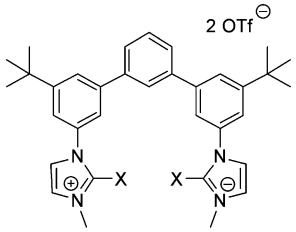

2 X = H $K_a(Cl^-) = 935\ M^{-1}$
X = Br $K_a(Cl^-) = 3.7 \cdot 10^4\ M^{-1}$

Figure 2. A bidentate XB/HB-based imidazolium system; OTf^- = triflate. **2**: K_a values obtained by ^1H NMR titration in CD_3CN/D_2O (99:1) at 289 K.[31]

solvent from neat CD_3CN to CD_3CN/D_2O (95:5), the XB-based system **2** (X = I) revealed only a 32% reduction. Hence, the potential of XBs to overcome competitive environments was demonstrated. In this context, Beer and co-workers very recently demonstrated selective anion recognition even in pure water by using a cyclodextrin-based receptor functionalized with two iodotriazole units.[32]

The affinity for a certain binding partner can be significantly increased by switching from bidentate complexation modes to multiple interaction points adjusted in a concerted manner. Although the design and synthesis of multidentate XB donors is rather challenging due to the strict linearity of the interaction, it also offers the advantage of creating more rigid and ordered structures with an improved selectivity.[25,26]

This general design strategy was successfully used in different studies by implementing pyridinium (**3**),[33] imidazolium (**4**, **5**),[34,35] or triazolium (**6**)[35] moieties to build a tridentate bowl-shaped cavity. These structures enabled anion binding in stable 1:1 (**3**, **5**, and **6**) or 1:3 (**4**) complexes through charge-assisted HB/XB interactions (Figure 3).

The Berryman research group designed a tridentate XB donor system consisting of three bridged 4-halopyridinium unites **7** (X = Br, I), which underwent an impressive self-assembly to form a triple helicate in solution as well as in the solid state (Figure 4).[36] In particular the tricationic strands of the 4-iodopyridinium derivative **7** (X = I) enabled the stable encapsulation of two iodide ions within the formed tubular anion channel with nine XB donor units in organic solvents ($CD_3CN/[D_7]DMF$ (4:1), stable up to 341 K) as well as aqueous media ($D_2O/[D_7]DMF$ (1:1) at 298 K). The formation of the triple helicate was encouraged by a combination of favorable π-stacking and the strict linearity of the strong XBs with the encapsulated guests.

2.2. Polymeric Multidentate Cationic Receptors and Supramolecular Polymers in Solution

In the last few years, the combination of XBs with polymeric architectures has also attracted growing interest for the design of supramolecular functional materials.[18] Nevertheless, a quantitative analysis of polymeric XB donors in solution is still missing to date. Accordingly, our group exploited isothermal titration calorimetry (ITC) experiments

Ronny Tepper studied chemistry at the Friedrich Schiller University Jena, where he has been a PhD student in the group of Prof. U. S. Schubert since 2013. His research interests focus on supramolecular chemistry, with a particular emphasis on anion recognition and sensing through halogen bonding in solution.

Ulrich S. Schubert studied chemistry in Frankfurt and Bayreuth as well as the Virginia Commonwealth University, Richmond (USA). He completed his PhD with Prof. C. D. Eisenbach (Bayreuth) and Prof. G. R. Newkome (South Florida, USA). After postdoctoral research with Prof. J.-M. Lehn at the University of Strasbourg (France), he moved to the TU Munich, where he habilitated in 1999. From 1999 to 2000 he was Professor at the University of Munich, and from 2000 to 2007 Full Professor at the TU Eindhoven in the Netherlands. Since 2007, he has been a Full Professor at the Friedrich Schiller University Jena.

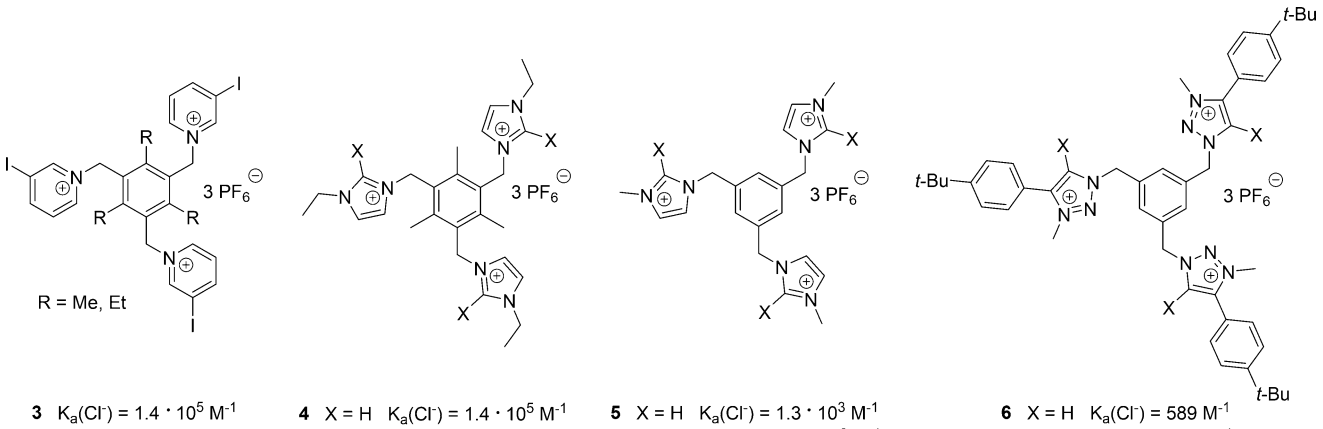

3 $K_a(Cl^-) = 1.4 \cdot 10^5\ M^{-1}$

4 X = H $K_a(Cl^-) = 1.4 \cdot 10^5\ M^{-1}$
X = I $K_a(Cl^-) = 6.0 \cdot 10^4\ M^{-1}$
$\beta_a(Cl^-) = 5.4 \cdot 10^{11}\ M^{-3}$
$K_a(Br^-) = 5.9 \cdot 10^5\ M^{-1}$
$\beta_a(Br^-) = 1.1 \cdot 10^{13}\ M^{-3}$

5 X = H $K_a(Cl^-) = 1.3 \cdot 10^3\ M^{-1}$
X = I $K_a(Cl^-) = 2.4 \cdot 10^3\ M^{-1}$

6 X = H $K_a(Cl^-) = 589\ M^{-1}$
X = I $K_a(Cl^-) = 829\ M^{-1}$

Figure 3. Tridentate XB/HB donor systems based on pyridinium, imidazolium, or triazolium moieties. K_a values obtained for **3**: by UV/Vis titration, CH_3CN, 298 K; **4**: ITC titration, CH_3CN, 298 K, β_a (1:3 complex); **5** and **6**: ^1H NMR titration in [D_6]DMSO at 298 K.[33–35]

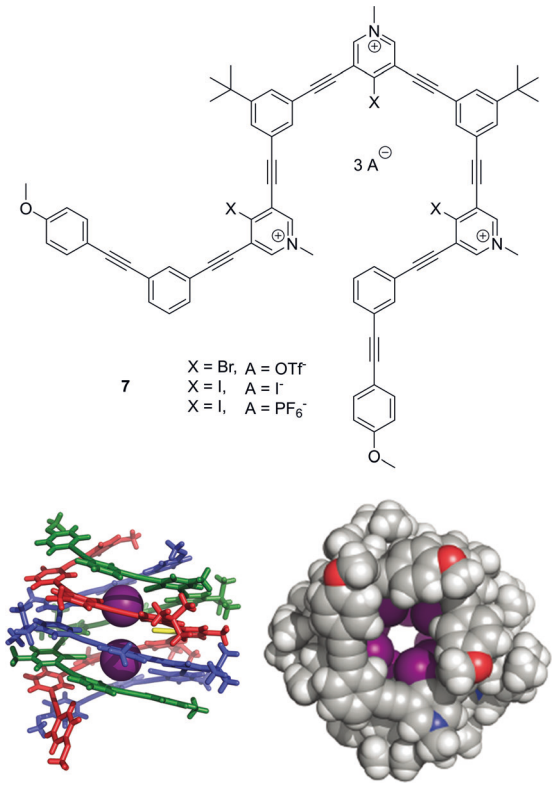

7

Figure 4. Top: Tridentate XB hosts based on 4-halopyridinium unites. Bottom: Solid-state representation of a triple helicate encapsulating two iodide ions.[36] Reprinted from Ref. [36] with permission. Copyright 2016 WILEY-VCH Verlag GmbH & Co. KGaA, Weinheim.

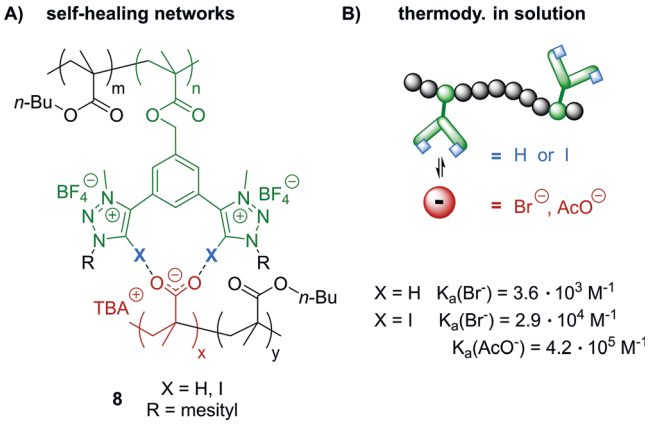

8 X = H, I
R = mesityl

X = H $K_a(Br^-) = 3.6 \cdot 10^3\ M^{-1}$
X = I $K_a(Br^-) = 2.9 \cdot 10^4\ M^{-1}$
$K_a(AcO^-) = 4.2 \cdot 10^5\ M^{-1}$

Figure 5. A) A polymeric bidentate XB/HB donor system interacting with a copolymer bearing accepting carboxylate groups. B) The thermodynamic behavior in solution. **8**: K_a values obtained by ITC titration in THF at 303 K.[37]

(in THF) on polymeric donor systems **8** (X = H, I) to evaluate the dependence of the anion affinity on different key parameters, namely, differences between monomeric and polymeric receptors, differences between XB- and HB-based units, and the effect of charge assistance (Figure 5B).[37] The combination of these donor systems with a copolymer bearing accepting carboxylate groups led to the formation of supramolecular cross-linked polymer networks that showed excellent intrinsic self-healing behavior (Figure 5A).

Quite recently, the Taylor research group studied the XB-driven self-assembly of a perfluoroiodoarene-substituted polystyrene **9** with an amino-functionalized methacrylate block copolymer (Figure 6).[38] The formation of the XBs in solution were analyzed by ^{19}F NMR spectroscopy, and revealed both an increased association constant (up to $K_a = 312\ M^{-1}$ in toluene at 298 K) as well as an increased donor site occupancy as a function of the degree of polymerization of the acceptor.

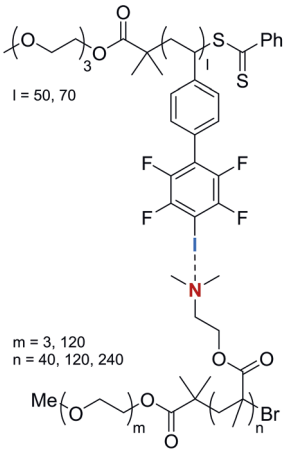

9 K_a(I=50, m=3, n=240) = 312 M^{-1}

Figure 6. A polymeric monodentate XB donor system forming XBs with a copolymer bearing accepting amine groups. **9**: K_a value obtained by ^{19}F NMR titration in toluene at 298 K.[38]

2.3. Electrochemistry and Enantioselectivity in Anion Sensing

Electrochemical sensors have received much attention because of their innate high sensitivity and facile integration into applicable devices. In 2015, the first example of XB-based redox-active receptors and their electrochemical anion-sensing properties were reported by the Beer research group.[39] Subsequently, XB motifs were also successfully integrated into other redox-active receptor frameworks containing, for example, ferrocene[40–43] or tetrathiafulvalene units.[44]

The fundamental studies of Lim et al.[39–41] concentrated, in particular, on ferrocene as the redox-active motif because of its chemical stability, wide synthetic repertoire, as well as favorable voltammetric properties. Their initial studies concerned different ferrocene motifs directly connected to the anion binding sites of **10** and **11** (X = H, I; Figure 7),[39] which were analyzed by ^1H NMR spectroscopy and electrochemical voltammetric investigations in organic and aqueous solvents. The XB-based binding site was found to significantly enhance the anion binding affinity as well as improve the electrochemical sensing of the anions compared to their HB analogues. Moreover, an anion-induced cathodic shift in the receptor's ferrocene/ferrocenium redox couple was observed, which indicated a stabilization of the ferrocenium oxidation state upon complexation of the anion.

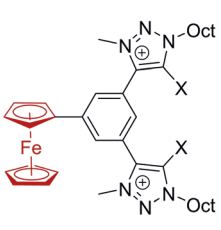

10

X = H $K_a(Cl^-)$ = 77 M^{-1}
X = I $K_a(Cl^-)$ = 286 M^{-1}

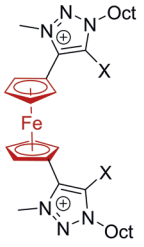

11

X = H $K_a(Cl^-)$ = 94 M^{-1}
X = I $K_a(Cl^-)$ = 312 M^{-1}

Figure 7. Bidentate XB/HB-based triazole systems with ferrocene as the redox-active unit (displayed in red). **10**, **11**: K_a values obtained by ^1H NMR titration in CD_3CN/D_2O (9:1) at 298 K.[39]

The dicationic system (**12**) of Beer and co-workers enabled the first example of enantiodiscrimination based on XBs (Figure 8).[41] The combination of the chiral, enantiopure (*S*)-BINOL core with the strict linearity of the XBs and the large steric demand of the XB donor iodine **12** (X = I) resulted in the ability to recognize a range of chiral anions (chiral amino acid carboxylates and BINOL phosphate) with a higher affinity and enhanced enantioselectivity compared to the HB analogue **12** (X = H). The discrimination of chiral anions was studied by ^1H NMR titration experiments in a CD_3CN/D_2O (99:1) solvent mixture and was further proven by a larger cathodic shift in the receptor's ferrocene/ferrocenium redox couple (in CD_3CN) for the preferred enantiomer. Recent studies also achieved enantiodiscrimination with various chiral triazole-based XB donors[45] or through the implementation of the (*S*)-BINOL core in a neutral tetradentate XB donor foldamer[46] as well as in chiral [2]rotaxanes[47] and even in [3]rotaxane[48] host systems.

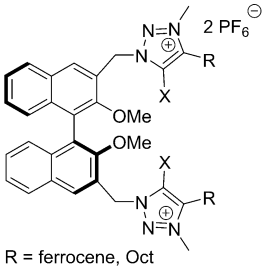

12

X = H (R=Oct) K_a(*N*Boc-(**S**)-Trp^-) = 34 M^{-1}
K_a(*N*Boc-(**R**)-Trp^-) = 37 M^{-1}
→ K(S)/K(R) = 0.9
X = I (R=Oct) K_a(*N*Boc-(**S**)-Trp^-) = 1.7 · 10^3 M^{-1}
K_a(*N*Boc-(**R**)-Trp^-) = 1.0· 10^3 M^{-1}
→ K(S)/K(R) = 1.7

Figure 8. A bidentate XB/HB-based triazolium system with a BINOL core that shows enantiodiscrimination; Oct = octyl, *N*Boc-(S/R)-Trp^- = *N-tert*-butoxycarbonyl-protected tryptophan.[41] **12**: K_a values obtained by ^1H NMR titration in CD_3CN/D_2O (99:1) at 298 K.

3. Anion Recognition and Sensing through Neutral Receptors

In comparison to charged XB donor systems (see Section 2), in which the binding efficiency strongly benefits from charge assistance, the interaction strength of neutral XB donors depends much more strongly on the electronic properties of the organic backbone. As most of the studies focus on XB donors where the halogen is bound to a carbon atom (C–X), the sp hybridization at this *ipso*-carbon atom

represents another important key factor for tuning the XB strength. It was revealed that the greater the degree of s character in a sp-hybridized carbon atom ($C(sp)-X > C(sp^2)-X > C(sp^3)-X$), the greater was its electron-withdrawing ability and, thus, the stronger the formed XB.[7]

The absence of charge also supports other design strategies, for example the possibility to create very hydrophobic scaffolds, which enable the use of less competing/low-polarity solvents, such as cyclohexane. Moreover, it was already observed for neutral systems that tuning of the XB donor is more efficient than tuning of the XB acceptor within the same system.[49] This also represents a useful design rule for the systematic optimization of new receptors.

3.1. Monodentate Receptors

As already mentioned, most of the studies concentrate on XB donors where the halogen is bound to a carbon atom (C–X) or to another halogen atom (Y–X). Nevertheless, nitrogen-bound donors (N–X), where the halogen is additionally strongly polarized by two electron-withdrawing groups, for example carbonyl groups in *N*-halosuccinimides (**13**, NXS) or sulfonyl units in *N*-halosaccharin derivatives (**14**, NXSac), also showed very strong monodentate XBs (Figure 9).[50,51] ^{1}H NMR titration experiments in solution were

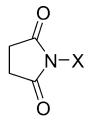

13 X = H, I, Br, Cl

X = I K_a(Me-PyNO) = 779 M^{-1}

X = H K_a(DMAP) = 2.1 M^{-1}
X = I K_a(DMAP) = $1.0 \cdot 10^4$ M^{-1}

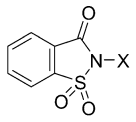

14 X = H, I, Br, Cl

X = I K_a(Me-PyNO) = $1.6 \cdot 10^4$ M^{-1}

Figure 9. Monodentate XB/HB donor systems based on *N*-succinimide and analogous *N*-saccharin derivatives.[50,51] **13**, **14**: K_a values for 2-methylpyridine *N*-oxide (Me-PyNO) obtained by ^{1}H NMR titration, in $CDCl_3$ at 298 K.[50] **13**: K_a value for 4-dimethylaminopyridine (DMAP) obtained by ITC titration in CH_3CN at 298 K.[51]

carried out to quantify the binding strength between different acceptors (pyridine *N*-oxides (PyNOs)[50] or *p*-substituted pyridine derivatives)[51] and the XB/HB donor moieties (**13**, **14**), and confirmed the expected larger association constants for the *N*-halosaccharin derivatives.[50]

The Lucarini research group coupled a monodentate tetrafluoroiodophenyl moiety to a nitroxide radical (**15**) to establish, for the first time, the use of radical spin probes for the detection and quantification of XBs in solution by EPR spectroscopy (Figure 10).[52] The formation of the XBs was reflected by a significant change in the benzylic hyperfine splitting initiated by geometric changes upon complexation to different XB acceptors. Shortly afterwards, other XB com-

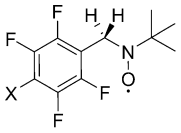

15 X = H, I

X = I $K_a(Cl^-)$ = 25 M^{-1} in CH_3CN at 243 K
K_a(quinuclidine) = 30 M^{-1} in CH_3CN at 243 K
K_a(quinuclidine) = 220 M^{-1} in TMP at 203 K

Figure 10. Monodentate XB/HB-based tetrafluorophenyl systems bearing a nitroxide radical. **15**: K_a values obtained by EPR titration; TMP = trimethylpentane.[52]

plexes with neutral nitroxide radicals as the Lewis base and pentafluoroiodobenzene as the XB donor were also analyzed by EPR spectroscopy.[53]

Philp and co-workers used the facile and modular copper-catalyzed azide-alkyne cycloaddition (CuAAC) reaction to synthesize a series of neutral 1,4-diaryl-5-iodo-1,2,3-triazoles containing both the iodotriazole as a Lewis-acidic donor and a variety of different Lewis-basic acceptor moieties (e.g. pyridine **16**,[54] phenol/phenoxide **17**,[55] or triphenylphosphine oxide (TPPO) **18**),[56] thereby generating molecules capable of undergoing dimerization (K_{dimer}) through self-complementary XBs (Figure 11). While the low acceptor strength of pyridine in **16** resulted in a rather low stability constant (K_{dimer}(**16**·**16**) = 3.4 M^{-1} in C_6D_6 at 298 K),[54] the pH-sensitive phenol unit (**17**) showed a greatly improved dimer stability in its negatively charged form ($K_{dimer}(\mathbf{17}\cdot\mathbf{17})^{2-} = 510\,M^{-1}$ in CD_3CN at 293 K; Figure 11 B).[55] The TPPO moiety (**18**), with a formal charge on the acceptor oxygen atom, led to a significant increase in the dimer stability compared to that of **16** (K_{dimer}(**18**·**18**) = 174 M^{-1} in [D_8]toluene at 295 K)[56] by simultaneously avoiding additional effects of counterions and the electrostatic repulsion observed with **17**.

In another approach, our group used the ambivalent character of the triazole for cooperative ion-pair recognition.[57] XB- (**19**) and HB-functionalized macrocycles were synthesized by CuAAC-type reactions under pseudo-high-dilution conditions. The heteroditopic character (i.e. iodotriazole for XB-based anion recognition and a Lewis-basic cavity consisting of a triethylene glycol chain and the nitrogen atoms of the triazole motif for cation binding) was illustrated by the calculated electrostatic potential surfaces (Figure 12 A, left) as well as comprehensive single-crystal X-ray analysis. Additionally, the cooperative effect of the cation complexation boosting the anion-binding affinity of **19** ($K_a(I^-)$ = 4.7 M^{-1} without cation complexation, $K_a(I^-) = 135\,M^{-1}$ with simultaneous complexation of Na^+ in CD_2Cl_2/CD_3CN (3:1) at 297 K) was quantified by detailed ^{1}H NMR and ^{13}C NMR binding studies in solution with sodium iodide as a representative ion pair.

3.2. Multidentate Receptors

Recently, the Kubik research group also designed a macrocyclic XB-based anion receptor comprising three iodotriazole subunits (Figure 12 B).[58] The rigid, highly preorganized macrocyclic pseudopeptide **20** showed an impressively high binding affinity for a neutral XB donor ($K_a(Cl^-) = 1.9 \times 10^3\,M^{-1}$ in 2.5% H_2O in [D_6]DMSO at 298 K) as well as

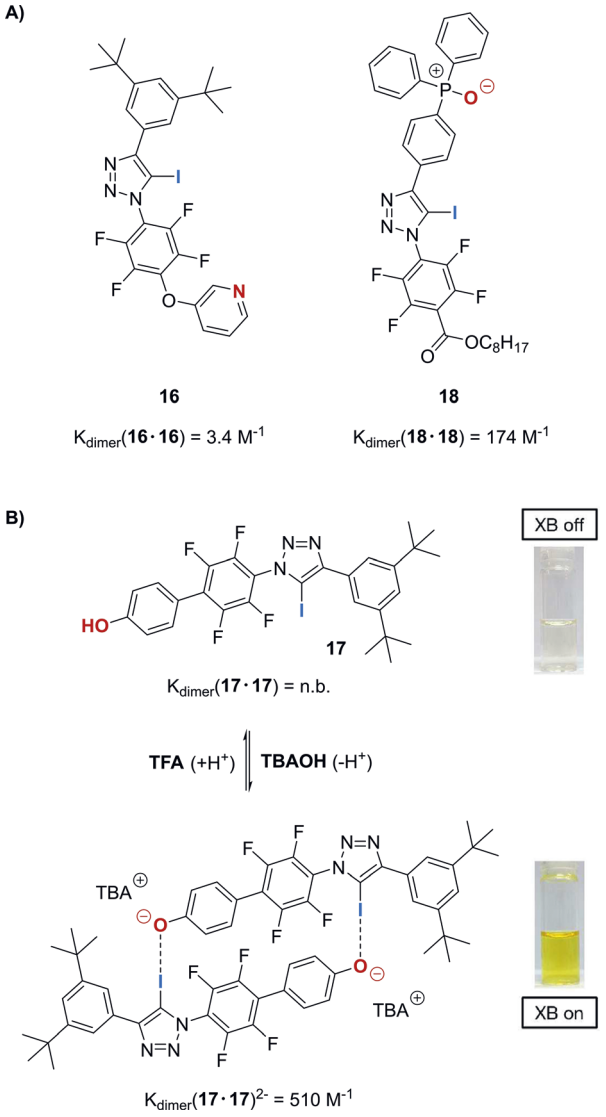

Figure 11. Series of neutral 1,4-diaryl-5-iodo-1,2,3-triazoles containing both a Lewis-acidic donor (blue) and a variety of different Lewis-basic acceptors (red); TBA = tetrabutylammonium, TFA = trifluoroacetic acid.[54–56] All K_{dimer} values obtained by dilution experiments followed by ^{1}H NMR in C_6D_6 at 298 K (**16**), ^{19}F NMR in CD_3CN at 293 K (**17**, n.d. = not determinable), ^{31}P NMR in [D_8]toluene at 295 K (**18**). Photos reprinted from Ref. [55] with permission. Copyright 2017 Royal Society of Chemistry.

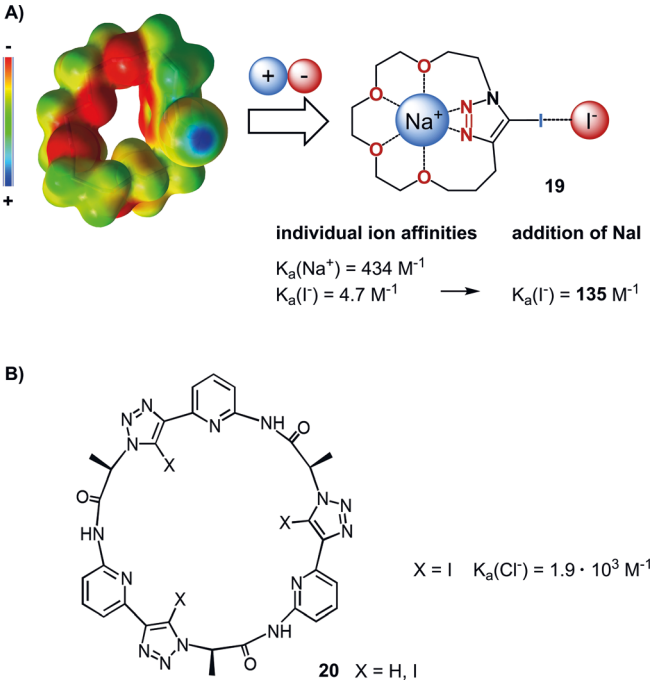

Figure 12. A) Calculated molecular electrostatic potential surface of the ion-pair receptor (left) and schematic representation of the binding mode (right).[57] B) Tridentate XB/HB-based macrocyclic pseudopeptide.[58] **19**: K_a values obtained by ^{1}H NMR (Na^+) and ^{13}C NMR (Na^+, I^-) titration in CD_2Cl_2/CD_3CN (3:1) at 297 K; **20**: K_a values obtained by ^{1}H NMR titration in 2.5% H_2O in [D_6]DMSO at 298 K.

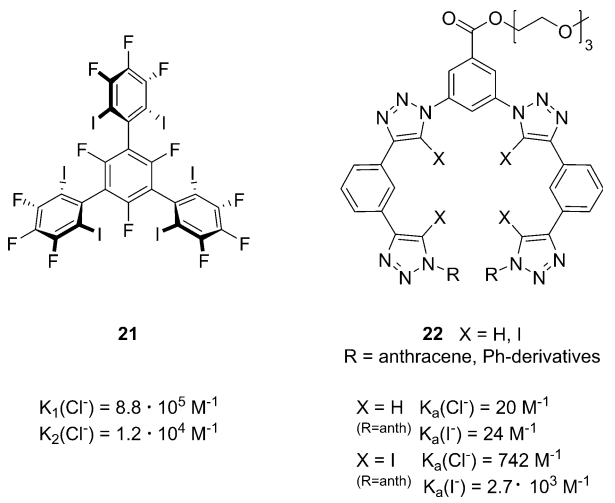

Figure 13. Multidentate neutral XB donors based on polyfluoroiodoarenes[59] and iodotriazoles.[46] **21**: K_a values obtained by ITC titration in THF at 303 K, $K_1 = K_a$(1:1 complex), $K_2 = K_a$(1:2 host/guest complex); **22**: K_a values obtained by ^{1}H NMR titration in $CDCl_3$ at 298 K.

exciting chirality, which was claimed to be interesting for the intended use in asymmetric organocatalysis. The example of Kubik and co-workers (**20**) nicely demonstrated that multiple XBs—adjusted in a concerted manner—offer the opportunity to significantly increase the affinity as well as selectivity for a certain binding partner.

Huber and co-workers designed a series of rigid multidentate polyfluoroiodoarene-based donors (e.g. **21**) with the ability to form multidentate XBs at two identical sides of the receptor (Figure 13).[59] A comprehensive study of the binding properties in the solid state revealed an anti-cooperative behavior of these two binding sides, namely, the tridentate binding on one side of the molecule and binding with reduced denticity on the remaining side. The negative cooperativity was further revealed by the characteristic biphasic shape of the ITC data indicating two successive binding events with different binding affinities (K_1, K_2) in solution.

Besides the tridentate system, the Beer research group also synthesized the first neutral tetradentate XB donor foldamers **22** (X = I). These showed enhanced anion affinities compared to the HB analogues, with a general preference for

heavier halides over oxoanions ($I^- > Br^- > Cl^- \approx AcO^- \approx H_2PO_4^-$ in $CDCl_3$ at 298 K; Figure 13).[46] This binding trend was attributed to an improved host–guest complementarity as well as to the absence of charge assistance that might favor the binding of larger, soft anions instead of small, hard anions, which are regularly preferred by charged XB donor systems.

3.2.1. Preorganized Multidentate Receptors

In contrast to flexible donor systems, which allow adaptive binding with usually low selectivity towards a certain substrate, the structural restriction in preorganized receptors leads to an improved selectivity being achieved by means of complementarity between the rigid receptor und the substrate. However, there are only a few examples that deal with this concept in combination with XBs. On the one hand, the design of efficient polydentate and simultaneously preorganized receptors is very challenging due to the strict linearity as well as the large size of the XB donor atom (mostly iodine). On the other hand, this building principle allows the design of charge-neutral receptors with very high binding affinities, which offer great potential for application as organocatalysts (see Section 4).

In this context, our group exploited the excellent XB donor ability as well as HB acceptor function of the iodo-1,2,3-triazole to generate a rigid and spring-loaded *syn* conformation of the carbazole-based receptor **24** with the help of intramolecular HBs (Figure 14).[29] Comparing the

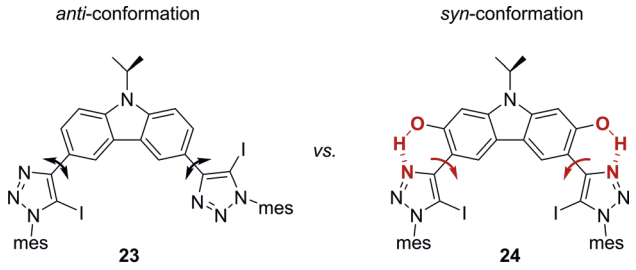

Figure 14. Bidentate XB donors based on a triazole unit preorganized by intramolecular HBs; mes = mesityl.[29] **23**, **24**: K_a values obtained by ITC titration in THF at 303 K.

ITC measurements of **23** and **24** with different halides (Br^-, Cl^- in THF at 303 K), an entropically driven increase in the binding affinity was revealed for the latter. The preorganization led to a restriction in the rotational freedom and, thus, to a minimized need for conformational reorganization of the system prior to halide complexation. Consequently, the entropic penalty for the complexation could be screened in **24** and, thus, the desolvation of the host and guest gave rise to a positive entropic contribution.

Jungbauer and Huber preorganized the halobenzimidazolium-containing bidentate XB donor **25** with the help of the sterically demanding trifluoromethyl group in the 2-position

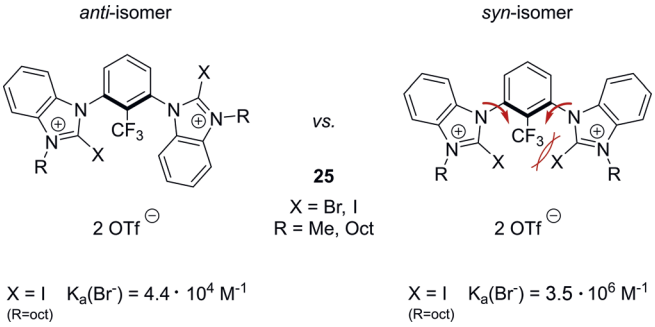

Figure 15. A bidentate haloimidazolium system preorganized by a sterically demanding trifluoromethyl group. **25**: K_a values obtained by ITC titration in CH_3CN at 303 K.[60]

of the benzene core (Figure 15).[60] ITC experiments revealed that the XB donor strength of the isolated *syn* isomer ($K_a(Br^-) = 3.5 \times 10^6\,M^{-1}$ in CH_3CN at 303 K) was significantly higher than that of the *anti* isomer ($K_a(Br^-) = 4.4 \times 10^4\,M^{-1}$ in CH_3CN at 303 K), which was also in line with the observed higher catalytic activity of the *syn* isomer (see Section 4.1, Figure 17).

4. Organocatalysis with XBs

Taking into account the similarities as well as beneficial differences between HBs and XBs (e.g. higher directionality, potential tuneability), the increasing number of investigations on the potential application of XB donor systems as catalysts (or at least as activators) in organic synthesis was a logical consequence.[22,24,61] There is an excellent review from the Huber group that provides a detailed overview of the historic development of XBs in organic synthesis as well as a summary of XB-based activators/catalysts up to the beginning of 2016.[22] Thus, this Minireview only focuses on some highly topical examples from mid-2015 onwards.

4.1. Activation by Halide Abstraction

In the first class of catalytic reactions, the XB donor interacts directly with the covalently bound halogen of the substrate, which in most cases leads to heterolytic cleavage of the bond followed by inhibition of the catalyst by the liberated halide. This is the main reason that most reactions published to date require stoichiometric amounts of the XB donor for the activation process (Figure 16).

For this purpose, the reaction of 1-chloroisochroman with a silyl enol ether was established as benchmark reaction for different XB donor catalysts (Figure 17).[22] The liberated

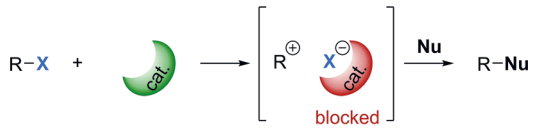

Figure 16. Proposed mechanism for XB-mediated halide abstraction reactions. Nu = nucleophile.

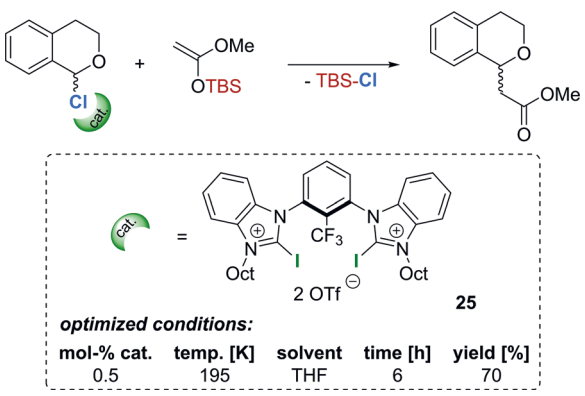

Figure 17. Benchmark reaction of 1-chloroisochroman with a silyl enol ether catalyzed by preorganized XB donor; TBS = *tert*-butyldimethylsilyl.[60]

chloride ion directly reacts with a silyl compound released from the nucleophile to form a very stable silyl chloride (TBS-Cl), which consequently prevents inhibition of the XB catalyst. In a recent example, Jungbauer and Huber tested the catalytic activity of their preorganized bidentate XB donor **25** in this benchmark reaction (Figure 17).[60] The catalytic activity of the *syn* isomer set a new record and could even be used at as low as 0.5 mol% (resulting in a 70% yield of the isolated product). The respective *anti* isomer showed lower activity (51% yield of isolated product with 0.5 mol% catalyst) as a result of its monodentate interaction. Nevertheless, the strength of the preorganized XB donor seemed to reach its limit under these reaction conditions (195 K in THF), as decomposition of compound **25** was already observed in the presence of chloride at room temperature. Recently, an analogous preorganized system with noncoordinating $BAr^{F}_{4}{}^{-}$ ($BAr^{F}_{4}{}^{-}$ = tetrakis[3,5-bis(trifluoromethyl)-phenyl]borate) counterions was used as the catalyst in a Michael addition reaction.[62]

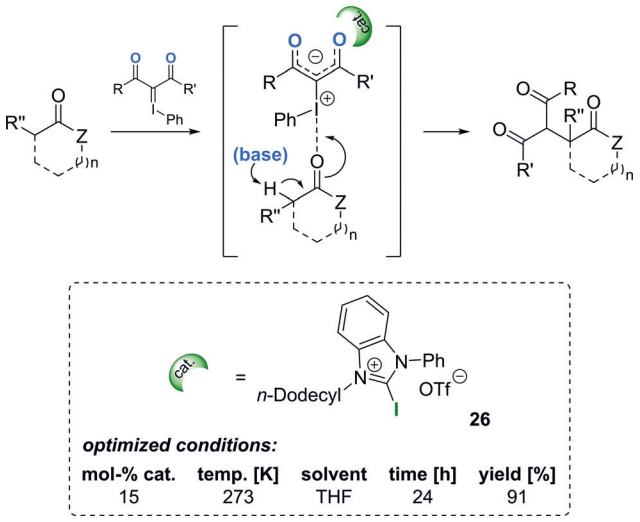

Figure 18. Proposed mechanisms of the umpolung alkylation of silyl enol ethers with an iodonium(III) ylide to afford various 1,4-dicarbonyl compounds.[63]

The Takemoto research group investigated the benzimidazolium system **26** for the XB-based activation of an umpolung alkylation of silyl enol ethers with an iodonium(III) ylide to synthesize various 1,4-dicarbonyl compounds (Figure 18).[63] To extend this approach to less nucleophilic silyl enol ethers, a catalytic amount of base (proton sponge) was added to preactivate the nucleophilic partner.

The XB-mediated halide abstraction reaction was used for the first time in mid-2017 for a controlled cationic living polymerization of isobutyl vinyl ether (IBVE).[64] The bidentate iodoimidazolium XB donor **27** enabled the formation of a dormant and an active species by a reversible halide transfer between the propagating chain end and the catalyst (Figure 19). 1-Chloroisochroman, bromodiphenylmethane, as

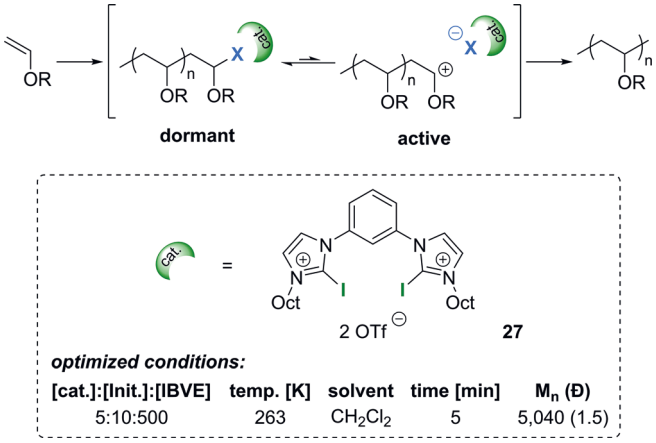

Figure 19. The iodoimidazolium system used for the living cationic polymerization of isobutyl vinyl ether (IBVE); Init = initiator.[64]

well as the HCl adduct of isobutyl vinyl ether were examined as initiators of the polymerization; the last was found to be the most suitable to start the controlled polymerization with narrow dispersities ($Đ = 1.5$, $M_n = 5040$) in CH_2Cl_2 at 263 K. The addition of small amounts of competing chloride ions (0.02 equiv) helped to regulate the equilibrium between the dormant and active species and, thus, to achieve improved control over the polymerization ($Đ = 1.3$, $M_n = 10100$).

4.2. Activation of Neutral Substances

In contrast to the first class of catalytic reactions, which often suffers from the inherent problem of catalyst blocking by the abstracted strong Lewis-basic halide, the second class focuses on the coordination to neutral and less Lewis basic substances such as carbonyl or imine compounds. As a consequence, the binding to the XB donor is much weaker, which on the one hand reduces the problem of forming inert catalyst complexes, but on the other hand hampers sufficient activation of the substance.

In most studies, strong charge-assisted XB donor systems were used for the efficient activation of the substrate; however, these systems sometimes suffer from a decreased stability at higher temperatures.[60] Consequently, different

neutral systems, for example, a chiral bis(imidazolidine)iodobenzene for a Michael/Henry reaction,[65] molecular iodine as the simplest catalytically active XB-based catalyst,[66,67] CBr_4 as the XB donor for the activation of benzaldehydes,[68] and recently the XB contribution in a side-chain iodination of electron-deficient benzylic hydrocarbons with iodohydantoins[69] were also investigated.

The first report of the use of the neutral iodoalkyne motif as a XB-based activator (**28**) was published in 2016 and described the effective activation of thioamides and their subsequent conversion into benzoxazoles (Figure 20).[70] This

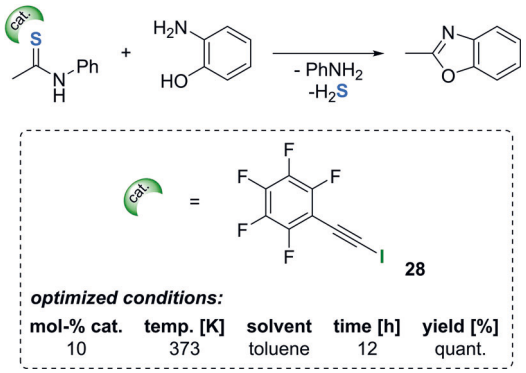

Figure 20. Iodoalkyne-based activation of thioamides and their conversion into benzoxazoles.[70]

study underlined the advantages of neutral XB donors over charge-assisted systems, namely, their better solubility in organic solvents as well as their higher stability towards nucleophiles and elevated temperatures. Control experiments with the analogous terminal alkyne as well as with the trimethylsilyl-protected system revealed product yields comparable to that obtained in the absence of the catalyst and, thus, further support the XB-mediated activation of the substrate.

5. XB-Templated Self-Assembly

The binding sites of receptors can be further used for anion-induced self-assembly to create mechanically interlocked rotaxane and catenane frameworks with an impressive selectivity towards complementary anionic guests.[71] Although the use of linear XBs can result in a notable enhancement of the binding strength and selectivity relative to HB-based analogues, the implementation of XBs as the driving force for the templation is relatively underdeveloped.[21]

In a very impressive example, a luminescent ruthenium(II)-based macrocycle was combined with a bis(iodotriazole)pyridinium motif equipped with permethylated β-cyclodextrin stoppering groups to create the fully water-soluble tricationic [2]rotaxane **29** (Figure 21).[72] Following on from the remarkable previous results,[73] the introduction of these water-solubilizing axle components enabled ^{1}H NMR binding titration experiments in pure D_2O, which revealed a strong

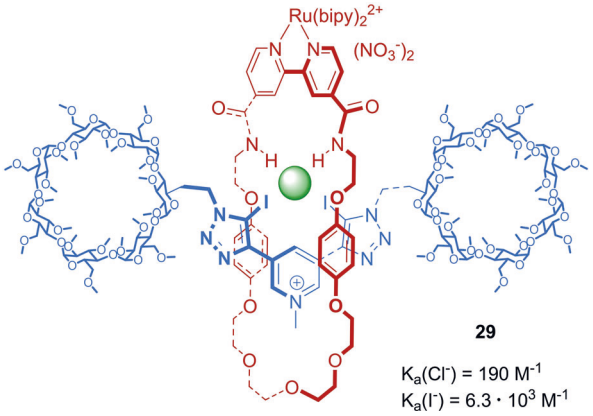

Figure 21. Fully water-soluble tricationic [2]rotaxane combined with a luminescent ruthenium(II) complex; bipy = 2,2′-bipyridine. **29**: K_a values obtained by ^{1}H NMR titration in pure D_2O at 298 K.[72]

preference for iodide ($K_a(I^-) = 6.3 \times 10^3\,M^{-1}$ in D_2O at 298 K) over the smaller halides and sulfate ($I^- > Br^- > SO_4^{2-} > Cl^-$ in D_2O). Moreover, the luminescent reporter group also allowed optical sensing of iodide in water through the enhanced intensity of the metal-centered metal-ligand charge-transfer (MLCT) emission band.

Recently, Beer and co-workers used an active-metal template approach to synthesize a variety of neutral XB rotaxanes containing two, three, and even four iodotriazole moieties (**30**) that exhibited strong and selective halide recognition even in wet organic ($(CD_3)_2CO/D_2O$ (98:2) at 298 K) solvent mixtures (Figure 22).[74] By varying the number and position of the XB donor moieties, which were found to contribute in an additive manner, the anion binding strength as well as the selectivity could be controlled.

Anion-induced conformational changes of the receptor system can be further used as a means of signal transduction. In this context, molecular shuttling of a macrocyclic wheel between a triazolium (X = H, I) axle motif and a naphthalene diimide moiety was reported for a [2]rotaxane[75] as well as for

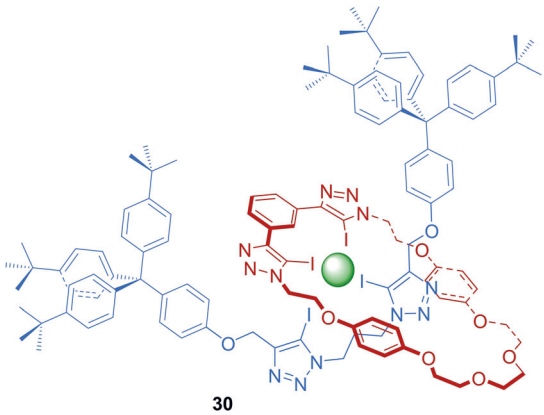

Figure 22. A neutral XB-based rotaxane containing four iodotriazole moieties for selective halide binding. **30**: K_a values obtained by ^{1}H NMR titration in $(CD_3)_2CO/D_2O$ (98:2) at 298 K.[74]

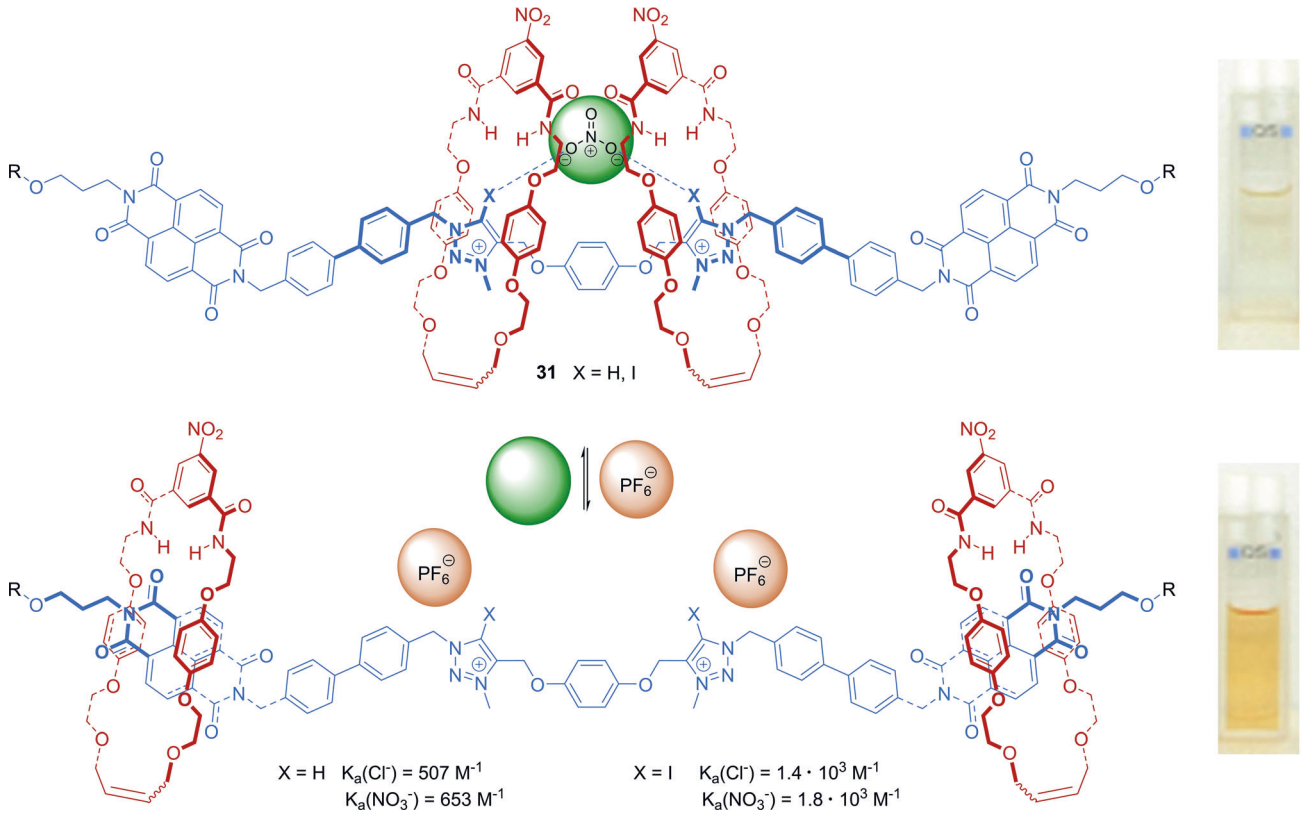

Figure 23. Anion-induced molecular shuttling of two macrocyclic wheels between a triazolium axle motif and a naphthalene diimide moiety in a XB/HB-based [3]rotaxane. **31**: K_a values obtained by ^{1}H NMR titration in $CDCl_3/CD_3OD$ (1:1) at 298 K.[76] Photos reprinted from Ref. [76] with permission. Copyright 2016 WILEY-VCH Verlag GmbH & Co. KGaA, Weinheim.

the first XB-based [3]rotaxane **31** (Figure 23).[76] In both systems, a distinct color change was achieved on exchanging the noncoordinating PF_6^- salt (orange solution) for a coordinating anion (colorless solution), which indicated a movement of the macrocycle from the naphthalene diimide (NDI) towards the central triazolium (X = H, I) anion recognition site. ^{1}H NMR titration experiments revealed an enhanced anion affinity and, thus, a superior shuttling behavior of the XB-based hosts relative to the HB analogues. Although the [2]rotaxane systems were only analyzed qualitatively for their halide affinities, a quantification of the binding constants for the [3]rotaxanes **31** showed a selectivity for nitrate ($K_a(NO_3^-) = 1.8 \times 10^3\,M^{-1}$ in $CDCl_3/CD_3OD$ (1:1) at 298 K) over more basic oxoanions ($H_2PO_4^-$, HCO_3^-, AcO^-) and chloride. This superior association of nitrate was assigned to the strict linearity of the XB interactions leading to a more geometrically defined recognition site that supports the binding of the multidentate oxoanion within the cavity.

6. Summary and Outlook

This Minireview gives an overview of new XB donor systems for anion recognition and sensing processes as well as for organocatalysis and the anionic templation of interlocked structures. Table 1 presents the binding affinities of the

Table 1: Overview of association constants K_a for representative XB complexes with a 1:1 stoichiometry.

	Denticity	Host	Guest	K_a (solvent)	Ref.	Related Ref.[d]
neutral host	1	**14**	Me-PyNO[c]	$1.6\times10^4\,M^{-1}$ ($CDCl_3$)	[50]	[51, 77]
	2	**24**	Cl^-	$7.1\times10^4\,M^{-1}$ (THF)	[29]	[59, 78]
	3[a]	**21**	Cl^-	$8.8\times10^5\,M^{-1}$ (THF)	[59]	[79]
	3	**20**	Cl^-	$1.9\times10^3\,M^{-1}$ (2.5% H_2O in DMSO)	[58]	
charged host	1	**1**	$H_2PO_4^-$	$1.9\times10^5\,M^{-1}$ (CH_3CN)	[30]	[80]
	2	**25**	Br^-	$3.5\times10^6\,M^{-1}$ (CH_3CN)	[60]	[27, 81]
	2 (+2)[b]	**29**	I^-	$6.3\times10^3\,M^{-1}$ (D_2O)	[72]	[2, 73]

[a] Anion recognition proceeds in a tridentate manner, although six donor atoms are available in total and thus a twofold tridentate XB donor is formed. [b] The binding cavity of the [2]rotaxane consists of two XBs supported by two HBs. [c] Me-PyNO = 2-methylpyridine *N*-oxide. [d] Related references of other exemplary studies which also exhibit very strong binding affinities in the respective class.

receptor classes described in this Minireview. The highlighted structures are all among the leading systems in terms of achievable binding affinities in their respective classes (see also the related references in Table 1), and demonstrate the significant progress made in the study of XBs in solution in the last few years.

Various limiting/key factors in terms of binding strengths always need to be considered when comparing different binding affinities:

1) number of accessible donor/acceptor sites,
2) preferred complex stoichiometry,
3) nature/polarity of the solvent and, in this context, also the solubility of the XB donor and acceptor,
4) strength of the XB donor (adjustable through the polarizability of X and the strength of the electron-withdrawing group R),
5) electron-withdrawing ability of R (includes factors such as charge assistance and sp hybridization at the *ipso*-carbon atom),
6) strength of the XB acceptor (includes factors such as solvation enthalpy, charge density, basicity),
7) host–guest geometric and size-complementary factors.

The utilization of XB interactions in solution-phase applications is still at a very early stage, but rapid advances are currently being made. In particular, the characteristic differences in the linearity, tuneability, solvent dependency, and hydrophobicity of XBs compared to the more established HBs has given rise to the construction of unique, highly selective, and functional binding sites for anion recognition with potential future applications in biological, medical, and environmental areas. Although both interactions (HB and XB) enable interaction strengths of up to about 180 kJ mol^{-1},[82,83] the stabilities of the XB-based complexes are much less sensitive to the polarity of the solvent,[84] which leads to the ability to outperform HB-based analogues in competitive solvents. In view of the promising results regarding both the enantiodiscrimination of chiral anions by XB-based systems and the huge potential to further tune the receptors, XBs will definitely have an impact on the development of powerful enantioselective organocatalytic transformations. Thus, a further rapid development of XB-based anion-recognition processes in solution can be anticipated.

Acknowledgements

We are grateful to the Deutsche Forschungsgemeinschaft (DFG) for financial support (SCHU1229/24-1), as well as Robert Schroot for very helpful comments on the manuscript.

Conflict of interest

The authors declare no conflict of interest.

[1] N. Busschaert, C. Caltagirone, W. Van Rossom, P. A. Gale, *Chem. Rev.* **2015**, *115*, 8038.
[2] M. J. Langton, C. J. Serpell, P. D. Beer, *Angew. Chem. Int. Ed.* **2016**, *55*, 1974; *Angew. Chem.* **2016**, *128*, 2012.
[3] P. A. Gale, C. Caltagirone, *Chem. Soc. Rev.* **2015**, *44*, 4212.
[4] P. Molina, F. Zapata, A. Caballero, *Chem. Rev.* **2017**, *117*, 9907.
[5] P. Metrangolo, F. Meyer, T. Pilati, G. Resnati, G. Terraneo, *Angew. Chem. Int. Ed.* **2008**, *47*, 6114; *Angew. Chem.* **2008**, *120*, 6206; G. R. Desiraju, P. S. Ho, L. Kloo, A. C. Legon, R. Marquardt, P. Metrangolo, P. Politzer, G. Resnati, K. Rissanen, *Pure Appl. Chem.* **2013**, *85*, 1711.
[6] Indeed, the terms XB donor and XB acceptor are somewhat confusing. In analogy to hydrogen bonds, the Lewis acidic halogen (i.e. the electron acceptor) is typically referred to as the XB donor, which "donates" the bond to the XB acceptor, namely the Lewis base (i.e. the electron donator).
[7] T. Clark, M. Hennemann, J. S. Murray, P. Politzer, *J. Mol. Model.* **2007**, *13*, 291.
[8] S. M. Huber, J. D. Scanlon, E. Jimenez-Izal, J. M. Ugalde, I. Infante, *Phys. Chem. Chem. Phys.* **2013**, *15*, 10350.
[9] P. A. Gale, J. T. Davis, R. Quesada, *Chem. Soc. Rev.* **2017**, *46*, 2497.
[10] A. V. Jentzsch, A. Hennig, J. Mareda, S. Matile, *Acc. Chem. Res.* **2013**, *46*, 2791.
[11] M. H. Kolář, O. Tabarrini, *J. Med. Chem.* **2017**, *60*, 8681.
[12] H. Wang, W. Wang, W. J. Jin, *Chem. Rev.* **2016**, *116*, 5072.
[13] M. H. Kolář, P. Hobza, *Chem. Rev.* **2016**, *116*, 5155.
[14] G. Resnati, E. Boldyreva, P. Bombicz, M. Kawano, *IUCrJ* **2015**, *2*, 675.
[15] B. Li, S.-Q. Zang, L.-Y. Wang, T. C. W. Mak, *Coord. Chem. Rev.* **2016**, *308*, 1.
[16] Z. Han, G. Czap, C.-l. Chiang, C. Xu, P. J. Wagner, X. Wei, Y. Zhang, R. Wu, W. Ho, *Science* **2017**, *358*, 206.
[17] A. Mukherjee, S. Tothadi, G. R. Desiraju, *Acc. Chem. Res.* **2014**, *47*, 2514.
[18] G. Berger, J. Soubhye, F. Meyer, *Polym. Chem.* **2015**, *6*, 3559.
[19] A. Priimagi, G. Cavallo, P. Metrangolo, G. Resnati, *Acc. Chem. Res.* **2013**, *46*, 2686.
[20] T. M. Beale, M. G. Chudzinski, M. G. Sarwar, M. S. Taylor, *Chem. Soc. Rev.* **2013**, *42*, 1667.
[21] A. Brown, P. D. Beer, *Chem. Commun.* **2016**, *52*, 8645.
[22] D. Bulfield, S. M. Huber, *Chem. Eur. J.* **2016**, *22*, 14434.
[23] M. Erdélyi, *Chem. Soc. Rev.* **2012**, *41*, 3547.
[24] Y. Zhao, Y. Cotelle, N. Sakai, S. Matile, *J. Am. Chem. Soc.* **2016**, *138*, 4270.
[25] L. C. Gilday, S. W. Robinson, T. A. Barendt, M. J. Langton, B. R. Mullaney, P. D. Beer, *Chem. Rev.* **2015**, *115*, 7118.
[26] G. Cavallo, P. Metrangolo, R. Milani, T. Pilati, A. Priimägi, G. Resnati, G. Terraneo, *Chem. Rev.* **2016**, *116*, 2478.
[27] S. M. Walter, F. Kniep, L. Rout, F. P. Schmidtchen, E. Herdtweck, S. M. Huber, *J. Am. Chem. Soc.* **2012**, *134*, 8507.
[28] O. Dumele, D. Wu, N. Trapp, N. Goroff, F. Diederich, *Org. Lett.* **2014**, *16*, 4722.
[29] R. Tepper, B. Schulze, H. Görls, P. Bellstedt, M. Jäger, U. S. Schubert, *Org. Lett.* **2015**, *17*, 5740.
[30] B. Chowdhury, S. Sinha, P. Ghosh, *Chem. Eur. J.* **2016**, *22*, 18051.
[31] N. B. Wageling, G. F. Neuhaus, A. M. Rose, D. A. Decato, O. B. Berryman, *Supramol. Chem.* **2016**, *28*, 665.
[32] S. P. Cornes, M. Sambrook, P. D. Beer, *Chem. Commun.* **2017**, *53*, 3866.
[33] V. Amendola, G. Bergamaschi, M. Boiocchi, N. Fusco, M. V. La Rocca, L. Linati, E. Lo Presti, M. Mella, P. Metrangolo, A. Miljkovic, *RSC Adv.* **2016**, *6*, 67540.
[34] S. Chakraborty, R. Dutta, P. Ghosh, *Chem. Commun.* **2015**, *51*, 14793.

[35] S. Ruiz-Botella, P. Vidossich, G. Ujaque, E. Peris, P. D. Beer, *RSC Adv.* **2017**, *7*, 11253.
[36] C. J. Massena, N. B. Wageling, D. A. Decato, E. M. Rodriguez, A. M. Rose, O. B. Berryman, *Angew. Chem. Int. Ed.* **2016**, *55*, 12398; *Angew. Chem.* **2016**, *128*, 12586.
[37] R. Tepper, S. Bode, R. Geitner, M. Jäger, H. Görls, J. Vitz, B. Dietzek, M. Schmitt, J. Popp, M. D. Hager, U. S. Schubert, *Angew. Chem. Int. Ed.* **2017**, *56*, 4047; *Angew. Chem.* **2017**, *129*, 4105.
[38] A. Vanderkooy, P. Pfefferkorn, M. S. Taylor, *Macromolecules* **2017**, *50*, 3807.
[39] J. Y. C. Lim, M. J. Cunningham, J. J. Davis, P. D. Beer, *Chem. Commun.* **2015**, *51*, 14640.
[40] J. Y. C. Lim, P. D. Beer, *Eur. J. Inorg. Chem.* **2017**, 220.
[41] J. Y. C. Lim, I. Marques, L. Ferreira, V. Félix, P. D. Beer, *Chem. Commun.* **2016**, *52*, 5527.
[42] F. Zapata, A. Caballero, P. Molina, *Eur. J. Inorg. Chem.* **2017**, 237.
[43] L. González, F. Zapata, A. Caballero, P. Molina, C. R. de Arellano, I. Alkorta, J. Elguero, *Chem. Eur. J.* **2016**, *22*, 7533.
[44] R. Oliveira, S. Groni, C. Fave, M. Branca, F. Mavre, D. Lorcy, M. Fourmigue, B. Schollhorn, *Phys. Chem. Chem. Phys.* **2016**, *18*, 15867.
[45] M. Kaasik, S. Kaabel, K. Kriis, I. Järving, R. Aav, K. Rissanen, T. Kanger, *Chem. Eur. J.* **2017**, *23*, 7337.
[46] A. Borissov, J. Y. C. Lim, A. Brown, K. Christensen, A. L. Thompson, M. D. Smith, P. D. Beer, *Chem. Commun.* **2017**, *53*, 2483.
[47] J. Y. C. Lim, I. Marques, V. Félix, P. D. Beer, *J. Am. Chem. Soc.* **2017**, *139*, 12228.
[48] J. Y. C. Lim, I. Marques, V. Félix, P. D. Beer, *Angew. Chem. Int. Ed.* **2017**, *57*, 584; *Angew. Chem.* **2017**, *130*, 593.
[49] O. Dumele, B. Schreib, U. Warzok, N. Trapp, C. A. Schalley, F. Diederich, *Angew. Chem. Int. Ed.* **2017**, *56*, 1152; *Angew. Chem.* **2017**, *129*, 1172.
[50] R. Puttreddy, O. Jurcek, S. Bhowmik, T. Makela, K. Rissanen, *Chem. Commun.* **2016**, *52*, 2338.
[51] V. Stilinović, G. Horvat, T. Hrenar, V. Nemec, D. Cinčić, *Chem. Eur. J.* **2017**, *23*, 5244.
[52] L. Gualandi, M. Lucarini, E. Mezzina, P. Franchi, *Chem. Eur. J.* **2016**, *22*, 16017.
[53] T. Lohmiller, A. V. Mahesh, W. Lubitz, A. Savitsky, *Z. Phys. Chem.* **2017**, *231*, 867.
[54] L. Maugeri, J. Asencio-Hernandez, T. Lebl, D. B. Cordes, A. Slawin, M.-A. Delsuc, D. Philp, *Chem. Sci.* **2016**, *7*, 6422.
[55] L. Maugeri, E. Jamieson, D. B. Cordes, A. Slawin, D. Philp, *Chem. Sci.* **2017**, *8*, 938.
[56] L. Maugeri, T. Lebl, D. B. Cordes, A. M. Z. Slawin, D. Philp, *J. Org. Chem.* **2017**, *82*, 1986.
[57] R. Tepper, B. Schulze, P. Bellstedt, J. Heidler, H. Görls, M. Jager, U. S. Schubert, *Chem. Commun.* **2017**, *53*, 2260.
[58] D. Mungalpara, S. Stegmuller, S. Kubik, *Chem. Commun.* **2017**, *53*, 5095.
[59] S. H. Jungbauer, S. Schindler, E. Herdtweck, S. Keller, S. M. Huber, *Chem. Eur. J.* **2015**, *21*, 13625.
[60] S. H. Jungbauer, S. M. Huber, *J. Am. Chem. Soc.* **2015**, *137*, 12110.
[61] M. Breugst, D. von der Heiden, J. Schmauck, *Synthesis* **2017**, *49*, 3224.
[62] J.-P. Gliese, S. H. Jungbauer, S. M. Huber, *Chem. Commun.* **2017**, *53*, 12052.
[63] M. Saito, Y. Kobayashi, S. Tsuzuki, Y. Takemoto, *Angew. Chem. Int. Ed.* **2017**, *56*, 7653; *Angew. Chem.* **2017**, *129*, 7761.
[64] K. Takagi, K. Yamauchi, H. Murakata, *Chem. Eur. J.* **2017**, *23*, 9495.
[65] T. Arai, T. Suzuki, T. Inoue, S. Kuwano, *Synlett* **2017**, *28*, 122.
[66] D. von der Heiden, S. Bozkus, M. Klussmann, M. Breugst, *J. Org. Chem.* **2017**, *82*, 4037.
[67] C. Xi, X. Yi, L. Jiao, *Org. Biomol. Chem.* **2016**, *14*, 9912.
[68] I. Kazi, S. Guha, G. Sekar, *Org. Lett.* **2017**, *19*, 1244.
[69] S. H. Combe, A. Hosseini, L. Song, H. Hausmann, P. R. Schreiner, *Org. Lett.* **2017**, *19*, 6156.
[70] A. Matsuzawa, S. Takeuchi, K. Sugita, *Chem. Asian J.* **2016**, *11*, 2863.
[71] M. Xue, Y. Yang, X. Chi, X. Yan, F. Huang, *Chem. Rev.* **2015**, *115*, 7398.
[72] M. J. Langton, I. Marques, S. W. Robinson, V. Félix, P. D. Beer, *Chem. Eur. J.* **2016**, *22*, 185.
[73] M. J. Langton, S. W. Robinson, I. Marques, V. Félix, P. D. Beer, *Nat. Chem.* **2014**, *6*, 1039.
[74] J. Y. C. Lim, T. Bunchuay, P. D. Beer, *Chem. Eur. J.* **2017**, *23*, 4700.
[75] T. A. Barendt, S. W. Robinson, P. D. Beer, *Chem. Sci.* **2016**, *7*, 5171.
[76] T. A. Barendt, A. Docker, I. Marques, V. Félix, P. D. Beer, *Angew. Chem. Int. Ed.* **2016**, *55*, 11069; *Angew. Chem.* **2016**, *128*, 11235.
[77] M. G. Sarwar, B. Dragisić, E. Dimitrijević, M. S. Taylor, *Chem. Eur. J.* **2013**, *19*, 2050.
[78] F. Kniep, S. H. Jungbauer, Q. Zhang, S. M. Walter, S. Schindler, I. Schnapperelle, E. Herdtweck, S. M. Huber, *Angew. Chem. Int. Ed.* **2013**, *52*, 7028; *Angew. Chem.* **2013**, *125*, 7166.
[79] M. G. Sarwar, B. Dragisic, S. Sagoo, M. S. Taylor, *Angew. Chem. Int. Ed.* **2010**, *49*, 1674; *Angew. Chem.* **2010**, *122*, 1718.
[80] M. Cametti, K. Raatikainen, P. Metrangolo, T. Pilati, G. Terraneo, G. Resnati, *Org. Biomol. Chem.* **2012**, *10*, 1329.
[81] R. Tepper, B. Schulze, M. Jäger, C. Friebe, D. H. Scharf, H. Görls, U. S. Schubert, *J. Org. Chem.* **2015**, *80*, 3139.
[82] P. Metrangolo, H. Neukirch, T. Pilati, G. Resnati, *Acc. Chem. Res.* **2005**, *38*, 386.
[83] F. Biedermann, H.-J. Schneider, *Chem. Rev.* **2016**, *116*, 5216.
[84] C. C. Robertson, R. N. Perutz, L. Brammer, C. A. Hunter, *Chem. Sci.* **2014**, *5*, 4179.

Manuscript received: August 4, 2017
Revised manuscript received: December 14, 2017
Accepted manuscript online: January 17, 2018
Version of record online: ■■ ■■, ■■■■

Minireviews

Suparmolecular Chemistry

R. Tepper,
U. S. Schubert* ———— ■■■■–■■■■

Halogen Bonding in Solution: Anion Recognition, Templated Self-Assembly, and Organocatalysis

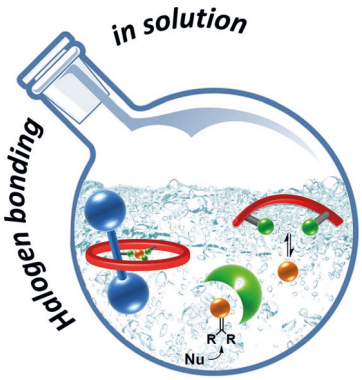

Giving direction: The utilization of highly directional halogen bonds for anion coordination and supramolecular chemistry has become increasingly apparent. In particular, their application for selective anion interactions in solution has attracted enormous interest. This Minireview focuses on fundamental advances in receptors based on halogen bonds in the area of anion recognition and sensing, anion-templated self-assembly, as well as organocatalysis.

Publication P2

”Preorganization in a cleft-type anion receptor featuring iodo-1,2,3-triazoles as halogen bond donors”

R. Tepper, B. Schulze, H. Görls, P. Bellstedt, M. Jäger, U. S. Schubert, *Org. Lett.* **2015**, *17*, 5740-5743.

The paper as well as the supporting information (free of charge) is available online under:
doi.org/10.1021/acs.orglett.5b02760

Organic LETTERS

Letter

pubs.acs.org/OrgLett

Preorganization in a Cleft-Type Anion Receptor Featuring Iodo-1,2,3-Triazoles As Halogen Bond Donors

Ronny Tepper,[†,‡] Benjamin Schulze,[†,‡,∥] Helmar Görls,[§] Peter Bellstedt,[†,§] Michael Jäger,[†,‡] and Ulrich S. Schubert*[,†,‡]

[†]Laboratory of Organic and Macromolecular Chemistry (IOMC), Friedrich Schiller University Jena, Humboldtstrasse 10, 07743 Jena, Germany

[‡]Jena Center for Soft Matter (JCSM), Friedrich Schiller University Jena, Philosophenweg 7, 07743 Jena, Germany

[§]Laboratory of Inorganic and Analytical Chemistry, Friedrich Schiller University Jena, Lessingstrasse 8, 07743 Jena, Germany

Supporting Information

ABSTRACT: Preorganization *via* intramolecular hydrogen bonds was applied in a cleft-type receptor by exploiting the excellent halogen bond donor ability as well as hydrogen bond acceptor function of iodo-1,2,3-triazoles. As investigated by isothermal calorimetric titrations, the restriction of conformational freedom causes an enhanced entropic contribution resulting in a strongly increased binding affinity. This efficient way to improve the binding strength of 5-halo-1,2,3-triazoles paves the way for applications of new charge-neutral halogen bond donors in solution.

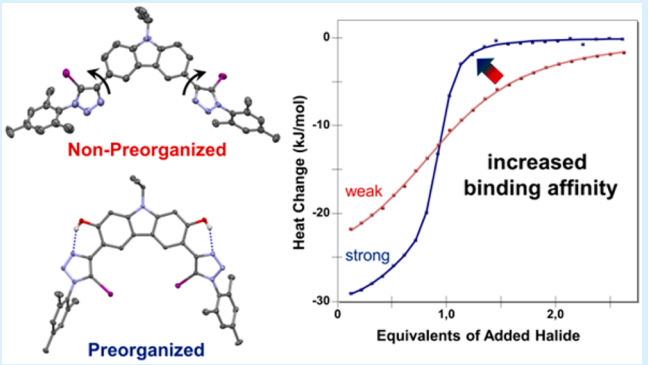

The halogen bond (XB) is a highly directional supramolecular interaction between a Lewis-acidic region of a covalently bound halogen (σ-hole) and a Lewis-base.[1] When compared to the hydrogen bond (HB), the XB features a higher preference for linearity[2] as well as a higher bond strength,[3] which constitutes the basis for application of XBs in selective anion detection[4] and transport,[5] organocatalysis,[6] and anion-templated construction of interlocked structures.[7] Beside cationic halo-imidazolium[4b,6a,8] and halo-1,2,3-triazolium[3b,4a,9] moieties, also charge-neutral systems based on perfluoroiodo arenes[2a,6b,10] and halo-1,2,3-triazoles[3b,7b−d,f,11] have been established as excellent XB donors.

While cationic XB donors achieve very high anion affinities due to charge assistance, their interaction with anions is less directional because of the isotropic nature of the additional Coulomb attraction.[11c] Evidently, this benefit only applies to anionic species. In addition, highly competitive solvents are usually required to dissolve the receptors and/or to prevent precipitation of the formed complex,[12] which lowers the effective binding strength in case of cationic XB donors. In contrast, charge-neutral XB donors offer an increased solubility in less competitive solvents and allow for a more directional binding. These characteristics of neutral systems might be advantageous when designing strong and selective receptors, *e.g.*, for application in asymmetric organocatalysis.[6b] For the latter, the use of charge-neutral catalysts is crucial, as the binding of anionic intermediates (*e.g.*, oxo-anions) or products (*e.g.*, halides) instead of the neutral substrate would be highly preferred in case of cationic receptors, *i.e.*, the catalyst would be blocked.[6f]

In particular, 5-halo-1,2,3-triazoles have been established as versatile, charge-neutral XB donors due to their good accessibility *via* facile and modular copper(I)-catalyzed cycloaddition reactions as well as their sufficient electron-withdrawing character.[11c,13] Nevertheless, the polarization of the XB donor atom and, consequently, the size of the σ-hole in this neutral unit is much smaller than that of positively charged halo-triazolium moieties.[3b] Hence, additional concepts as for instance chelation through polydentate donors[4c,6f,10a,d,11b] are required to increase the binding affinity. Furthermore, the concept of preorganization *via* intramolecular HBs represents a very efficient method to improve the binding affinity.

The 1,2,3-triazole ring is ideally suited to establish intramolecular preorganization as it offers both donor and acceptor function. In the case of HB-based receptors, this has been demonstrated by the seminal work by Flood *et al.*[14] Notably, the preorganization by intramolecular HBs does not only screen the entropic penalty for the binding event, but also increases the effective binding enthalpy since the free receptor cannot adopt a relaxed conformation and because the polarization of the 1,2,3-triazole is enhanced (dipole moment of 4.4 D[11c] and 6.1 D[14b] for the flexible and preorganized triazole, respectively). However, to

Received: September 24, 2015
Published: November 20, 2015

DOI: 10.1021/acs.orglett.5b02760
Org. Lett. 2015, 17, 5740−5743

the best of our knowledge, no comparative XB-based system has been published to date.[15]

Because of the strict linearity of XBs as well as the large size of the XB donor atom, the design of efficient polydentate XB-based receptors is not trivial.[3b] In contrast to flexible receptors, which can adapt to the size of the binding partner, the design of preorganized receptors is more challenging. In this case, the cavity of the preorganized receptor molecule has to match the size of the guest, otherwise the breaking of the intramolecular HB upon binding would hinder the binding event. In this contribution, we demonstrate that the carbazole spacer is ideally suited to enable a bidentate binding of halides by two iodo-1,2,3-triazoles in a coplanar fashion (Scheme 1, top).[16] Building on this finding, we demonstrate the effect of preorganization in XB donors based on iodo-triazoles (Scheme 1, bottom).

Scheme 1. Schematic Representation of Studied Receptors[a]

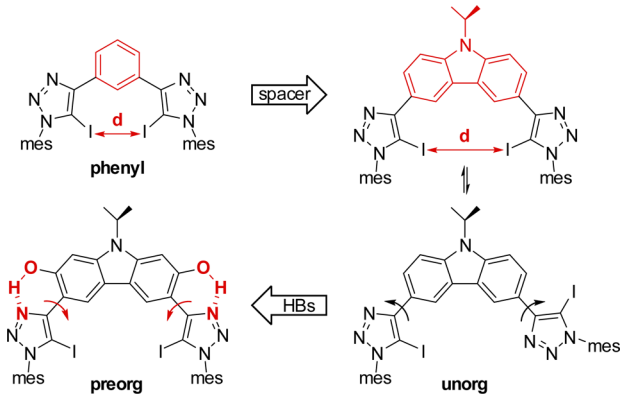

[a]Top: influence of spacer unit 1,3-benzene (**phenyl**) or 3,6-carbazole (**unorg**) on distance (*d*) between two donor moieties. Bottom: preorganization via intramolecular HBs (**preorg**).

Besides the already established phenyl-based receptor system (**phenyl**),[3b] the two carbazole-based receptors were synthesized using copper(I)-catalyzed cycloaddition reactions. **Unorg** was prepared directly from the corresponding iodo-alkyne (**3**) and mesityl azide in moderate yields (Scheme 2). In the case of the preorganized receptor, the 1,2,3-triazoles were formed first (**8**) and the iodination was achieved by metalation using *n*-BuLi and subsequent treatment with iodine to obtain the methoxy-decorated precursor (**9**). Remarkably, even in the presence of the iodo-1,2,3-triazoles, the final receptor **preorg** was obtained in excellent yields by BBr_3-induced ether cleavage. In addition, the formation of intramolecular HBs in case of **preorg** was revealed by selective ROESY studies as well as ^{1}H NMR experiments in solvents with different polarity.[17]

To discuss the influence of the receptor design in the solid state, single crystals of free and complexed receptors were grown by slow vapor diffusion of different nonsolvents into a concentrated solution.[17] Obviously, because of the conformational freedom of **unorg**, the anti/anti or syn/anti conformation of the XB donors can be adapted in the free receptor.[18] In contrast, the formation of intramolecular HBs in **preorg** leads to a limitation of the rotational freedom, and thus, the required syn/syn conformation for the bidentate complexation is already preformed, which could be also supported by quantum chemical calculations using density functional theory (DFT).[17]

Furthermore, all three receptors revealed the expected cleft-type complexation of the anion through the formation of two

Scheme 2. Schematic Representation of the Synthesis of Receptors unorg and preorg

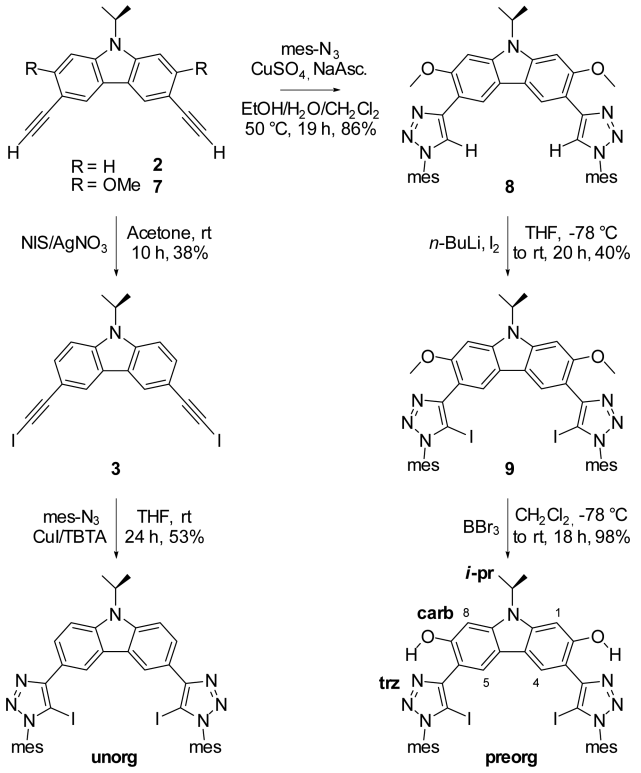

nearly linear XBs, which are significantly shorter than the sum of the van der Waals radii (I···Cl 3.73 Å).[19] Moreover, the preorganization of **preorg** led to an additional binding process (*vide infra*).

Comparing the 1:1 complexes of **phenyl** and **unorg** with chloride (Figure 1), the larger distance (*d*) between the two

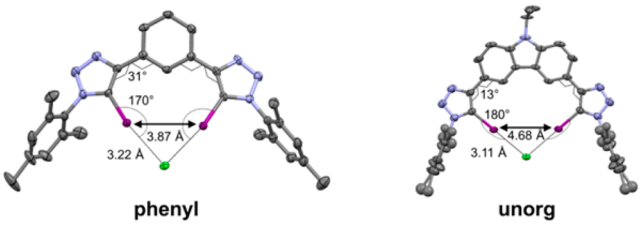

Figure 1. Molecular structure of **phenyl** (left) and **unorg** (right) interacting with chloride (thermal ellipsoids at 50% probability level, hydrogen atoms, counterions, and solvent molecules are omitted for clarity).

iodine atoms in the carbazole-based receptor enables an improved coplanarization (dihedral angle of 31° and 13°, respectively), which allows an increased linearity of the XBs and, as a net result, a decreased I···Cl distance.

Isothermal titration calorimetry (ITC) experiments were performed with the three receptors and two different tetra-*n*-butylammonium (TBA^+) halides to obtain a detailed understanding of the complex stoichiometry, the binding affinity, and the thermodynamic effect of preorganization in solution (Table 1). All titrations were performed in the guest-into-host setup in THF. In addition, also inverse titrations, *i.e.*, addition of a host solution into a guest solution, were performed to confirm the reliability of the calculated values.[17] Unfortunately, a direct

DOI: 10.1021/acs.orglett.5b02760
Org. Lett. 2015, 17, 5740−5743

Table 1. Thermodynamic Parameters for the Complexation of Various Receptors with Different TBA$^+$ Halides[a]

host	guest	K [M^{-1}]	ΔH [kJ mol^{-1}]	$T\Delta S$[kJ mol^{-1}]	N
phenyl	Br$^-$	2.22×10^3	−24.5	−5.1	0.99
	Cl$^-$	3.52×10^3	−22.9	−2.3	1.08
unorg	Br$^-$	1.58×10^3	−27.4	−8.8	1.03
	Cl$^-$	2.34×10^3	−24.9	−5.4	1.05
preorg[b]	Br$^-$	3.85×10^3	−7.2	13.6	0.52
		5.45×10^4	−23.5	4.0	0.89
	Cl$^-$	3.17×10^3	−15.1	5.3	0.45
		7.09×10^4	−17.8	10.3	0.90

[a]Thermodynamic parameters calculated from guest-into-host titrations in THF at 303 K. [b]The formation of a 2:1 complex (host−guest) could be further supported by a solid-state structure and selective NOESY experiments (*vide infra*).

comparison between **preorg** and **9** was not possible because of the insufficient solubility of **9** in THF.

In line with the binding in the solid state, a cleft-type complexation of the halides by **phenyl** and **unorg** in solution was deduced from the ITC titration experiments. For **unorg**, a slightly increased enthalpic contribution toward the binding was revealed, which may be due to the optimized XB formation (Figure 1). On the other hand, the entropic term is decreased for **unorg**, which is tentatively explained by a smaller extent of desolvation of the receptor and/or the anion upon binding. However, there are only subtle differences in the overall binding affinities of **phenyl** and **unorg** and the effect of the spacer unit seems to be negligible for the two flexible receptors.

Comparing the complexation of chloride and bromide, the trend for the K values (Table 1) shows a general preference for the more charge-dense/basic chloride, which allows a stronger electrostatic as well as charge-transfer interaction.[3b,8b] For the same reason, the solvent interaction is more pronounced for chloride, resulting in a reduced enthalpic contribution toward the binding, which is, however, overcompensated by a more favorable entropic term due to the enhanced desolvation upon anion complexation.[20]

When comparing **unorg** and **preorg**, the tendency to form a 1:1 complex with chloride is enhanced by a factor of about 30 for the preorganized receptor ($K_1^{\text{unorg}} = 2.34 \times 10^3$ M^{-1} and $K_1^{\text{preorg}} = 7.09 \times 10^4$ M^{-1}). As a result of the increased anion affinity, even a 2:1 complex is formed (*vide infra*). The same behavior is observed for bromide. Regarding the overall chloride affinity, the accumulated binding constant has to be considered, which even amounts to $K_1K_2 = 2.24 \times 10^8$ M^{-2}, corresponding to $\Delta G = -48.5$ kJ mol^{-1}. Notably, in contrast to the association constants, the observed binding enthalpy for the formation of a 1:1 complex with **unorg** cannot be directly compared to the binding enthalpy of a 1:1 complex with **preorg** since a 2:1 complex is formed simultaneously in the case of the latter. Thus, the released heat accounts for two processes both being related to the complexation of a single anion. Furthermore, the observed enthalpies for the formation of 1:1 and 2:1 complexes depend on the titration setup (guest-to-host *vs* host-to-guest).[21] However, the sum of both enthalpies, which corresponds to the total interaction with the anion, is the same irrespective of the titration order and is slightly more negative in the case of **preorg**. This slightly enhanced enthalpic contribution is attributed to the preorganization, which prevents a relaxation of the free receptor, *i.e.*, the preorganized receptor is spring-loaded for complexation. Additionally, the polarization of the triazole rings may be slightly enhanced;[14b] however, no significant difference of the computed σ-hole was observed.[17,22] Most importantly, however, the entropic term for the complexation with **preorg** is positive, while it is negative for **unorg**. This striking difference can be explained by the restriction of rotational freedom already in the uncomplexed **preorg** due to the intramolecular HBs. Consequently, the entropy penalty for the complexation is screened in the preorganized receptor[14b] and the desolvation of host and guest give rise to a positive entropic term.

The formation of a 2:1 complex could also be observed in the solid state (Figure 2A).[17] Accordingly, the anion is complexed in

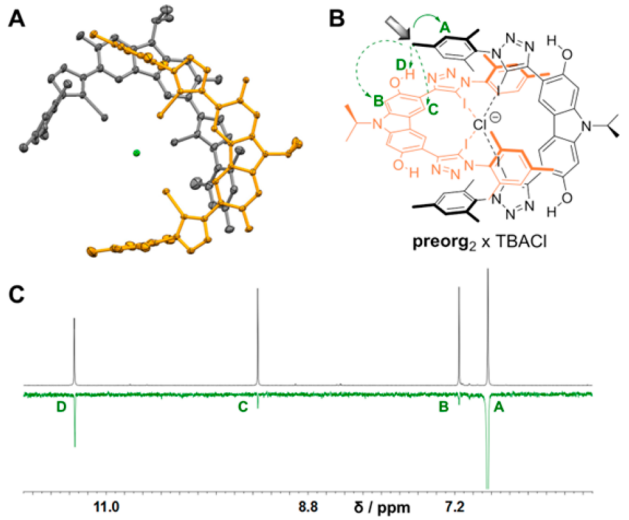

Figure 2. (A) Molecular structure of **preorg** interacting with chloride forming a 2:1 complex (thermal ellipsoids at 50% probability level, hydrogen atoms, counterions, and solvent molecules are omitted for clarity). (B) Schematic representation of the NOE contacts; the excited protons are marked with a shaded arrow and strong and medium contacts are indicated with solid and dashed arrows, respectively. (C) ^{1}H NMR and selective ROESY spectra for **preorg** in the presence of 0.5 equiv of TBACl in THF-d_8.

a *bis*-bidentate fashion *via* four highly directional XBs (167° to 177°), which are all significantly shorter than the sum of the van der Waals radii (3.09−3.23 Å).[17] Moreover, the hydroxyl groups serve only as intramolecular HB donors and are not involved in the anion complexation.

This coordination mode is also present in solution as revealed by selective ROESY experiments (Figure 2B, C). For this experiment, a 2:1 mixture of the receptor and the anion was dissolved in THF-d_8 and the NOE signals after excitation of the methyl group of the mesityl substituent (CH_3-4$^{\text{mes}}$) were recorded. Beside a strong contact to the adjacent aromatic proton, further contacts to the central carbazole spacer and the hydroxyl groups were visible (Figure 2B, C). These additional NOE signals are not observed for the free receptor[17] and can only be explained by an orthogonal arrangement of two receptors within a *bis*-bidentate complex.

In conclusion, three different bidentate XB-based anion receptors were synthesized using facile and modular copper(I)-catalyzed cycloaddition reactions. Subsequently, the halide complexation was characterized by ITC experiments, X-ray diffraction, and selective ROESY experiments. While **phenyl** and **unorg** showed only moderate association constants, a strongly increased binding affinity was revealed for **preorg** *via* formation of intramolecular HBs between the central carbazole spacer and

DOI: 10.1021/acs.orglett.5b02760
Org. Lett. 2015, 17, 5740−5743

the adjacent iodo-1,2,3-triazoles, a rigid bidentate XB donor was formed, which enabled a strong complexation of halides without entropic penalty. Notably, the central carbazole is an almost ideal spacer for this assignment as it enables a bidentate complexation by a nearly planar receptor system. Following these building principles, charge-neutral, cleft-type receptors with high anion affinities can be designed. Owing to the highly directional and strong XBs as well as to the absence of isotropic Coulomb interactions, these receptors offer great potential for application as organocatalysts.

■ ASSOCIATED CONTENT

Supporting Information

The Supporting Information is available free of charge on the ACS Publications website at DOI: 10.1021/acs.orglett.5b02760.

DFT data and crystal structures (CIF)
Experimental details, NMR spectra, binding studies (PDF)

■ AUTHOR INFORMATION

Corresponding Author

*E-mail: ulrich.schubert@uni-jena.de.

Present Address

[‖]B.S.: Novaled GmbH, Tatzberg 49, 01307 Dresden, Germany

Notes

The authors declare no competing financial interest.

■ ACKNOWLEDGMENTS

The authors are grateful to the Deutsche Forschungsgemeinschaft (DFG) for financial support (Grants SCHU 1229/24-1 and SPP 1568). We also thank C. Friebe, W. Günther, G. Sentis, T. Schlotthauer, as well as N. Fritz (all Friedrich Schiller University Jena, IOMC, Germany) for discussions and performing experiments.

■ REFERENCES

(1) (a) Gale, P. A.; Caltagirone, C. *Chem. Soc. Rev.* **2015**, *44*, 4212. (b) Metrangolo, P.; Resnati, G. *Science* **2008**, *321*, 918. (c) Desiraju, G. R.; Ho, P. S.; Kloo, L.; Legon, A. C.; Marquardt, R.; Metrangolo, P.; Politzer, P.; Resnati, G.; Rissanen, K. *Pure Appl. Chem.* **2013**, *85*, 1711. (d) Beale, T. M.; Chudzinski, M. G.; Sarwar, M. G.; Taylor, M. S. *Chem. Soc. Rev.* **2013**, *42*, 1667. (e) Erdelyi, M. *Chem. Soc. Rev.* **2012**, *41*, 3547. (f) Gilday, L. C.; Robinson, S. W.; Barendt, T. A.; Langton, M. J.; Mullaney, B. R.; Beer, P. D. *Chem. Rev.* **2015**, *115*, 7118. (g) Clark, T.; Hennemann, M.; Murray, J. S.; Politzer, P. *J. Mol. Model.* **2007**, *13*, 291.

(2) (a) Chudzinski, M. G.; McClary, C. A.; Taylor, M. S. *J. Am. Chem. Soc.* **2011**, *133*, 10559. (b) Kilah, N. L.; Wise, M. D.; Beer, P. D. *Cryst. Growth Des.* **2011**, *11*, 4565.

(3) (a) Politzer, P.; Lane, P.; Concha, M. C.; Ma, Y.; Murray, J. S. *J. Mol. Model.* **2007**, *13*, 305. (b) Tepper, R.; Schulze, B.; Jäger, M.; Friebe, C.; Scharf, D. H.; Görls, H.; Schubert, U. S. *J. Org. Chem.* **2015**, *80*, 3139. (c) Priimagi, A.; Cavallo, G.; Metrangolo, P.; Resnati, G. *Acc. Chem. Res.* **2013**, *46*, 2686.

(4) (a) Zapata, F.; Caballero, A.; Molina, P.; Alkorta, I.; Elguero, J. *J. Org. Chem.* **2014**, *79*, 6959. (b) Caballero, A.; White, N. G.; Beer, P. D. *Angew. Chem., Int. Ed.* **2011**, *50*, 1845. (c) Sarwar, M. G.; Dragisic, B.; Sagoo, S.; Taylor, M. S. *Angew. Chem., Int. Ed.* **2010**, *49*, 1674.

(5) Vargas Jentzsch, A.; Emery, D.; Mareda, J.; Metrangolo, P.; Resnati, G.; Matile, S. *Angew. Chem., Int. Ed.* **2011**, *50*, 11675.

(6) (a) Takeda, Y.; Hisakuni, D.; Lin, C.-H.; Minakata, S. *Org. Lett.* **2015**, *17*, 318. (b) Kniep, F.; Jungbauer, S. H.; Zhang, Q.; Walter, S. M.; Schindler, S.; Schnapperelle, I.; Herdtweck, E.; Huber, S. M. *Angew. Chem., Int. Ed.* **2013**, *52*, 7028. (c) Jungbauer, S.; Walter, S.; Schindler, S.; Rout, L.; Kniep, F.; Huber, S. M. *Chem. Commun.* **2014**, *50*, 6281. (d) Castelli, R.; Schindler, S.; Walter, S. M.; Kniep, F.; Overkleeft, H. S.; Van der Marel, G. A.; Huber, S. M.; Codée, J. D. C. *Chem. - Asian J.* **2014**, *9*, 2095. (e) Walter, S. M.; Kniep, F.; Herdtweck, E.; Huber, S. M. *Angew. Chem., Int. Ed.* **2011**, *50*, 7187. (f) Kniep, F.; Rout, L.; Walter, S. M.; Bensch, H. K. V.; Jungbauer, S. H.; Herdtweck, E.; Huber, S. M. *Chem. Commun.* **2012**, *48*, 9299. (g) Jungbauer, S. H.; Huber, S. M. *J. Am. Chem. Soc.* **2015**, *137*, 12110. (h) Bruckmann, A.; Pena, M. A.; Bolm, C. *Synlett* **2008**, *2008*, 900.

(7) (a) Caballero, A.; Swan, L.; Zapata, F.; Beer, P. D. *Angew. Chem., Int. Ed.* **2014**, *53*, 11854. (b) Mullaney, B. R.; Thompson, A. L.; Beer, P. D. *Angew. Chem.* **2014**, *126*, 11642. (c) Robinson, S. W.; Mustoe, C. L.; White, N. G.; Brown, A.; Thompson, A. L.; Kennepohl, P.; Beer, P. D. *J. Am. Chem. Soc.* **2015**, *137*, 499. (d) Cornes, S. P.; Davies, C.; Blyghton, D.; Sambrook, M.; Beer, P. D. *Org. Biomol. Chem.* **2015**, *13*, 2582. (e) Gilday, L. C.; Lang, T.; Caballero, A.; Costa, P. J.; Félix, V.; Beer, P. D. *Angew. Chem., Int. Ed.* **2013**, *52*, 4356. (f) Mullaney, B. R.; Partridge, B. E.; Beer, P. D. *Chem. - Eur. J.* **2015**, *21*, 1660.

(8) (a) Zapata, F.; Caballero, A.; White, N. G.; Claridge, T. D. W.; Costa, P. J.; Félix, V.; Beer, P. D. *J. Am. Chem. Soc.* **2012**, *134*, 11533. (b) Walter, S. M.; Kniep, F.; Rout, L.; Schmidtchen, F. P.; Herdtweck, E.; Huber, S. M. *J. Am. Chem. Soc.* **2012**, *134*, 8507. (c) Cametti, M.; Raatikainen, K.; Metrangolo, P.; Pilati, T.; Terraneo, G.; Resnati, G. *Org. Biomol. Chem.* **2012**, *10*, 1329.

(9) (a) Lim, J. Y. C.; Beer, P. D. *Chem. Commun.* **2015**, *51*, 3686. (b) Mercurio, J. M.; Knighton, R. C.; Cookson, J.; Beer, P. D. *Chem. - Eur. J.* **2014**, *20*, 11740.

(10) (a) Dimitrijevic, E.; Kvak, O.; Taylor, M. S. *Chem. Commun.* **2010**, *46*, 9025. (b) Jungbauer, S. H.; Bulfield, D.; Kniep, F.; Lehmann, C. W.; Herdtweck, E.; Huber, S. M. *J. Am. Chem. Soc.* **2014**, *136*, 16740. (c) Takezawa, H.; Murase, T.; Resnati, G.; Metrangolo, P.; Fujita, M. *Angew. Chem., Int. Ed.* **2015**, *54*, 8411. (d) Jungbauer, S. H.; Schindler, S.; Herdtweck, E.; Keller, S.; Huber, S. M. *Chem. - Eur. J.* **2015**, *21*, 13625.

(11) (a) Langton, M. J.; Robinson, S. W.; Marques, I.; Félix, V.; Beer, P. D. *Nat. Chem.* **2014**, *6*, 1039. (b) Gilday, L. C.; White, N. G.; Beer, P. D. *Dalton Trans.* **2013**, *42*, 15766. (c) Schulze, B.; Schubert, U. S. *Chem. Soc. Rev.* **2014**, *43*, 2522.

(12) Schulze, B.; Friebe, C.; Hager, M. D.; Günther, W.; Köhn, U.; Jahn, B. O.; Görls, H.; Schubert, U. S. *Org. Lett.* **2010**, *12*, 2710.

(13) Hua, Y.; Flood, A. H. *Chem. Soc. Rev.* **2010**, *39*, 1262.

(14) (a) McDonald, K. P.; Ramabhadran, R. O.; Lee, S.; Raghavachari, K.; Flood, A. H. *Org. Lett.* **2011**, *13*, 6260. (b) Lee, S.; Hua, Y.; Park, H.; Flood, A. H. *Org. Lett.* **2010**, *12*, 2100. (c) McDonald, K. P.; Qiao, B.; Twum, E. B.; Lee, S.; Gamache, P. J.; Chen, C.-H.; Yi, Y.; Flood, A. H. *Chem. Commun.* **2014**, *50*, 13285.

(15) In the course of our investigations, Beer *et al.* published an interesting study including iodo-1,2,3-triazoles which were preorganized by the help of a covalent metal coordination: Mole, T. K.; Arter, W. E.; Marques, I.; Félix, V.; Beer, P. D. *J. Organomet. Chem.* **2015**, *792*, 206 Nevertheless, there is no detailed characterization of the effect of preorganization.

(16) In the course of our investigations, Beer *et al.* published rotaxane systems with related cationic XB donors based on a carbazole spacer. See references 7b and 7f.

(17) See the Supporting Information for more detailed explanations.

(18) Zornik, D.; Meudtner, R. M.; El Malah, T.; Thiele, C. M.; Hecht, S. *Chem. - Eur. J.* **2011**, *17*, 1473.

(19) Bondi, A. *J. Phys. Chem.* **1964**, *68*, 441.

(20) Schmidtchen, F. P. *Chem. Soc. Rev.* **2010**, *39*, 3916.

(21) Dobrawa, R.; Ballester, P.; Saha-Möller, C. R.; Würthner, F. In *Metal-Containing and Metallosupramolecular Polymers and Materials*; American Chemical Society: Washington, DC, 2006; Vol. *928*, Chapter 4.

(22) Electrostatic potential calculations were performed for **unorg** and **preorg** to visualize the σ-hole.

DOI: 10.1021/acs.orglett.5b02760
Org. Lett. 2015, 17, 5740−5743

Publication P3

”Halogen-bond-based cooperative ion-pair recognition by a crown-ether-embedded 5-iodo-1,2,3-triazole”

R. Tepper, B. Schulze, P. Bellstedt, J. Heidler, H. Görls, M. Jäger, U. S. Schubert, *Chem. Commun.* **2017**, *53*, 2260-2263.

The paper as well as the supporting information (free of charge) is available online under:
doi.org/10.1039/C6CC09749A

ChemComm

COMMUNICATION

View Article Online
View Journal | View Issue

Cite this: *Chem. Commun.*, 2017, 53, 2260

Received 7th December 2016,
Accepted 26th January 2017

DOI: 10.1039/c6cc09749a

rsc.li/chemcomm

Halogen-bond-based cooperative ion-pair recognition by a crown-ether-embedded 5-iodo-1,2,3-triazole†

Ronny Tepper,[ab] Benjamin Schulze,‡[ab] Peter Bellstedt,[ac] Jan Heidler,[ab] Helmar Görls,[c] Michael Jäger[ab] and Ulrich S. Schubert*[ab]

A crown-ether containing the iodo-triazole moiety for simultaneous cation–anion binding through Lewis-basic nitrogen atoms and C–I···I halogen-bond-donating iodine atoms was prepared. The complexation of the heteroditopic receptor was illustrated by X-ray and DFT analysis. The cooperative effect boosting the anion affinity was quantified by $^{1}H/^{13}C$ NMR titration experiments.

The selective recognition and sensing of ions has attracted enormous interest in supramolecular chemistry; however, the design of ditopic receptors capable of the simultaneous binding of both cation and anion is still an underexplored area.[1–3] Nevertheless, the combination of allosteric and electrostatic cooperative effects offer the opportunity to fine tune the affinity as well as selectivity of these ion-pair receptors, which enables a better control over the binding event in potential applications like, *e.g.*, salt extraction/solubilization, membrane transport, or sensing.[3]

While the cation binding sites in these ditopic systems usually take advantage of crown-ether or calixarene derivatives, the anion binding sites typically involve Lewis-acidic sites, electrostatic interactions or, most frequently, use hydrogen bond (HB) interactions.[1] Beside the commonly used urea, amide, or hydroxyl groups, also 1,2,3-triazoles have been employed recently as HB donors for ion-pair receptors[4,5] due to their good accessibility *via* facile and modular copper(I)-catalyzed azide–alkyne cycloaddition (CuAAC) reactions as well as due to their CH-acidic and highly polar character.[6,7] Additionally, the Lewis-basic part of this heterocycle offers the opportunity to simultaneously coordinate metal cations and, thus, the possibility for a concurrent recognition of both cation and anion guest species through the triazole motif is given.[5,8,9]

While the usage of HBs in solution has already been well established, the application of halogen bond (XB) interactions in solution has attracted enormous interest over the last years.[10,11] In general, an XB is a highly directional supramolecular interaction between a Lewis-acidic region of a covalently bound halogen (σ-hole)[12] and a Lewis base. When compared to HB, the XB features a higher preference for linearity as well as a higher bond strength,[13] which constitutes the basis for applications of XBs in selective anion detection,[14–16] organocatalysis,[17,18] and anion-templated construction of interlocked structures.[19] Nevertheless, their application in the field of ion-pair recognition is very sparse,[20,21] which might be due to a combination of synthetic challenges and experimental complexities associated with the simultaneous as well as reliable quantification of different binding affinities.

In this communication, we report a macrocyclic ion-pair receptor comprising an iodo-triazole moiety for XB-based anion recognition and a Lewis-basic cavity consisting of a triethylene glycol chain and the nitrogen atoms of the triazole motif for cation binding. The heteroditopic character of the receptor is demonstrated by the calculated electrostatic potential surface (Scheme 1 and Fig. S51, ESI†). Accordingly, a possible ion-pair

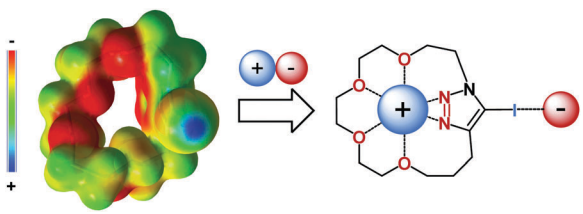

Scheme 1 Calculated molecular electrostatic potential surface (red: 0.00 to blue: 0.15) mapped on total density (isovalue 0.01) for the studied ion pair system (left); schematic representation of ion pair recognition by an iodo-triazole containing crown-ether. Red color indicates Lewis-basic regions, blue color Lewis-acidic regions (right).

[a] *Laboratory of Organic and Macromolecular Chemistry (IOMC), Friedrich Schiller University Jena, Humboldtstr. 10, 07743 Jena, Germany. E-mail: ulrich.schubert@uni-jena.de*
[b] *Jena Center of Soft Matter (JCSM), Friedrich Schiller University Jena, Philosophenweg 7, 07743 Jena, Germany*
[c] *Laboratory of Inorganic and Analytical Chemistry, Friedrich Schiller University Jena, Humboldtstr. 8, 07743 Jena, Germany*

† Electronic supplementary information (ESI) available: Experimental details, crystal structures, NMR spectra as well as detailed explanations towards NMR binding studies are included. See DOI: 10.1039/c6cc09749a

‡ Present address: Novaled GmbH, Tatzberg 49, 01307 Dresden, Germany.

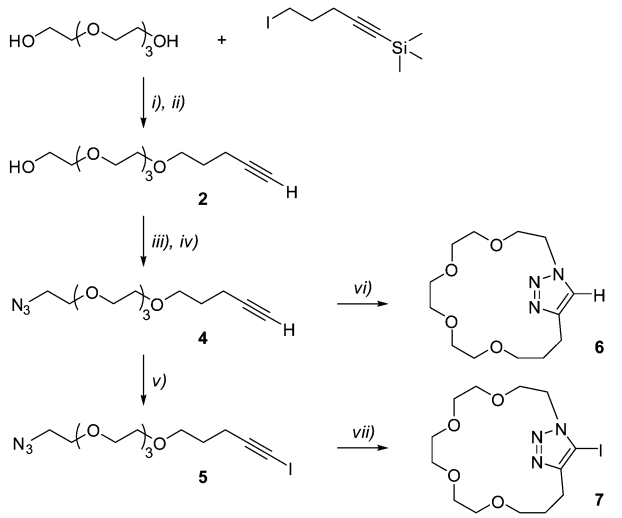

Scheme 2 (i) NaH, THF, 0 °C, 30% (**1**); (ii) TBAF, THF/MeOH (2 : 3), room temperature (rt), 99% (**2**); (iii) TosCl, DMAP, Et_3N, CH_2Cl_2, 0 °C, 86% (**3**); (iv) NaN_3, DMSO, rt, 89% (**4**); (v) NIS, $AgNO_3$, acetone, rt, 87% (**5**); (vi) $CuSO_4$, NaAsc., $EtOH/H_2O/CH_2Cl_2$ (2 : 1 : 1), 50 °C, 74% (**6**); (vii) CuI, TBTA, THF, 40 °C, 75% (**7**).

binding mode that simultaneously employs the iodo-triazole's function as a Lewis base and as XB donor is illustrated in Scheme 1. The flexibility of the macrocyclic backbone should enable an adaption for the size of the cation, while the monodentate interaction simplifies the analysis of the binding affinity.

The HB- and XB-donating crown-ether-based macrocycles **6** and **7**, respectively, were accessible by taking advantage of highly efficient CuAAC-type reactions. For this purpose, unsymmetrically substituted triethylene glycols equipped with an azide as well as an alkyne (**4**)/iodo-alkyne (**5**) function were synthesised (Scheme 2). Subsequently, the fundamental synthetic challenge of forming well-defined monomeric macrocycles instead of larger macrocycles or linear oligomers was achieved using pseudo-high-dilution-conditions.[22] Hence, a solution of the linear precursor (**4** or **5**) was added dropwise to a heated solution containing the catalyst system ($CuSO_4$/NaAsc. for **4** or CuI/TBTA for **5**) required to initiate the intramolecular cyclization. Indeed, owing to the high efficiency of the cyclization reaction, the desired products were obtained in good yields and were characterized by NMR spectroscopy, mass spectrometry, and, ultimately, single-crystal X-ray diffraction (Fig. 1).

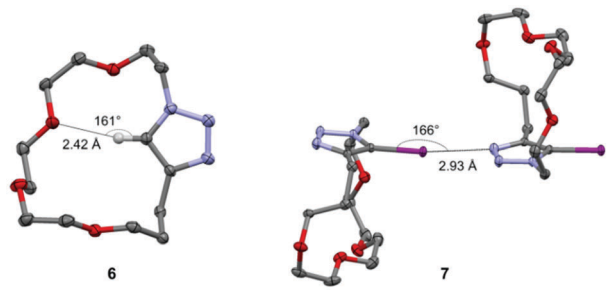

Fig. 1 Single crystal X-ray structures of **6** (left, with intramolecular HB) and **7** (right, with intermolecular XB) (thermal ellipsoids at 50% probability level, hydrogen atoms and solvent molecules are omitted for clarity).

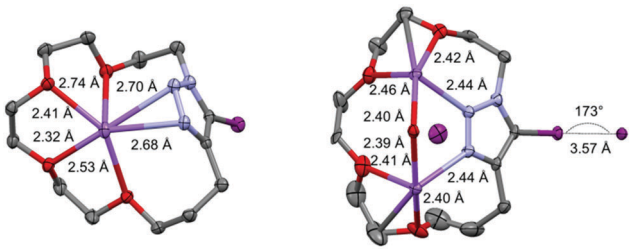

Fig. 2 Single crystal X-ray structure of **7** interacting with Na^+ forming a 1 : 1 complex (left) as well as the structure of **7** interacting with NaI forming a 1 : 2 complex (right); (sodium added as $NaBPh_4$, thermal ellipsoids at 50% probability level, hydrogen atoms, BPh_4^- counter ions, and solvent molecules are omitted for clarity).

The participation of the Lewis-basic nitrogen atoms of the iodo-triazole moiety in the cation complexation was confirmed by single-crystal X-ray diffraction of the macrocycles **6** and **7** interacting with sodium and a non-coordinating anion (see Fig. 2 for **7** and Fig. S48 for **6**, ESI†).[23] The expected simultaneous interaction of the four oxygen atoms and the two triazole nitrogen atoms with the cation was observed. Nonetheless, sodium is apparently not an ideal guest for the binding cavity, which is indicated by several observations: (1) the $Na^+\cdots O$ distances in the 1 : 1 complex range from 2.32 Å to 2.74 Å indicating a slightly strained binding pocket and (2) depending on the added amount of sodium salt, the stoichiometry can adapt to a 1 : 1 as well as a 1 : 2 complex.

Nevertheless, the capability of the iodo-triazole moiety to coordinate simultaneously cationic and anionic guests was proven by the molecular structure of **7** interacting with sodium iodide in a 1 : 2 complex (Fig. 2). In this case, the nitrogen atoms still contribute towards the cation binding while the anion is complexed through the formation of a nearly linear (173°) XB, which is significantly shorter than the sum of the van der Waals radii ($d(I\cdots I)$ = 3.96 Å).[24] Additionally, both iodides are stabilized by HBs formed between the anion and bridging water molecules (Fig. S50C, ESI†). The close contact distances between Na^+ and I^- range from 4.6 Å to 5.1 Å, which falls between the $Na^+\cdots I^-$ contact ion pair distance (3.2 Å)[4] and the completely host-separated ion pair distance (5.6 Å)[20] observed for other sodium iodide complexes with organic receptor molecules.

After this proof of principle, the cooperative effect of the cation complexation on the anion-binding affinity was quantified by detailed binding studies in solution. For this purpose, the cation and anion binding of the macrocyclic receptors were investigated by ^1H NMR and ^{13}C NMR spectroscopy (Scheme 3). A mixture of CD_2Cl_2 and CD_3CN (3 : 1) was found to offer good solubility for both the receptor and all titrated salts, in particular sodium iodide (Table 1).

Initially, the individual cation and anion binding affinity of the receptor system was studied by using sodium tetraphenylborate ($NaBPh_4$) and tetra-*n*-butyl ammonium iodide (TBAI), respectively. Here, characteristic sodium- as well as iodide-induced chemical shift migrations in the ^1H NMR and ^{13}C NMR spectra were observed, while their respective bulky, non-coordinating counter

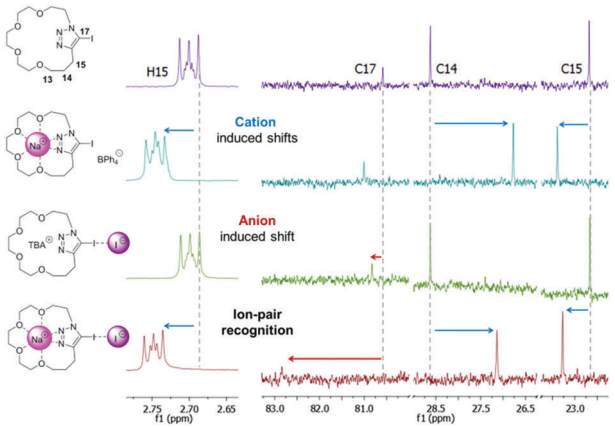

Scheme 3 Schematic representation of the $^{1}H/^{13}C$ NMR (500/126 MHz, $CD_2Cl_2:CD_3CN$ 3 : 1) of host **7** [1 mM] with 8 eq. of different guests illustrating the chemical shifts used for the calculation of the cation or anion binding affinities.

ions did not show any significant influence on the chemical shifts in a control experiment (Fig. S22, ESI†).[23]

Noteworthy, the analysis of the anion affinity represents a basic experimental challenge in this study owing to a fundamental difference between HB- and XB-based receptors. While the binding analysis of the HB-based systems benefit from mostly large chemical shift migrations of the HB-forming protons, the distance between XB-based anion-binding sites and adjacent hydrogen atoms is often too large to see any significant chemical shift migrations in the ^{1}H NMR spectrum. Consequently, alternatives like *e.g.* UV/Vis, ^{19}F NMR, or ^{13}C NMR analysis have to be used.[25]

In this work, the anion binding could only be exemplified by the ^{13}C NMR chemical shift migration of the quaternary carbon atom (C_{17}) directly connected to the XB-donating iodine atom (Scheme 3). In combination with the very low concentrations of the host solutions ([1 mM]), which were dictated by the limited solubility of sodium iodide in organic solvents (Table S1, ESI†), very long ^{13}C NMR acquisition times and a cryogenic NMR probe were thus required.[23] Moreover, owing to the even worse organosolubility of other salts, *e.g.*, NaBr/NaCl (to study the influence of the basicity of the anion) or KI (to study the influence of the cavity size on the cation affinity), a more comprehensive binding study was prevented. Despite these limitations, the found characteristic cation- and anion-induced chemical shift migrations in the NMR data (Scheme 3) allowed the calculation of sodium- and iodide-binding affinities (K_{Na} and K_I, respectively) applying a 1 : 1 binding model (Table 1).[26]

The comparatively weak cation-binding affinity of the macrocycle ($K_{Na} < 10^3\ M^{-1}$ compared to $K_{Na} > 10^4\ M^{-1}$ for optimized crown-ether systems)[27] is in line with the non-ideal geometry of the cavity for the sodium ion as concluded from the X-ray analysis (Fig. 2). Furthermore, the binding affinity of **7** towards mere iodide (added as TBA salt) is very weak, which is caused by: (1) the charge-neutrality of the triazole moiety, *i.e.* the absence of charge-assistance; (2) the monodentate interaction; (3) the rather low charge density/basicity of iodide; (4) the absence of cooperative effects through cation complexation. Accordingly, the reliable quantification of the anion affinity was rather challenging; however, comparable monodentate iodo-triazole-based receptors gave very similar results.[28]

Table 1 Overview of the binding constants calculated from NMR titration data for **6** and **7** with different guests (sodium added as $NaBPh_4$ and iodide added as TBAI, measurements at 297 K in a $CD_2Cl_2:CD_3CN$ (3 : 1) solvent mixture)

Host	Guest	NMR	K_{Na} [M^{-1}]	K_I [M^{-1}]
7	Na^+	^{1}H	434 ± 6^a	—
	I^-	^{13}C	—	4.7 ± 0.4^d
	NaI	^{1}H	394 ± 14^a	N/S
		^{13}C	406 ± 60^b	135 ± 17^d
6	Na^+	^{1}H	126 ± 6^c	—
	I^-	^{13}C	—	N/D
	NaI	^{1}H	155 ± 19^c	N/S
		^{13}C	174 ± 30^b	N/D

Signal used for the calculation of the corresponding association constant: $a = H_{15}$, $b = C_{14}$, $c = H_{13}$, $d = C_{17}$; N/S = no shift; no anion induced shift observable in the ^{1}H NMR; N/D = not determined, no reliable quantification of K_I due to an insufficiently large chemical shift.

The good comparability between different NMR titration experiments was proven by the coincidence of the K_{Na} values obtained by ^{1}H NMR ($K_{Na} = 394 \pm 14\ M^{-1}$) and ^{13}C NMR ($K_{Na} = 406 \pm 60\ M^{-1}$) of **7** with NaI. The larger error in the case of the latter is attributed to the fewer data points that were accessible for the fitting process.[23]

Regarding the cooperativity of the ion-pair recognition, the cation-binding affinity calculated by the titration of **7** with $NaBPh_4$ ($K_{Na} = 434 \pm 6\ M^{-1}$) revealed nearly the same result as the titration of **7** with NaI ($K_{Na} = 394 \pm 14\ M^{-1}$) indicating that the cation binding is clearly dominated by the multidentate coordination within the macrocycle. Potentially, the cation binding of **7** could be enhanced in the presence of iodide due to the additional Coulomb attraction and a cooperative polarization of the 1,2,3-triazole ring; however, as NaI is not expected to be fully solvent-separated in $CD_2Cl_2:CD_3CN$ (3 : 1), the enhanced ion-pair separation in **7** with NaI deteriorates the cooperative effects. In contrast, the presence of the coordinated cation significantly enhanced the anion-binding affinity of **7**. Noteworthy, as the anion recognition only relies on a monodentate XB interaction with the iodo-triazole, cooperativity is still observed in this case. This cooperative effect is ascribed to an additional electrostatic contribution[29] and, in particular, an enhancement of the C–I bond polarization (Fig. S51, ESI†). While the ability to partially separate two ions underlined the strength of the XB interaction, the relatively large ion-pair distance expected for **7** with NaI (Fig. S52, ESI†) also caused a reduction of the electrostatic contribution and, consequently, cooperative effects in the ion-pair recognition are not fully exploited for the presented receptor type.

The expected decrease of the binding affinity by changing from the XB- to the analogous HB-based interaction[13] led to an insufficient chemical-shift migration during the NMR titration and, thus, precluded a reliable quantification of the anion-binding affinity of **6**. Moreover, comparing the cation-binding

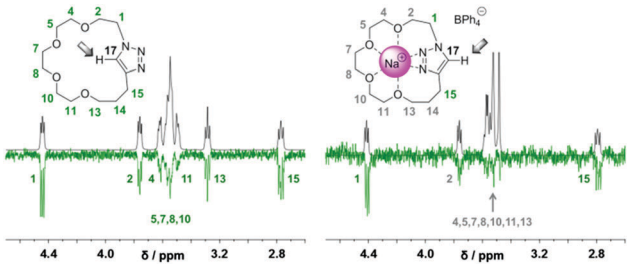

Fig. 3 Schematic representation of the ROE contacts; the selectively excited proton (H_{17}) is marked with a shaded arrow and strong as well as weak contacts are indicated with green and grey numbers, respectively. ^{1}H NMR (black) and selective ROESY spectra (green) for **6** [20 mM] in the absence (left) as well as in the presence of 8 equiv. of $NaBPh_4$ (right) in a CD_2Cl_2 : CD_3CN (3 : 1) solvent mixture.

affinities of the XB- and the HB-based receptor ($K_{Na} = 434 \pm 6\ M^{-1}$ for **7** and $K_{Na} = 126 \pm 6\ M^{-1}$ for **6**, respectively), also a significantly decreased K_{Na} was observed for the latter. This lowered cation-binding affinity was attributed to a possible intramolecular HB formation, which was also observed for the solid-state structures (Fig. 1) and would cause an interference with the cation complexation of the crown ether. To prove this assumption, selective ROESY experiments of **6** in a CD_2Cl_2 : CD_3CN (3 : 1) solvent mixture were performed (Fig. 3).[23] After selective excitation of the triazole proton (H_{17}) in the free macrocycle **6**, strong ROE signals of all protons indicated a freely rotatable triazole moiety and, thus, also a possible formation of an intramolecular HB between H_{17} and oxygen atoms of the crown ether. In contrast, upon addition of $NaBPh_4$ (Fig. 3 and Fig. S46, ESI†), the ROE signals of all protons located at the cation-binding site decreased (Table S2, ESI†).[23] Consequently, the possibility of an intramolecular HB formation is lowered as the triazole moiety is involved in the complexation of the cation within the macrocycle. Conversely, the intramolecular HB lowers the cation affinity of **6**. While this behavior cannot be studied for **7**, the size of the macrocycle's binding pocket is simply too small to establish an analogous intramolecular XB, which is in line with the intermolecular XB observed in the solid state (Fig. 1).

In conclusion, well-defined macrocycles capable of HB (**6**) and XB (**7**) interactions were synthesised using highly efficient CuAAC-type reactions under pseudo-high-dilution-conditions. Subsequently, the capability of a crown-ether-embedded 5-iodo-1,2,3-triazole to coordinate simultaneously cation and anion guests was proven by solid-state analysis and supported by quantum chemical calculations. Subsequently, detailed ^{1}H and ^{13}C NMR titration experiments in solution were performed with sodium iodide as representative ion pair to quantify the cooperative effect of the cation complexation on the anion-binding affinity. For this purpose, several challenges had to be overcome first, namely (1) the low organosolubility of sodium iodide and, thus, the very low concentrations of the host solutions; (2) low anion-binding affinities; (3) comparatively weak cation-binding affinity of the macrocycle due to the non-ideal fit of the sodium with the cation cavity; (4) interference of an intramolecular HB with the cation-binding site in case of **6**. Nonetheless, a consistent and reliable analysis of the binding affinities as well as the determination of the cooperative effect was successfully demonstrated for the presented 5-iodo-1,2,3-triazole-derived model system. Considering both, the already observed promising cooperative effect of the simultaneous metal coordination on the XB-based anion recognition by the iodo-triazole and the potential to further improve the cation-binding cavity using highly efficient CuAAC-type reactions, more powerful ion-pair receptors can be designed building on this fundamental study.

Notes and references

1 S. K. Kim and J. L. Sessler, *Chem. Soc. Rev.*, 2010, **39**, 3784.
2 P. D. Beer and M. J. Langton, *Macrocyclic and Supramolecular Chemistry*, 2016, , DOI: 10.1002/9781119053859.ch3.
3 A. J. McConnell and P. D. Beer, *Angew. Chem., Int. Ed.*, 2012, **51**, 5052.
4 B. Qiao, A. Sengupta, Y. Liu, K. P. McDonald, M. Pink, J. R. Anderson, K. Raghavachari and A. H. Flood, *J. Am. Chem. Soc.*, 2015, **137**, 9746.
5 S. C. Picot, B. R. Mullaney and P. D. Beer, *Chem. – Eur. J.*, 2012, **18**, 6230.
6 B. Schulze and U. S. Schubert, *Chem. Soc. Rev.*, 2014, **43**, 2522.
7 Y. Hua and A. H. Flood, *Chem. Soc. Rev.*, 2010, **39**, 1262.
8 H. Tomiyasu, N. Shigyo, X.-L. Ni, X. Zeng, C. Redshaw and T. Yamato, *Tetrahedron*, 2014, **70**, 7893.
9 M. A. D. C. González, F. Otón, R. A. Orenes, A. Espinosa, A. Tárraga and P. Molina, *Organometallics*, 2014, **33**, 2837.
10 G. Cavallo, P. Metrangolo, R. Milani, T. Pilati, A. Priimägi, G. Resnati and G. Terraneo, *Chem. Rev.*, 2016, **116**, 2478.
11 L. C. Gilday, S. W. Robinson, T. A. Barendt, M. J. Langton, B. R. Mullaney and P. D. Beer, *Chem. Rev.*, 2015, **115**, 7118.
12 M. H. Kolář and P. Hobza, *Chem. Rev.*, 2016, **116**, 5155.
13 R. Tepper, B. Schulze, M. Jäger, C. Friebe, D. H. Scharf, H. Görls and U. S. Schubert, *J. Org. Chem.*, 2015, **80**, 3139.
14 T. M. Beale, M. G. Chudzinski, M. G. Sarwar and M. S. Taylor, *Chem. Soc. Rev.*, 2013, **42**, 1667.
15 M. Erdelyi, *Chem. Soc. Rev.*, 2012, **41**, 3547.
16 R. Tepper, B. Schulze, H. Görls, P. Bellstedt, M. Jäger and U. S. Schubert, *Org. Lett.*, 2015, **17**, 5740.
17 D. Bulfield and S. M. Huber, *Chem. – Eur. J.*, 2016, **22**, 14434.
18 Y. Zhao, Y. Cotelle, N. Sakai and S. Matile, *J. Am. Chem. Soc.*, 2016, **138**, 4270.
19 A. Brown and P. D. Beer, *Chem. Commun.*, 2016, **52**, 8645.
20 A. Mele, P. Metrangolo, H. Neukirch, T. Pilati and G. Resnati, *J. Am. Chem. Soc.*, 2005, **127**, 14972.
21 A. Vargas Jentzsch, D. Emery, J. Mareda, P. Metrangolo, G. Resnati and S. Matile, *Angew. Chem., Int. Ed.*, 2011, **50**, 11675.
22 S. Binauld, C. J. Hawker, E. Fleury and E. Drockenmuller, *Angew. Chem., Int. Ed.*, 2009, **48**, 6654.
23 See ESI† for more detailed explanations.
24 A. Bondi, *J. Phys. Chem.*, 1964, **68**, 441.
25 P. Thordarson, *Chem. Soc. Rev.*, 2011, **40**, 1305.
26 Although a possible formation of a 1 : 2 complex was also indicated by the solid state structures, the 1 : 1 binding model was chosen since it should describe the complexation in solution most properly (see Fig. S27 and S28 (ESI†) for detailed explanations).
27 Z. Wang, S. H. Chang and T. J. Kang, *Spectrochim. Acta, Part A*, 2008, **70**, 313.
28 L. Maugeri, J. Asencio-Hernandez, T. Lebl, D. B. Cordes, A. Slawin, M.-A. Delsuc and D. Philp, *Chem. Sci.*, 2016, **7**, 6422.
29 Calculated $Na^+ \cdots I^-$ distance of 5.6 Å (Fig. S52, ESI†) is below the expectable Bjerrum-length (see for example R. Moritz, G. Zardalidis, H.-J. Butt, M. Wagner, K. Müllen and G. Floudas, *Macromolecules*, 2014, **47**, 191) of ions in an unpolar solvent mixture.

Publication P4

”Polymeric halogen-bond-based donor systems showing self-healing behavior in thin films”

R. Tepper, S. Bode, R. Geitner, M. Jäger, H. Görls, J. Vitz, B. Dietzek, M. Schmitt, J. Popp, M. D. Hager, U. S. Schubert, *Angew. Chem. Int. Ed.* **2017**, *56*, 4047-4051; *Angew. Chem.* **2017**, *129*, 4105-4110.

The paper as well as the supporting information (free of charge) is available online under: doi.org/10.1002/anie.201610406

Self-Healing Systems

International Edition: DOI: 10.1002/anie.201610406
German Edition: DOI: 10.1002/ange.201610406

Polymeric Halogen-Bond-Based Donor Systems Showing Self-Healing Behavior in Thin Films

Ronny Tepper, Stefan Bode, Robert Geitner, Michael Jäger, Helmar Görls, Jürgen Vitz, Benjamin Dietzek, Michael Schmitt, Jürgen Popp, Martin D. Hager, and Ulrich S. Schubert**

Abstract: *The synthesis and comprehensive characterization of a systematic series of cleft-type anion receptors imbedded into a polymeric architecture is presented. For the first time, isothermal calorimetric titrations on polymeric halogen-bond-based donors were exploited to evaluate the dependence of the anion affinity on different key parameters (i.e. monomeric versus polymeric receptor, halogen versus hydrogen bonding, charge assistance). The combination of these donor systems with a copolymer bearing accepting carboxylate groups led to supramolecular cross-linked polymer networks showing excellent intrinsic self-healing behavior. FT-Raman spectroscopy and nano-indentation measurements were utilized to clarify the thermally induced self-healing mechanism based on the formation of halogen bonds. These first self-healing materials based on halogen bonds pave the way for new applications of halogen-bond donors in polymer and material science.*

The halogen bond (XB) is a supramolecular interaction between a Lewis-acidic region of a covalently bound halogen (σ-hole) and a Lewis base.[1] As an analogue of hydrogen bonds (HB), the XB is utilized in various fields of solution-phase applications (e.g. selective anion detection[2] and transport,[3] organocatalysis,[4] and anion-templated construction of interlocked structures[5]) and has attracted enormous interest in the last decades.[6] In particular, the greater preference for linearity[7] compared to HBs combined with the potential tuneability of the interaction strength[8] gives rise to the construction of very selective and highly functional anion-binding sites. Recently, the combination of XBs with polymeric architectures has also attracted growing interest in regard to the design of functional supramolecular materials.[9] Nevertheless, the use of XBs in polymer science is still in its infancy, with a current concentration on halogenated perfluoroalkanes and perfluoroarenes as XB donor moieties that interact with different pyridine and amine derivatives.[9a] However, there is potentially a much larger variety of conceivable XB donor–acceptor pairs with a broad range of interaction strengths as well as complex stoichiometries, as already known from solution-phase investigations. Hence, transferring this knowledge to polymeric systems allows the design of novel functional materials with on-demand properties. In this context, it is conceivable that designing a new class of intrinsic self-healing polymer networks based on XBs has great potential, but was, to the best of our knowledge, not reported up to now.

In general, the concept of self-healing polymers relies on the formation of a reversible network, which is able to heal, for example, a mechanical damage and to restore the mechanical properties.[10] Different supramolecular interactions have already been utilized to prepare such materials.[11] In this regard, the aim of this study is to generate self-healing materials by utilization of highly directional and strong XBs. In particular, the influence of the different binding affinities of analogous HB- and XB-based receptor systems as well as the effect of charge assistance were analyzed, which allowed a straightforward variation of the polymer properties for the later application. Thus, a systematic series of cleft-type anion receptors based on HB and XB interactions were imbedded into a polymeric architecture and were comprehensively characterized by isothermal titration calorimetry (ITC) and extensive self-healing tests.

The synthesis of the polymeric donor–acceptor systems as well as of the required reference systems employed in this study is depicted in Figure 1. Reversible addition-fragmentation chain-transfer polymerization (RAFT) was utilized to prepare well-defined copolymers with a low dispersity and precise molar masses.[12] In all cases, butyl methacrylate (BMA) was chosen as co-monomer since it features a low glass transition temperature (around 20 °C).

In the case of the polymeric donor systems (**P1** and **P2**), co-monomers containing HB (**M1**) or XB (**M2**) donor units were designed, which already revealed an efficient binding behavior in their analogous monomeric forms (see reference

[*] R. Tepper, Dr. S. Bode, Dr. M. Jäger, Dr. J. Vitz, Dr. M. D. Hager, Prof. U. S. Schubert
Laboratory of Organic and Macromolecular Chemistry (IOMC)
Friedrich Schiller University Jena
Humboldtstrasse 10, 07743 Jena (Germany)
E-mail: martin.hager@uni-jena.de
ulrich.schubert@uni-jena.de

R. Tepper, Dr. S. Bode, Dr. M. Jäger, Dr. J. Vitz, Prof. B. Dietzek, Prof. M. Schmitt, Prof. J. Popp, Dr. M. D. Hager, Prof. U. S. Schubert
Jena Center for Soft Matter (JCSM)
Friedrich Schiller University Jena
Philosophenweg 7, 07743 Jena (Germany)

R. Geitner, Prof. B. Dietzek, Prof. J. Popp
Institute for Physical Chemistry and Abbe Center of Photonics (ACP)
Friedrich Schiller University Jena
Helmholtzweg 4, 07743 Jena (Germany)

Dr. H. Görls
Laboratory of Inorganic and Analytical Chemistry
Friedrich Schiller University Jena
Humboldtstrasse 8, 07743 Jena (Germany)

Prof. B. Dietzek, Prof. J. Popp
Leibniz Institute for Photonic Technology (IPHT) Jena
Albert-Einstein-Strasse 9, 07745 Jena (Germany)

Supporting information and the ORCID identification number(s) for the author(s) of this article can be found under: http://dx.doi.org/10.1002/anie.201610406.

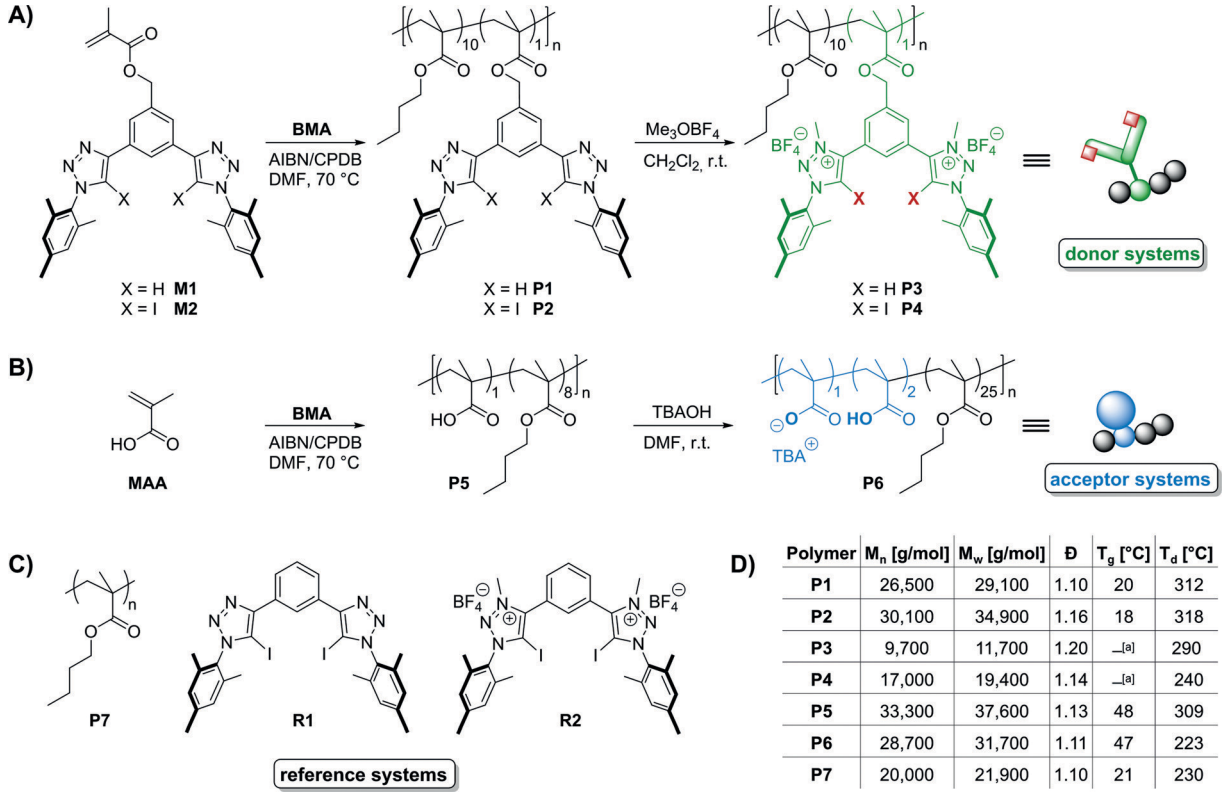

D)

Polymer	M_n [g/mol]	M_w [g/mol]	Đ	T_g [°C]	T_d [°C]
P1	26,500	29,100	1.10	20	312
P2	30,100	34,900	1.16	18	318
P3	9,700	11,700	1.20	–[a]	290
P4	17,000	19,400	1.14	–[a]	240
P5	33,300	37,600	1.13	48	309
P6	28,700	31,700	1.11	47	223
P7	20,000	21,900	1.10	21	230

Figure 1. A) Monomers **M1** and **M2** (see the Supporting Information for the synthetic procedures) were subjected to RAFT polymerization with BMA to prepare the donor-containing copolymers **P1** and **P2**, which were further methylated to obtain **P3** and **P4**. B) Acceptor copolymers **P5** and **P6** were obtained by RAFT polymerization of BMA with MAA and subsequent treatment with TBAOH. C) Overview of synthesized polymeric and monomeric reference compounds. D) Summary of the molar masses obtained by SEC and the Đ values of all polymers. [a] T_g not determinable.

compound **R1**)[13] as well as in comparable salt extraction studies.[14] Furthermore, **M1** and **M2** exhibit a good accessibility through facile and modular copper(I)-catalyzed azide–alkyne cycloaddition (CuAAC) reactions and simultaneously introduce the triazole group with sufficient electron-withdrawing character.[15] Additionally, quantitative alkylation of the triazole moieties (e.g. using trimethyloxonium tetrafluoroborate) allows the formation of the corresponding triazolium salts (**P3**, **P4**, and reference compound **R2**), which causes an increased C–H/C–I polarization as well as an additional charge assistance.[13a] Moreover, this post-functionalization guarantees the same BMA/receptor ratio (see Figure 1) in the neutral and positively charged forms of the copolymers (**P1** versus **P3** and **P2** versus **P4**) and, thus, ensures comparability.

In the case of the polymeric acceptor systems (**P5** and **P6**), BMA was copolymerized with methacrylic acid (MAA) and the resulting copolymer **P5** was subsequently treated with an excess of tetrabutylammonium hydroxide (TBAOH) to obtain the analogous anionic system (**P6**). However, ^{1}H NMR spectroscopy revealed a maximum degree of deprotonation of the acid groups of around 30%. All the copolymers were analyzed by NMR spectroscopy as well as size-exclusion chromatography (SEC), and revealed molar masses (M_n) of around 25000 g mol^{-1} (Figure 1 D).

The ability of the synthesized donor systems to effectively bind anions was subsequently evaluated by ITC experiments. Since ITC is a less common method in polymer and material science and was not performed on polymeric XB-based donor systems up to now, important parameters concerning the complex stoichiometry (N), the binding affinity (K), and the thermodynamic parameters (ΔH and ΔS) of different receptor systems in solution were obtained (Table 1). Notably, to compare the different binding behaviors of polymer-imbedded receptor units and the analogous monomeric structure, the reference system **R1**[13b] was also investigated in detail. Unfortunately, experiments with the charged reference

Table 1: Thermodynamic parameters for the complexation behavior of various donor–acceptor systems determined by ITC.[a]

Host	Guest	K [M^{-1}]	ΔH [kJ mol^{-1}]	$T\Delta S$ [kJ mol^{-1}]	N
P1[b]	Br^-	–	–	–	–
P3	Br^-	3.55×10^3	−13.9	6.8	1.06
R1	Br^-	2.22×10^3	−24.5	−5.1	1.00
P2	Br^-	2.36×10^3	−28.4	−8.8	0.79
P4	Br^-	2.87×10^4	−31.8	−5.9	1.05
P4	AcO^-[c]	4.17×10^5	−12.9	19.7	0.96
		2.11×10^3	−22.8	−3.5	1.50

[a] Thermodynamic parameters calculated from guest-into-host titration experiments in THF at 303 K. All anions were added as their tetra-*n*-butylammonium (TBA^+) salts. [b] No sufficient heat effect was observed in the ITC measurement. [c] The formation of a 1:2 complex (host/guest) could be further supported by inverse titration experiments (see Table S3).

system **R2** under identical conditions could not be performed because of its low solubility in THF.

First, a systematic analysis of the binding behavior of all the prepared donor systems with bromide was performed to enable a reliable prediction of the binding motif and to allow the classification of these donor moieties with respect to literature data.[13a,16] As expected, the HB-based host systems (**P1** and **P3**) revealed significantly smaller association constants than the XB-based analogues (**P2** and **P4**). In the case of the uncharged HB system **P1**, the anion affinity to bromide was even too low to be determined by ITC (Table 1).

Comparing the polymeric system **P2** with the analogous monomeric XB-based reference system **R1**, there seemed to be only minor influences of the polymer backbone on the complexation behavior of the receptor unit. In both cases, 1:1 complexes with nearly the same binding affinities were revealed by the ITC experiments (Table 1), thus indicating a cleft-type complexation as a result of the formation of two XBs between the two iodotriazole donors and the bromide ion. However, a slightly more unfavorable entropic term for the binding as well as a slightly decreased stoichiometric value ($N = 0.79$) was determined for **P2** (see the Supporting Information for details).

The tendency of the doubly positive charged systems (**P3** and **P4**) to form a 1:1 complex with bromide is enhanced by about one order of magnitude compared to the charge-neutral (**P1** and **P2**) receptor systems ($K_{\mathbf{P2}} = 2.36 \times 10^3\,\text{M}^{-1}$ and $K_{\mathbf{P4}} = 2.87 \times 10^4\,\text{M}^{-1}$). The enhanced enthalpic term for the doubly positive charged systems can be explained by the additional Coulomb interaction (charge assistance) as well as by a stronger C–H/C–X bond polarization of the triazolium moiety compared to the charge-neutral triazole moiety.[13a] At the same time, adjacent positively charged receptor units repel each other, thereby leading to a less-tangled conformation of the polymer chain. This results in a better accessibility of the receptor units, which is in line with the increased stoichiometric value for **P4** compared to **P2** ($N_{\mathbf{P4}} = 1.05$ and $N_{\mathbf{P2}} = 0.79$).

After the evaluation of different receptor-related parameters on the binding behavior to a simple spherical guest, the interaction with the polyatomic acetate was exemplarily studied with the strongest donor system (**P4**). Notably, acetate mimics the carboxylate group of the polymeric acceptor system (**P6**). The observed preference of **P4** for acetate over bromide (Table 1) is in line with previous results of monomeric receptor systems, and is rationalized by the higher basicity of the oxoanion.[13a] As a result of the increased anion affinity, the tendency to even form 1:2 complexes ($N_2 = 1.50$ for **P4** × AcO^-) was observed for acetate. Therefore, quantum chemical calculations using density functional theory (DFT) methods were performed to visualize and corroborate the different binding modes of the polyatomic acetate (see Figures S53 and S54 in the Supporting Information).

Finally, complete polymer-based donor–acceptor pairs (**P4** with **P5** as well as **P4** with **P6**) were also studied with regard to their complexation behavior in solution (see Figure S28). In general, an attractive interaction between the two polymeric systems was found, that is, even the completely neutral system **P5** showed an exothermic signal, which was even stronger for the partially anionic species **P6**. Unfortunately, a reliable quantification is precluded by the unknown degree of accessible donor and/or acceptor sites (see the Supporting Information for more detailed explanations). Nevertheless, a titration of **P4** with a pure BMA-based reference polymer **P7** revealed no significant heat change, which is a strong indication that the attractive interaction with **P5** and **P6** is based on the formation of XBs between the receptor unit and the acid function of the MAA co-monomer (see Figure S29).

Having established the general binding behavior of the polymeric donor and acceptor systems in solution, we turned our attention to the material properties of the corresponding films. Thereby, we focused on the new and strong XB-based networks and the strongest HB-based reference system. For this purpose, solutions of the polymeric donor–acceptor pairs were mixed in stoichiometric amounts according to the degree of functionality to obtain cross-linked polymeric networks after solvent evaporation (e.g. **P46** from **P4** and **P6** in Figure 2a; see the Supporting Information for details).

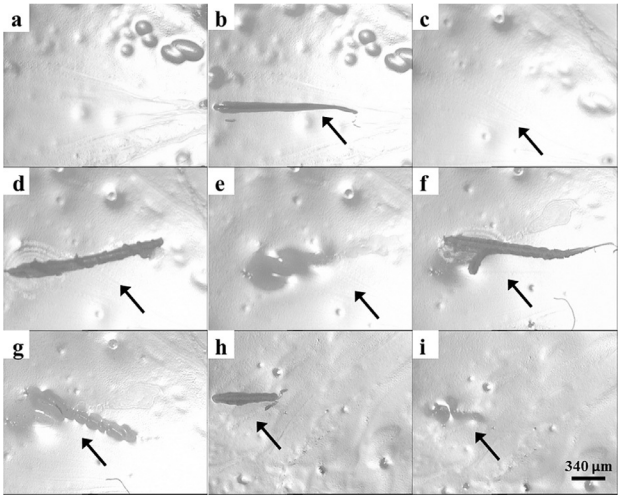

Figure 2. Self-healing behavior of the copolymer network **P46**: a) Film, b) first scratch, c) healing after 17 h at 100 °C, d) second scratch, e) healing after 17 h at 100 °C, f) third scratch, g) partial healing after 4 h at 100 °C, h) fourth scratch, and i) healing after 69 h at 80 °C.

Successful cross-linking was demonstrated by the help of nano-indentation measurements, which revealed relatively hard materials[11c,17] with indentation moduli (E_i) up to 1.82 GPa (**P25**) and, thus, a significantly higher stiffness than the non-cross-linked reference polymer **P7** (0.98 GPa). Moreover, when comparing analogous HB (**P36**) and XB (**P46**) based donor systems, the slightly increased stiffness and hardness of the film is also in line with the higher binding affinity of the iodotriazolium system in solution (Table 1). Remarkably, the completely charge-neutral network **P25**, which is characterized on the one hand by a weaker host–guest interaction compared to the charge-assisted donor moieties and on the other hand through the absence of counterions, exhibits an even slightly higher indentation modulus than **P46**. Hence, the additional counterions tenta-

tively act as a kind of plasticizer which reduces the stiffness of the films.

Afterwards, the applicability of these hard materials as self-healing films was investigated. The strong but reversible formation of supramolecular bonds between the polymeric donor–acceptor pairs constitutes the basis for this application. Satisfactorily, scratch tests on all the networks at 100 °C revealed self-healing behaviors (Figure 2 and Figures S30–S33). The different copolymer networks showed slight differences regarding the healing times and the healing temperatures (see Table S4). Interestingly, the combination of a XB-based donor with the partially anionic acceptor (**P26** and **P46**) required slightly higher temperatures for complete scratch healing. This result is in accord with the stronger host–guest interaction obtained by ITC and corresponds to the anticipated stronger cross-linking.

Furthermore, FT-Raman spectroscopy, an established method for the characterization of self-healing processes,[18] was applied to study the self-healing behavior. Thereby, **P4** (charge-assisted donor) as well as **P2** (neutral donor) were exemplarily studied in their corresponding donor–acceptor networks **P46** and **P26** (Figure 3 and Figure S49, respectively). The shift in the wavenumber of the C–I stretching vibration of the network **P46** (285 cm^{-1}) compared to that of **P4** (295 cm^{-1}; **P4**→**P46** = 10 cm^{-1}) is a clear indication for a C–I bond lengthening[19] and, thus, is consistent with a charge transfer and partial population of the σ*(C–I) orbital upon formation of XBs.[20] Moreover, the larger shift of the C–I band of the charge-assisted network **P46** (**P4**→**P46** = 10 cm^{-1}) compared to that of **P26** (**P2**→**P26** = 5 cm^{-1}) is in line with the expected formation of a stronger XB in the charge-assisted donor system **P4**.

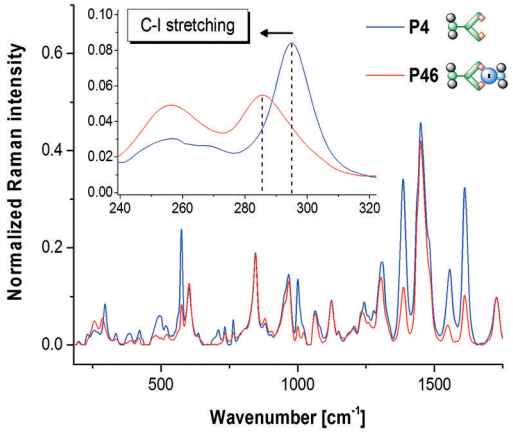

Figure 3. Normalized and background-corrected FT-Raman spectrum of the copolymer **P4** (blue line) and the polymer network **P46** (red line) as well as (inset) the shift of the C–I bond from **P4** (295 cm^{-1}) to **P46** (285 cm^{-1}), which proves the network formation through XBs.

In accord with the resulting bond weakening, a comparison of the C–I bond lengths in the solid-state structures of the free receptor **R2** (2.06 Å) and of the acetate complex (2.09 Å) also revealed a slight bond lengthening upon formation of a XB with a strongly coordinating anion (see Figure S52). Thus, the anion is complexed through the formation of two nearly linear XBs (177°–173°, cleft-type complexation) between the iodine atoms and the two different oxygen atoms of the acetate (I···O bond length of 2.61 Å). Moreover, the solid-state bond lengths as well as bond angles of the 1:1 complex (**R2** × AcO^-) are reproduced by quantum chemical calculations using DFT (see Figure S53). Additionally, two distinct conformations of 1:2 complexes that mimic the coordination of a second acetate to the host from the same or the opposite side were investigated by DFT (see Figure S54). For both, the XB angles (C–I···O) remain nearly linear, whereas a slight I···O bond shortening (−0.08 Å) as well as a C–I bond elongation (+0.02 Å) was calculated. Moreover, both studied conformations are comparable in energy, thus suggesting a variety of conceivable coordination modes for 1:2 complexes even for non-ideal arrangements in restricted media, for example, polymeric donor–acceptor networks.

Subsequently, the copolymer network **P46** was studied by temperature-dependent Raman spectroscopy to understand the underlying self-healing mechanism in more detail (see Figure S51). However, no changes in the Raman signals could be detected during heating, even after a longer heating time or after several heating–cooling cycles. Hence, the self-healing mechanism is presumably based on exchange reactions between two functional moieties, which has already been reported for other self-healing systems such as acylhydrazones.[21]

In conclusion, four different polymeric donor systems based on HBs (**P1** and **P3**) or XBs (**P2** and **P4**) were synthesized by facile and modular copper(I)-catalyzed cycloaddition reactions followed by RAFT polymerization. Subsequently, the first systematic ITC study with polymer-based XB donor systems was reported, which provided detailed information concerning their complexation behavior in solution and, thus, allows distinction between the effects of individual parameters (e.g. influence of polymeric backbone with respect to the monomeric systems, effect of charge assistance, and difference between HB- and XB-based receptor units). The complexation mode was further investigated by X-ray diffraction and computational modeling of the analogous monomeric receptor system (**R2**). After also imbedding the acceptor part into a polymer backbone, the thermally induced multiple self-healing behavior of the resulting polymer network was examined by scratch-healing tests. The XB-based induced cross-linking could be clearly revealed by a characteristic shift of the C–I band in the Raman spectra and could be further proven by the evaluated elastic moduli and hardness values of the coatings by nanoindentation. Consequently, the coupling of XBs with the concept of self-healing polymer networks allows the formation of hard coatings that have a multiple self-healing capability; further variations of the donor–acceptor part are currently under investigation to improve the self-healing ability and to gain a more detailed understanding of the self-healing mechanism. We believe that these first results will aid in the exploitation of the rich application potential of XB-based supramolecular polymer architectures (e.g. stimulus-responsive materials, stabilization of polymer blends).

Acknowledgements

We are grateful to the Deutsche Forschungsgemeinschaft (DFG) for financial support (SCHU1229/24-1, PO563/25-2, DI1517/9-1, SPP 1568). We also thank P. Bellstedt, G. Sentis, T. Schlotthauer, M. Enke, and N. Fritz for discussions and performing experiments.

Conflict of interest

The authors declare no conflict of interest.

Keywords: halogen bonding · host–guest systems · polymers · self-healing · supramolecular chemistry

How to cite: *Angew. Chem. Int. Ed.* **2017**, *56*, 4047 – 4051
Angew. Chem. **2017**, *129*, 4105 – 4110

[1] a) T. Clark, M. Hennemann, J. S. Murray, P. Politzer, *J. Mol. Model.* **2007**, *13*, 291 – 296; b) M. H. Kolář, P. Hobza, *Chem. Rev.* **2016**, *116*, 5155 – 5187.
[2] P. A. Gale, C. Caltagirone, *Chem. Soc. Rev.* **2015**, *44*, 4212 – 4227.
[3] A. Vargas Jentzsch, D. Emery, J. Mareda, P. Metrangolo, G. Resnati, S. Matile, *Angew. Chem. Int. Ed.* **2011**, *50*, 11675 – 11678; *Angew. Chem.* **2011**, *123*, 11879 – 11882.
[4] a) D. Bulfield, S. M. Huber, *Chem. Eur. J.* **2016**, *22*, 14434 – 14450; b) Y. Zhao, Y. Cotelle, N. Sakai, S. Matile, *J. Am. Chem. Soc.* **2016**, *138*, 4270 – 4277.
[5] A. Brown, P. D. Beer, *Chem. Commun.* **2016**, *52*, 8645 – 8658.
[6] a) T. M. Beale, M. G. Chudzinski, M. G. Sarwar, M. S. Taylor, *Chem. Soc. Rev.* **2013**, *42*, 1667 – 1680; b) M. Erdélyi, *Chem. Soc. Rev.* **2012**, *41*, 3547 – 3557; c) L. C. Gilday, S. W. Robinson, T. A. Barendt, M. J. Langton, B. R. Mullaney, P. D. Beer, *Chem. Rev.* **2015**, *115*, 7118 – 7195; d) G. Cavallo, P. Metrangolo, R. Milani, T. Pilati, A. Priimägi, G. Resnati, G. Terraneo, *Chem. Rev.* **2016**, *116*, 2478 – 2601.
[7] M. G. Chudzinski, C. A. McClary, M. S. Taylor, *J. Am. Chem. Soc.* **2011**, *133*, 10559 – 10567.
[8] a) A. Priimagi, G. Cavallo, P. Metrangolo, G. Resnati, *Acc. Chem. Res.* **2013**, *46*, 2686 – 2695; b) P. Politzer, P. Lane, M. C. Concha, Y. Ma, J. S. Murray, *J. Mol. Model.* **2007**, *13*, 305 – 311.
[9] a) G. Berger, J. Soubhye, F. Meyer, *Polym. Chem.* **2015**, *6*, 3559 – 3580; b) A. Vanderkooy, M. S. Taylor, *J. Am. Chem. Soc.* **2015**, *137*, 5080 – 5086; c) N. Houbenov, R. Milani, M. Poutanen, J. Haataja, V. Dichiarante, J. Sainio, J. Ruokolainen, G. Resnati, P. Metrangolo, O. Ikkala, *Nat. Commun.* **2014**, *5*, 4043; d) L. Meazza, J. A. Foster, K. Fucke, P. Metrangolo, G. Resnati, J. W. Steed, *Nat. Chem.* **2013**, *5*, 42 – 47; e) F. Meyer, P. Dubois, *CrystEngComm* **2013**, *15*, 3058 – 3071.
[10] a) M. D. Hager, P. Greil, C. Leyens, S. van der Zwaag, U. S. Schubert, *Adv. Mater.* **2010**, *22*, 5424 – 5430; b) S. J. Garcia, *Eur. Polym. J.* **2014**, *53*, 118 – 125.
[11] a) F. Herbst, D. Döhler, P. Michael, W. H. Binder, *Macromol. Rapid Commun.* **2013**, *34*, 203 – 220; b) P. Cordier, F. Tournilhac, C. Soulie-Ziakovic, L. Leibler, *Nature* **2008**, *451*, 977 – 980; c) S. Bode, L. Zedler, F. H. Schacher, B. Dietzek, M. Schmitt, J. Popp, M. D. Hager, U. S. Schubert, *Adv. Mater.* **2013**, *25*, 1634 – 1638; d) M. Burnworth, L. Tang, J. R. Kumpfer, A. J. Duncan, F. L. Beyer, G. L. Fiore, S. J. Rowan, C. Weder, *Nature* **2011**, *472*, 334 – 337.
[12] J. Chiefari, Y. K. Chong, F. Ercole, J. Krstina, J. Jeffery, T. P. T. Le, R. T. A. Mayadunne, G. F. Meijs, C. L. Moad, G. Moad, E. Rizzardo, S. H. Thang, *Macromolecules* **1998**, *31*, 5559 – 5562.
[13] a) R. Tepper, B. Schulze, M. Jäger, C. Friebe, D. H. Scharf, H. Görls, U. S. Schubert, *J. Org. Chem.* **2015**, *80*, 3139 – 3150; b) R. Tepper, B. Schulze, H. Görls, P. Bellstedt, M. Jäger, U. S. Schubert, *Org. Lett.* **2015**, *17*, 5740 – 5743.
[14] K. P. McDonald, B. Qiao, E. B. Twum, S. Lee, P. J. Gamache, C.-H. Chen, Y. Yi, A. H. Flood, *Chem. Commun.* **2014**, *50*, 13285 – 13288.
[15] a) B. Schulze, U. S. Schubert, *Chem. Soc. Rev.* **2014**, *43*, 2522 – 2571; b) Y. Hua, A. H. Flood, *Chem. Soc. Rev.* **2010**, *39*, 1262 – 1271.
[16] S. M. Walter, F. Kniep, L. Rout, F. P. Schmidtchen, E. Herdtweck, S. M. Huber, *J. Am. Chem. Soc.* **2012**, *134*, 8507 – 8512.
[17] M. L. Oyen, R. F. Cook, *J. Mech. Behav. Biomed. Mater.* **2009**, *2*, 396 – 407.
[18] L. Zedler, M. D. Hager, U. S. Schubert, M. J. Harrington, M. Schmitt, J. Popp, B. Dietzek, *Mater. Today* **2014**, *17*, 57 – 69.
[19] a) M. T. Messina, P. Metrangolo, W. Navarrini, S. Radice, G. Resnati, G. Zerbi, *J. Mol. Struct.* **2000**, *524*, 87 – 94; b) R. Bertani, P. Metrangolo, A. Moiana, E. Perez, T. Pilati, G. Resnati, I. Rico-Lattes, A. Sassi, *Adv. Mater.* **2002**, *14*, 1197 – 1201.
[20] S. V. Rosokha, C. L. Stern, J. T. Ritzert, *Chem. Eur. J.* **2013**, *19*, 8774 – 8788.
[21] N. Kuhl, S. Bode, R. K. Bose, J. Vitz, A. Seifert, S. Hoeppener, S. J. Garcia, S. Spange, S. van der Zwaag, M. D. Hager, U. S. Schubert, *Adv. Funct. Mater.* **2015**, *25*, 3295 – 3301.

Manuscript received: November 25, 2016
Final Article published: March 7, 2017

Publication P5

”A healing ionomer crosslinked by a bis-bidentate halogen bond linker: a route to hard and healable coatings”

J. Dahlke, R. Tepper, R. Geitner, S. Zechel, J. Vitz, R. Kampes, J. Popp, M. D. Hager, U. S. Schubert*, Polym. Chem*. **2018**, *9*, 2091-2197.

The paper as well as the supporting information (free of charge) is available online under:
doi.org/10.1039/C8PY00149A

Polymer Chemistry

PAPER

View Article Online
View Journal | View Issue

Cite this: *Polym. Chem.*, 2018, **9**, 2193

A healing ionomer crosslinked by a bis-bidentate halogen bond linker: a route to hard and healable coatings†

J. Dahlke, [a,b] R. Tepper,[a,b] R. Geitner,[c,d] S. Zechel,[a,b] J. Vitz,[a,b] R. Kampes,[a,b] J. Popp, [b,c,d] M. D. Hager *[a,b] and U. S. Schubert *[a,b]

Received 26th January 2018,
Accepted 21st March 2018

DOI: 10.1039/c8py00149a

rsc.li/polymers

In this work we present the first incorporation of bis-bidentate halogen bond linkers into an organic healing ionomer system resulting in the formation of crosslinked supramolecular networks. The obtained supramolecular coatings feature an excellent healing ability as well as an enhanced mechanical performance.

With the increasing usage of plastics in everyday life, the design of synthetic polymers with tailor-made properties is one of the largest challenges at the present time. Polymers containing supramolecular interactions are able to answer the expectations for modern high-performance materials due to their unique characteristics and defined tunability.[1,2] The usual concepts that come to mind when thinking about supramolecular bonds in polymers are, *e.g.*, metal ligand bonds[3] or hydrogen bond (HB) interactions.[4] A less popular but emerging class of strong supramolecular forces are halogen bond (XB) interactions.[5] Even though XBs are known for several decades, the advances in their research have gained more and more interest recently.[6] In general, XB interactions can occur if a strongly polarized halogen atom (X) interacts with an electron rich acceptor. In this context, the halogen atom can function as a Lewis acidic electron acceptor due to the formation of the so-called σ-hole and is, therefore, defined as an XB donor.[7]

The strength of these interactions can be comparable to and even stronger than those of more common HBs depending on the polarizability of the used halogen atom.[8] Moreover, XBs feature unique properties compared to the familiar HB systems such as strong directionality and hydrophobicity as well as the tunability of the interaction strength and the donor atom size.[9] The strength and versatility of XBs allow, *e.g.*, the formation of gels or fibrils.[10] Further applications of XBs are anion sensing,[11] liquid crystals,[12] magnetic and conductive materials[13] or catalytic systems.[14] However, the beneficial combination of highly functional polymers and XBs still remains a challenging approach.

We reported the first healing polymers based on XB interactions only recently in which the formation of a reversible supramolecular polymer network by two functional copolymers (*i.e.* polymeric halogen bond donor and acceptor) resulted in an intrinsically healable material.[15] In general, these kinds of healing polymers can be designed by using certain functional moieties in the structure, which can form reversible bonds based on covalent or supramolecular interactions.[16] However, the introduction of supramolecular bonds, which in most cases are weaker than covalent bonds, usually results in a reduced mechanical performance of the materials. Thus, the goal to design a material with sufficient mobility, enabling crack healing and still retaining high mechanical stability to prevent damage in the first place, is challenging.[17]

Accordingly, the aim of this work is the investigation of the influence of XB donors on an organic healing ionomer system based on phosphate moieties. Ionomers are low dielectric constant polymers, which contain up to 20% of ionic groups within their side chain structures.[18] Furthermore, the ion pairs can form aggregates, known as multiplets and clusters, which lead to very unique mechanical properties. As a consequence, ionomers can be considered as thermoplastic elastomers. The most intensively investigated example of this material class is poly(ethylene-*co*-methacrylic acid) partially neutralized with metal bases. Interestingly, this commercial ionomer, which is

[a]*Laboratory of Organic and Macromolecular Chemistry (IOMC), Friedrich Schiller University Jena, Humboldtstrasse 10, 07743 Jena, Germany. E-mail: ulrich.schubert@uni-jena.de, martin.hager@uni-jena.de*
[b]*Jena Center for Soft Matter (JCSM), Friedrich Schiller University Jena, Philosophenweg 7, 07743 Jena, Germany*
[c]*Institute for Physical Chemistry and Abbe Center of Photonics (ACP), Friedrich Schiller University Jena, Helmholtzweg 4, 07743 Jena, Germany*
[d]*Leibniz Institute for Photonic Technology (IPHT) Jena, Albert-Einstein-Strasse 9, 07745 Jena, Germany*

†Electronic supplementary information (ESI) available: Experimental details including NMR, DSC, TGA, Raman and nanoindentation data as well as detailed explanations towards ITC binding studies and healing experiments. See DOI: 10.1039/c8py00149a

also known as Surlyn®, shows healing behavior upon the damage of projectiles.[2,19] Due to the fact that ionomers usually contain anionic groups, they are potentially suitable as polymeric XB acceptors, which to the best of our knowledge has not yet been tested.

In combination with a bi-functional XB donor (Fig. 1B) it should be possible to improve the mechanical properties while maintaining the reversible nature of the network by crosslinking the polymer chains. In particular, phosphate groups are known to be effective Lewis basic XB acceptors[20] and, thus, we decided to attach phosphate moieties with a flexible ethyl bridge to the polymer backbone to ensure a good accessibility for the XB based crosslinker. Additionally, in order to study the effect of XBs on the ionomer network, an analogous HB-based donor was designed for comparison (Fig. 1B).

The synthesis of the precursors (**1** to **4**, see ESI†) for the preparation of the linkers **A** and **B** proceeded as described earlier.[15] The three step synthesis was completed by a reaction of octanedioyl dichloride with the educts **3** and **4**. The alkyl chain, which connects the two bidentate binding sites, increases the flexibility of the linker and, thus, enables an efficient crosslinking in the later polymer network (Fig. 1C). Furthermore, iodine was chosen as the XB donor atom for the linker **A** due to its tendency to form stronger interactions compared to other halogen atoms, presumably increasing the later mechanical performance of the formed network.[9]

In order to obtain a defined and comparable network structure, the linear polymer with the functional moieties had to be synthesized in the first place. One method to achieve tailor-made molar masses and low $Đ$ values with high reproducibility is reversible addition–fragmentation chain transfer (RAFT) polymerization.[21] The preparation of **P1** was performed by RAFT polymerization (M_n = 15 100 g mol^{-1}, M_w = 18 200 g mol^{-1}, $Đ$ =1.21) resulting in a neutral copolymer consisting of butyl methacrylate (BMA) and the phosphate based functional moiety (**5**, see ESI†). In order to calculate the required amount of a base (tetrabutylammonium hydroxide, NBu_4OH) for the subsequent quantitative deprotonation to obtain ionomer **P2**, the content of the phosphate groups in **P1** (10%) was determined by acid–base titration (see ESI†).

Afterwards, the ionomer **P2** was crosslinked by the addition of either linker **A** or **B** (ratio of the bifunctional linker to phosphate moieties 1 : 2) resulting in the supramolecular networks **P2A** (XB-based) and **P2B** (HB-based), respectively. Additionally, the non-charged network **P1A** was prepared using the neutral polymer **P1** and the linker **A**, which is expected to be weakly crosslinked because of the lack of ionic charges in the side chains.

To evaluate the anion binding behavior of the synthesized linkers **A** and **B**, isothermal titration calorimetry (ITC) measurements in solution were performed. Comparing the bromide affinity of the bi-functional linker **A** ($K_a(Br^-)$ = 2.76 × 10^3 M^{-1}) with the analogous mono-functional reference compound **R1** ($K_a(Br^-)$ = 2.22 × 10^3 M^{-1}, see ESI†), nearly the same association constant was determined indicating only minor interactions between the two adjacent binding sites of linker **A**. Moreover, the complex stoichiometry of **A** (N = 1.78) further supports the expected bis-bidentate complexation mode of the linker. In contrast, the binding affinity of the HB-based linker **B** is expectably much smaller and, therefore, not detectable with this method.

In order to validate the XB interactions also directly in the solid polymer film, Raman measurements of the linker **A**, the ionomer **P2** and the XB network **P2A** were performed. The supramolecular bond formation is indicated by a shift of the donor signals at 1524 cm^{-1} to 1520 cm^{-1} (triazole) and at 1612 cm^{-1} to 1608 cm^{-1} (phenyl/mesityl) (Fig. 2), which is in line with previous investigations on a similar system.[15]

Besides the structural composition of the network, the mechanical and thermal properties were investigated in order

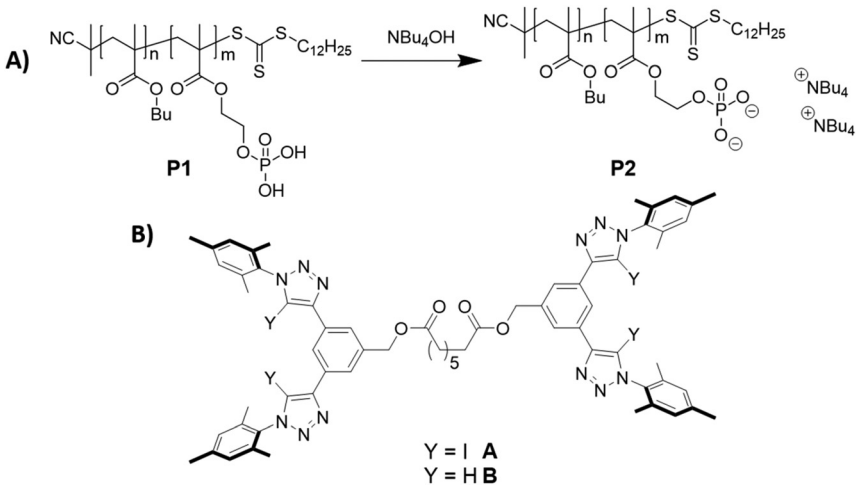

C)

P1	+	A	⟶	P1A
P2	+	A	⟶	P2A
P2	+	B	⟶	P2B

D)

Polymer	M_n [g/mol]	M_w [g/mol]	Đ
P1	15,100	18,200	1.21

E)

Polymer	T_g [°C]	T_d [°C]
P1	44.0	217
P2	33.3	224
P1A	41.5	212
P2A	35.3	229
P2B	–[a)]	231

Fig. 1 (A) Schematic representation of **P1** and the synthesis path towards the ionomer **P2**. (B) Chemical structure of the XB-based linker **A** and the corresponding HB-based model system **B**. (C) Simplified reaction scheme of the network synthesis. (D) SEC results for the neutral copolymer **P1**. (E) Summary of the thermal properties of all tested polymers determined by DSC and TGA. [a] No T_g detectable.

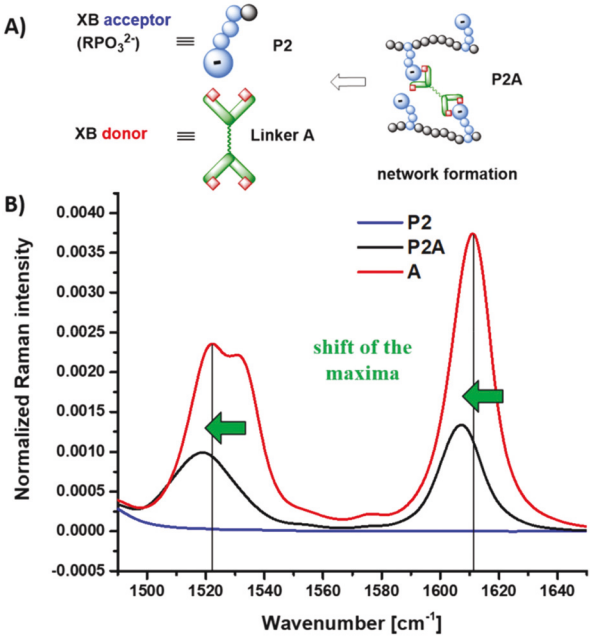

Fig. 2 (A) Schematic representation of the XB network formation. (B) Normalized and background-corrected FT-Raman spectra of the polymer **P2** (blue line), the polymer network **P2A** (black line) as well as the XB-based linker **A** (red line).

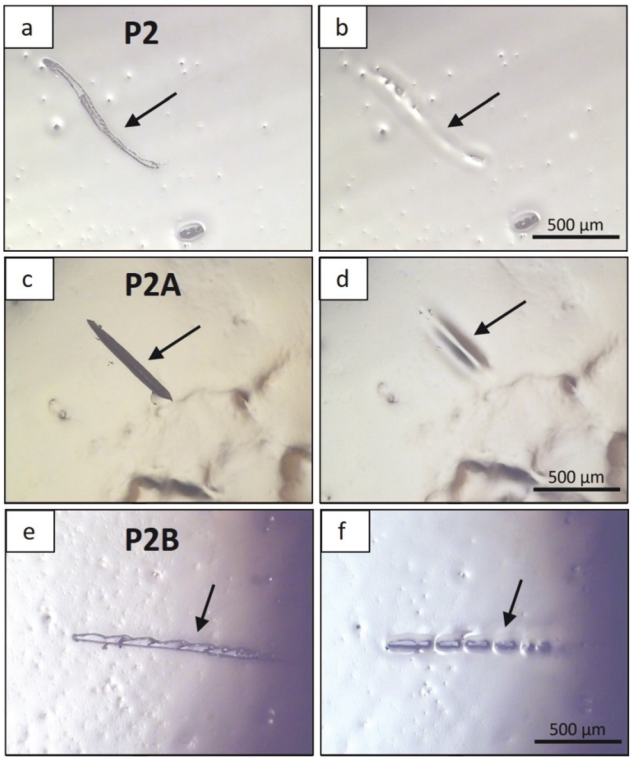

Fig. 3 Scratch healing experiments of the polymers **P2** (a,b), **P2A** (c,d) and **P2B** (e,f). Left: Scratch, right: scratch after 3.5 h at 100 °C.

to evaluate the suitability of the polymers as healing materials. Common healing temperatures for supramolecular, BMA containing copolymers range from 60 to 100 °C.[22] Thus, the thermal properties were studied *via* differential scanning calorimetry (DSC) and thermal gravimetric analysis (TGA). The detected T_g values of the samples (33 to 44 °C, see Fig. 1E and ESI†) as well as their observed thermal stability for temperatures up to 200 °C (see Fig. 1E and ESI†) indicate the suitability of the materials for healing tests at 100 °C.

In order to further evaluate the influences of XB crosslinks in the polymer networks, the healing abilities of the prepared films were compared with the help of the common scratch healing test.[23] Thus, the neutral copolymer **P1** and the ionomer **P2** without any bidentate linker were tested initially (see ESI†). As expected, only the ionomer **P2** revealed healing at 100 °C within 3.5 h, whereas **P1** was not able to heal the scratches. In addition, the XB crosslinked networks **P2A** and **P1A** were tested under the same conditions. Thereby, the best healing properties were observed for **P2A**, which contains ionic groups and the iodine containing linker **A** (Fig. 3). The network was able to heal the scratches within the same timescale as that of **P2** (3.5 h at 100 °C). In contrast, the neutral copolymer with the same linker **A** (**P1A**) revealed only partial healing after 3.5 h at 100 °C, which is slightly slower compared to the ionic network (**P2A**), but better in comparison with the sole neutral polymer **P1** indicating a beneficial influence of the XB crosslinker. This valuable influence was further underlined by comparing the XB-based network (**P2A**) with the HB-based one (**P2B**). Considering the ITC results in solution, the HB-based network is indicated to be weaker crosslinked, which is in line with the observed partial healing properties. In order to quantify the results, the optical images from the microscopy study for the most relevant polymers (**P2**, **P2A** and **P2B**) were analyzed. The area of the scratch before and after the temperature treatment was calculated and the ratio was utilized to calculate the healing efficiency according to the literature.[24] The details regarding the calculations can be found in the ESI (see Table S9†). The resulting values for **P2** (86%), **P2A** (80%) and **P2B** (63%) support the conclusions discussed above.

A crucial point when designing healing systems besides actual healing ability is the mechanical stability and performance of the material. Very soft polymers, *e.g.*, hydrogels with weak supramolecular interactions, show superior healing behavior at very low temperatures.[25] However, for the potential application as a coating material, a certain resistance to the mechanical damage/hardness of the material is indispensable. In order to evaluate the mechanical properties and the hardness of the material, even with very little amounts of the material, nanoindentation represents the method of choice (Fig. 4).[26] The nanoindentation measurements were performed at room temperature. The neutral copolymer **P1** features a hardness of approximately 0.045 to 0.05 GPa at indentation depths between 300 and 1500 nm. After the neutralization of the acidic groups with NBu_4OH, the hardness decreases significantly by one order of magnitude to about 0.005 GPa. This

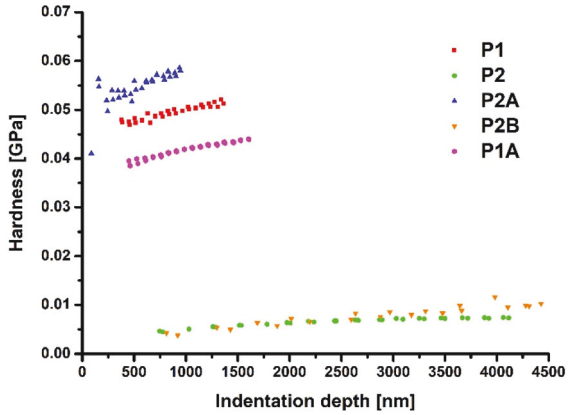

Fig. 4 Nanoindentation results for the polymers **P1** (red), **P2** (green) and the polymer networks **P2A** (blue), **P2B** (orange) and **P1A** (purple).

behavior can be explained by a softener effect of the introduced organic and flexible bulky tetrabutyl ammonium cations. However, the ionomer **P2** revealed much better healing properties than **P1**. A similar softener effect could be observed for **P2B**, which contains the bidentate HB linker **B**. Since the hydrogen atoms in **B** resulted in no significant crosslinking of the copolymer, the linker simply acts as an additional softener. The investigations of **P2A** and **P1A** on the other hand showed a strong influence of the linker **A** on the hardness of the materials. The formed XBs increased the hardness significantly by a factor of 10 in comparison to the pure ionomer **P2**. The neutral **P1A** featured slightly lower hardness properties compared to **P2A** due to the lack of ionic groups and, therefore, a weaker XB interaction.

Considering the results presented herein, the effect of the XB can be explained best by the comparison of the ionomer **P2** and the ionic XB network **P2A**. The ionomer **P2** revealed very good healing behavior at 100 °C. The healing behavior of the ionic XB network **P2A** certainly was similar to this ionomer, however, the mechanical stability in terms of hardness significantly increased for **P2A**. Thus, the combination of a XB-based crosslinker with Lewis basic ionomers allows the design of materials with a good healing behavior and the ability to have a specific material flow at moderate temperatures while still maintaining the mechanical strength required for applications like coating materials. XB type interactions can clearly influence the properties and enable the development of new, superior healing polymer systems with excellent mechanical performance.

Conclusions

The new healing polymer network presented in this study consists of a fully organic phosphate based ionomer crosslinked by a bis-bidentate iodine containing XB linker. The thermal, chemical and mechanical properties were investigated comprehensively using advanced methods such as DSC, TGA, NMR, SEC, ITC, Raman and nanoindentation. Additionally, a neutral polymer network as well as an ionomer with a HB analogous linker, which only imitates the structure of the linker due to the very weak interaction strength, were tested in order to identify the influences of the XB interactions on the properties of the material. We were able to demonstrate the design of a system which, does not only feature excellent healing behavior but also high mechanical strength in terms of hardness. This beneficial combination of ionic and XB interactions in a healing polymer opens a new pathway towards tailor-made highly functional materials, presumably interesting as coating materials.

Conflicts of interest

There are no conflicts to declare.

Acknowledgements

The authors gratefully acknowledge the Deutsche Forschungsgemeinschaft (DFG) for financial support (SPP 1568, SCHU1229/24-1, PO563/25-2). The authors further thank Marcus Abend for support with the analysis of the healing images. S. Z. is grateful to the Carl-Zeiss foundation for funding.

Notes and references

1 (*a*) L. Yang, X. Tan, Z. Wang and X. Zhang, *Chem. Rev.*, 2015, **115**, 7196–7239; (*b*) M. D. Hager, P. Greil, C. Leyens, S. van der Zwaag and U. S. Schubert, *Adv. Mater.*, 2010, **22**, 5424–5430; (*c*) M. Enke, D. Döhler, S. Bode, W. H. Binder, M. D. Hager and U. S. Schubert, *Adv. Polym. Sci.*, 2016, **273**, 59–112.

2 L. Zhang, N. R. Brostowitz, K. A. Cavicchi and R. A. Weiss, *Macromol. React. Eng.*, 2014, **8**, 81–99.

3 G. R. Whittell, M. D. Hager, U. S. Schubert and I. Manners, *Nat. Mater.*, 2011, **10**, 176–188.

4 L. Brunsveld, B. J. B. Folmer, E. W. Meijer and R. P. Sijbesma, *Chem. Rev.*, 2001, **101**, 4071–4098.

5 (*a*) F. Meyer and P. Dubois, *CrystEngComm*, 2013, **15**, 3058–3071; (*b*) G. Berger, J. Soubhye and F. Meyer, *Polym. Chem.*, 2015, **6**, 3559–3580.

6 G. Cavallo, P. Metrangolo, R. Milani, T. Pilati, A. Priimagi, G. Resnati and G. Terraneo, *Chem. Rev.*, 2016, **116**, 2478–2601.

7 M. H. Kolář and P. Hobza, *Chem. Rev.*, 2016, **116**, 5155–5187.

8 L. C. Gilday, S. W. Robinson, T. A. Barendt, M. J. Langton, B. R. Mullaney and P. D. Beer, *Chem. Rev.*, 2015, **115**, 7118–7195.

9 A. Priimagi, G. Cavallo, P. Metrangolo and G. Resnati, *Acc. Chem. Res.*, 2013, **46**, 2686–2695.

10 (*a*) Y. Huang, H. Li, Z. Li, Y. Zhang, W. Cao, L. Wang and S. Liu, *Langmuir*, 2017, **33**, 311–321; (*b*) L. Meazza,

J. A. Foster, K. Fucke, P. Metrangolo, G. Resnati and J. W. Steed, *Nat. Chem.*, 2013, **5**, 42–47; (*c*) A. Bertolani, L. Pirrie, L. Stefan, N. Houbenov, J. S. Haataja, L. Catalano, G. Terraneo, G. Giancane, L. Valli, R. Milani, O. Ikkala, G. Resnati and P. Metrangolo, *Nat. Commun.*, 2015, **6**, 7574.

11 A. Brown and P. D. Beer, *Chem. Commun.*, 2016, **52**, 8645–8658.

12 (*a*) H. L. Nguyen, P. N. Horton, M. B. Hursthouse, A. C. Legon and D. W. Bruce, *J. Am. Chem. Soc.*, 2004, **126**, 16–17; (*b*) P. Metrangolo, C. Präsang, G. Resnati, R. Liantonio, A. C. Whitwood and D. W. Bruce, *Chem. Commun.*, 2006, **31**, 3290–3292.

13 (*a*) M. Fourmigué and P. Batail, *Chem. Rev.*, 2004, **104**, 5379–5418; (*b*) T. Imakubo, H. Sawa and R. Kato, *J. Chem. Soc., Chem. Commun.*, 1995, **73**, 1667–1668.

14 D. Bulfield and S. M. Huber, *Chem. – Eur. J.*, 2016, **22**, 14434–14450.

15 R. Tepper, S. Bode, R. Geitner, M. Jager, H. Gorls, J. Vitz, B. Dietzek, M. Schmitt, J. Popp, M. D. Hager and U. S. Schubert, *Angew. Chem., Int. Ed.*, 2017, **56**, 4047–4051.

16 (*a*) F. Herbst, D. Döhler, P. Michael and W. H. Binder, *Macromol. Rapid Commun.*, 2013, **34**, 203–220; (*b*) M. D. Hager, S. van der Zwaag and U. S. Schubert, *Self-healing materials*, Springer, Switzerland, 2016, vol. 273.

17 (*a*) R. Hoogenboom, *Angew. Chem., Int. Ed.*, 2012, **51**, 11942–11944; (*b*) S. Zechel, R. Geitner, M. Abend, M. Siegmann, M. Enke, N. Kuhl, M. Klein, J. Vitz, S. Gräfe, B. Dietzek, M. Schmitt, J. Popp, U. S. Schubert and M. D. Hager, *NPG Asia Mater.*, 2017, **9**, e420.

18 (*a*) R. J. Varley and S. van der Zwaag, *Polym. Test.*, 2008, **27**, 11–19; (*b*) A. Eisenberg, B. Hird and R. B. Moore, *Macromolecules*, 1990, **23**, 4098–4107.

19 S. J. Kalista, J. R. Pflug and R. J. Varley, *Polym. Chem.*, 2013, **4**, 4910.

20 R. Tepper, B. Schulze, M. Jäger, C. Friebe, D. H. Scharf, H. Görls and U. S. Schubert, *J. Org. Chem.*, 2015, **80**, 3139–3150.

21 G. Moad, E. Rizzardo and S. H. Thang, *Aust. J. Chem.*, 2012, **65**, 985.

22 (*a*) S. Bode, M. Enke, R. K. Bose, F. H. Schacher, S. J. Garcia, S. van der Zwaag, M. D. Hager and U. S. Schubert, *J. Mater. Chem. A*, 2015, **3**, 22145–22153; (*b*) J. Dahlke, R. K. Bose, S. Zechel, S. J. Garcia, S. van der Zwaag, M. D. Hager and U. S. Schubert, *Macromol. Chem. Phys.*, 2017, **218**, 1700340.

23 S. Bode, M. Enke, M. Hernandez, R. K. Bose, A. M. Grande, S. van der Zwaag, U. S. Schubert, S. J. Garcia and M. D. Hager, *Adv. Polym. Sci.*, 2016, **273**, 113–142.

24 R. K. Bose, M. Enke, A. M. Grande, S. Zechel, F. H. Schacher, M. D. Hager, S. J. Garcia, U. S. Schubert and S. van der Zwaag, *Eur. Polym. J.*, 2017, **93**, 417–427.

25 A. Phadke, C. Zhang, B. Arman, C.-C. Hsu, R. A. Mashelkar, A. K. Lele, M. J. Tauber, G. Arya and S. Varghese, *Proc. Natl. Acad. Sci. U. S. A.*, 2012, **109**, 4383–4388.

26 G. M. Pharr and W. C. Oliver, *MRS Bull.*, 1992, **17**, 28–33.